BESS for Electrification of Aviation on Bonaire

Analysis of the contribution of a BESS enabling electric aviation on the island Bonaire

Master Thesis

Floris van Buren

Delft University of Technology

TU Delft

BESS for Electrification of Aviation on Bonaire

Analysis of the contribution of a BESS enabling electric aviation on the island Bonaire

by

Floris van Buren

Master of Science in Sustainable Energy Technology
DC systems, Energy conversion and Storage

Floris van Buren 4719549

To be defended in public on 2023/11/17

Thesis Committee and Guidance:

Dr.ir. (Pavol) Bauer - TU Delft
Dr.ir (Rudi) Hakvoort - TU Delft
Dr.ir. (Laura) Ramírez Elizondo - TU Delft
Ir. (Patrick) Groenewoud - Krado

TU Delft

Foreword

This report was written to obtain the Master's degree in Sustainable Energy Technology at the Delft University of Technology. For the past few months, I have been working on a project that concerns the increased electricity demand of electric aviation and the contribution of a BESS to enable electric aviation at Bonaire. This thesis was conducted with the help and guidance of Krado, Water- en Energiebedrijf Bonaire (WEB), and Bonaire International Airport (BIA).

Going into the topic of aviation, especially electric aviation was new for me. Moreover, I learned to optimize a battery energy storage system in combination with a PV system and deepened my knowledge in the field of energy storage. Secondly, working on this thesis gave me many opportunities to develop myself personally. Working on a project with multiple stakeholders' views has taught me a lot as well as planning such a long-term project. I want to thank my supervisor from the TU Delft, Laura Ramírez Elizondo, for guiding me through the phase of setting up research questions and for the interesting meetings. To Rudi Hakvoort, for the critical view, useful feedback, and jokes during the meetings. And special thanks to Patrick Groenewoud and Roy Silberie for the intensive guidance and for creating the opportunity to do an international thesis project which has brought me a lot of new experiences. I am proud to successfully finished the Master of Sustainable Energy Technology. I have truly enjoyed my time as a Sustainable Energy Technology student at the Delft University of Technology.

Abstract

Currently, the entire aviation sector accounts for 2.5% of global emissions. To commit to the Paris Agreement by 2050, new emerging technology is necessary. Electric aircraft emerged as one of the promising solutions to decarbonize the aviation sector. However, the introduction of electric aviation (EA) causes a shift from kerosene to electricity. With the minimized turnaround times of aircraft, high charging powers are encountered with the adoption of electric aircraft. This can in turn lead to grid instability and costly grid infrastructure upgrades for the grid operator. A battery energy storage system (BESS) can potentially be a promising solution capable of addressing the high power rates associated with electric aircraft charging. Moreover, it provides opportunities for the battery owner to reduce costs and increase the utilization of renewable energy.

This thesis aims to gain insight into the contribution of the deployment of a BESS compared to the business-as-usual situation to enable electric aviation while facilitating the interests of both the grid operator and the airport. In particular, this is done for the case study of Bonaire International Airport (BIA) and the grid operator Water- en Energiebedrijf Bonaire (WEB). For the grid operator, the impact on the grid is analyzed focusing on the voltage fluctuations, the load on the distribution cables, and the airport's transformer (over)loading. From the airport's perspective, the airport system's LCOE, and the CO_2 emissions from grid electricity are investigated. Lastly, as electric aviation is currently not commercially used, and faces a lot of uncertainty, the sensitivity of the control strategies to various future scenarios for 2030 is analyzed. This is investigated by a mathematical optimization model for the three battery control strategies, Self-Consumption, Peak-Shaving, and Cost-Optimal.

The results showed that in the absence of a BESS, the business-as-usual situation, independent of the adoption level of electric aviation at BIA, the transformer required a capacity upgrade. With the deployment of a BESS, it was found that a Self-consumption-controlled BESS could not effectively reduce the peak loads and defer a transformer capacity upgrade. While voltage fluctuations remained within the acceptable operational range for each control strategy and adoption level of EA. On the other hand, future scenarios with high demand growth could lead voltage fluctuations to reach the allowable threshold. The Self-Consumption strategy is susceptible to an increased electricity demand and adoption level of EA, which substantially influences the load on the distribution cables. Conversely, the Peak-Shaving and Cost-Optimal battery significantly reduces the peak loads in both electricity demand and injection even in scenarios with increased electricity demand and higher adoption levels of EA. Economically, it was shown that a BESS substantially reduced the LCOE depending on the control strategy. Furthermore, it is feasible to reduce CO_2 emissions originating from grid electricity production, albeit the reduction is strongly affected by increased electricity demand over time.

The research concluded that a BESS is able to defer grid infrastructure upgrades and reduce costs for the airport, although, the extent of these results is highly dependent on the control strategy. Regardless of the control strategies, a battery is able to achieve a reduction in CO_2 emissions from the grid given the on-site PV system.

Contents

List of Figures

List of Tables

1 Introduction

1.1. Problem Definition

Currently, there is a growing concern about the emissions originating from the transportation sector, in particular the aviation sector. The entire aviation sector amounts to 2.5% in global CO_2 emissions, which is expected to keep on growing [89]. According to forecasts of Airbus and Boeing the aviation sector is expected to annually increase by 4.8%, while the energy efficiency improvements of conventional aircraft are reaching a plateau [6].
Therefore, new emerging technology is necessary to reduce environmental impact. Electric aircraft emerged as a promising solution because of this need to decarbonize the aviation sector, aligning with the objective of reaching net-zero carbon emissions at airports by 2050 according to the Paris Agreement [49]. In the same timeframe, the aviation industry should reduce its emissions by 75% [40]. Other key aspects of objectives in the aviation sector are to make aviation more cost-effective, energy-efficient, and reliable while concurrently reducing noise-related impact [90] [111]. However, state-of-the-art battery technology hinders the breakthrough of commercial electric aircraft. A major barrier to the realization of an electric aircraft is the high battery energy density and the subsequent increase in aircraft weight. This limits the range and passenger capacity of electric aircraft [111]. Nevertheless, taking into account the development of battery technology, companies like Eviation anticipate market entry with small electric aircraft for short regional flights in 2027 [32], followed by more designs of electric aircraft of other companies by 2030 [82] [7].

The introduction of electric aviation (EA) entails a fuel shift from kerosene to electricity as the primary energy source, resulting in an increased electricity demand profile of airports. Moreover, due to the short turnaround times of aircraft, this results in substantial electricity peak demands for airports. As a consequence of this high peak demand, problems can arise with grid stability resulting in grid infrastructure upgrades [109], which are associated with costly investments [45].

In response to the aforementioned challenges, a Battery Energy Storage System (BESS) can potentially be a promising solution capable of addressing the high charging rates of electric aircraft. From a technical perspective, a BESS can reduce the impact on the grid by diminishing peak loads [109] [86] which aligns with the interest of the grid operator. Additionally, from the airport's perspective, a BESS can provide an opportunity to reduce the total costs associated with aircraft charging [40]. Moreover, given the collective commitment of both the grid operator and the airport to increase the share of renewable energy utilization, and to achieve sustainable goals in electric aviation, the deployment of a BESS and a PV system can be effective in reducing emissions [59] [64].
However, these technical, economic, and environmental outcomes are achieved to varying degrees through different BESS control strategies. Considering these indicators, the research question in this thesis is:

'What is the effect of different BESS control strategies on the technical, economic, and environmental performance so that it can facilitate both the grid operator and the airport to enable electric aviation?'

This research is structured as follows: Chapter 2 provides the background theory into electric aviation, the renewable energy system, and battery control strategies. In Chapter 3 the methodology of the research is outlined. Subsequently, the results are presented in Chapter 4. The thesis ends with the conclusion, discussion, and future work in Chapter 5.

1.2. Context

In the previous section, it was stated that this research is conducted for Bonaire International Airport (BIA) and Water- en Energiebedrijf Bonaire (WEB) located on Bonaire. This section discusses general information about Bonaire, its energy system, and WEB and BIA.

Bonaire is an island located to the north of Venezuela in the Caribbean Sea as depicted in figure 1.1. As of 2023, Bonaire counts around 23,000 inhabitants, which will grow further with a 15% increase over the years according to forecasts [99]. Bonaire is relatively small with an area of approximately 250 square km.
The islands's economy heavily relies on tourism, and the tourism sector faced difficulties during the pandemic. Nevertheless, in 2021, 111,300 tourists (pre-pandemic 2019: 152,000) came by plane and 56,600 (pre-pandemic 2019: 457,700) arrived by cruise ship [73]. Currently, the tourism sector has picked up the pace. The same holds for the electricity use of the Bonairean people. The growth rates of electricity demand have returned to pre-pandemic rates of 6.7% [28]. The average income in 2021 of the Bonairean population is 25,810 USD [74]. Together with St. Eustatius and Saba, Bonaire is one of the BES islands and a special municipality of the Netherlands. Also, Bonaire is actively engaged in the energy transition. Since the Netherlands Caribbean is under the indirect influence of the European part of the Netherlands, the governance of this part of the Kingdom will work through the BES-islands. Therefore, the policy regarding sustainability should be taken into account. The energy policy of Bonaire is striving for an energy system in 2050 that is in accordance with the reduction in CO_2 of the Paris climate agreement [27].

Figure 1.1: Location of Bonaire in Caribbean sea with an enlargement of the island Bonaire in the right top corner.[117][62]

1.2.1. Water- en Energiebedrijf Bonaire (WEB)

The primary function of Water- en Energiebedrijf Bonaire (WEB) is to distribute electricity, drinking water, and irrigation water throughout Bonaire, while the energy production is exclusively provided by Contour Global. As mentioned in the previous section Bonaire is undergoing rapid development,

due to the growing population and tourism. Therefore, WEB has the challenge of ensuring a reliable, sustainable, and affordable supply of these products for the population of Bonaire [28]. These three core values of WEB will be elaborated in this section.

The first core value of WEB is sustainability, where WEB tries to accelerate and stimulate the energy transition according to the Global Sustainable Development Goals [28]. The introduction of electric aviation in Bonaire is according to the sustainability goals of WEB and therefore WEB takes a sympathetic view of the introduction of electric aviation at Bonaire.
However, the increased electricity demand of BIA for EA purposes could impede the grid, which could lead to conflicts with the two other core values of WEB; quality and reliability, and affordability. WEB is a public organization and therefore works with a social perspective. As a result, a reliable grid connection and an affordable electricity price for the Bonairian residents is important for WEB [28].
The electricity grid should be able to handle sudden peak loads associated with the demand profile of electric aircraft charging. In case EA necessitates substantial grid upgrades to be able to introduce aircraft charging, WEB is less supportive of the introduction of EA. This would lead to significant investments reflected in the electricity price for the consumer and so be at the expense of the Bonairian residents. In that case, the Bonairian residents will pay for the BIA's increased energy consumption which is in conflict with the core value of affordability of electricity of WEB [28].
The demand profile for EA can cause sudden peak loads on the grid that pose significant challenges for the Bonairian grid as an islanded microgrid [86]. These sudden peak loads causing problems with the grid stability run contrary to the main value of quality and reliability of electricity of WEB.
In short, the introduction of EA aligns with WEB's values in terms of sustainability goals but can potentially clash with the reliability and affordability of electricity. Consequently, under certain circumstances, WEB supports EA, as long as this does not grossly affect the reliability and affordability of electricity.
The operational core values of WEB are summarized in table 1.1

Table 1.1: The core values of Water- en Energiebedrijf Bonaire summarized [28].

Core Values of WEB	
1. Sustainability	The main function of WEB is distributing electricity and water, in which WEB also tries to be supportive in the acceleration of the energy transition on Bonaire.
2. Quality and Reliability	As WEB is the electricity distributor of the islanded grid of Bonaire, WEB has the challenge of maintaining grid stability. Therefore one of the core values of WEB is to provide a reliable and qualitative grid connection to citizens and businesses as customers.
3. Affordability	Affordability is the third main value of WEB. As a public organization, WEB operates with a social perspective. WEB strives to lower the electricity price of electricity and water for the Bonairian citizens. Where WEB wants to contribute to the quality of life of the present and future generations.

1.2.2. Energy System of Bonaire

The Bonairian energy system currently relies on a combination of energy production assets, including diesel generators, wind energy, a battery management system, and to a lesser extent solar energy, with renewable energy sources (RES) account for approximately 30% of the total energy production [28].

At the east side of Bonaire at Morotin, twelve wind turbines account for 900 kW each, and at Sorobon a 330 kW wind turbine is located [113]. Even though Bonaire is located near the equator in the Caribbean Sea and is associated with a sun-drenched environment, the current share of PV generation is minimal. Nevertheless, there is a current pilot PV project going on at Barcadera that consists of 792 panels powering around 60 houses [113]. The solar pilot was used for future projects to investigate the efficiency, return on investment, and impact on the grid [104] [28].
Lastly, ten diesel generators are used for the remaining share of the energy production, being able to provide 22 MW of electricity. A reserve of diesel generators is installed in case of emergency. The energy

system is summarized in table 1.2.

In 2021 the total generation of electricity was nearly 120 GWh, from which 22.4% was provided by renewable energy [28]. The peak load on the island was approximately 18MW, with peak demand typically occurring in September driven by an increased electricity usage for air conditioning, while the lowest peak is during January-February [36]. Figure 1.2 shows the locations of all the power plants and their respective power output.

Table 1.2: *Energy production at Bonaire 2023*

Bonaire Energy System	Number	Available Capacity	Total Capacity
Wind Turbine I	1	330 kW	330 kW
Wind Turbine II	12	900 kW	10.8 MW
PV solar park	1	200 kWp	200 kWp
Diesel I (P nominal 2.85 MW)	5	2.50 MW	12.5 MW
Diesel II (P nominal 1.8 MW)	5	1.8 MW	9 MW
Diesel Reserve (P nominal 1.8 MW)	4	1.75 MW	7 MW
BESS	1	6 MWh/6MW	6 MWh/6MW

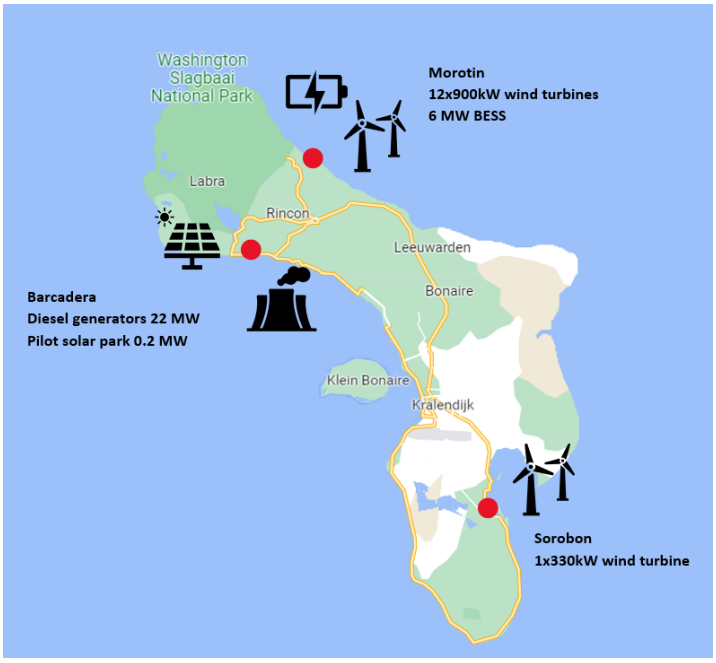

Figure 1.2: Map of Bonaire with the solar pilot and the diesel generators located on the west side of Bonaire at Barcadera. On the north side of Bonaire at Morotin 12 wind turbines are located (900 kW each), together with the battery energy storage system (BESS). Lastly, in the south of Bonaire, one single wind turbine is located at Sorobon.

Bonaire is actively pursuing the transition to an energy system with a larger share of RES, however, the current efforts are in line with the desired objective. The objective is to adopt a level of sustainable energy to reduce CO_2 emissions in accordance with the Paris Agreement in 2050 [27].

In addition to the environmental reason for driving the push for the energy transition, Bonaire is striving for less reliance on the import of fossil fuels. With the current energy system, a significant share is generated using diesel generators. As a consequence, the electricity price is highly affected by the global oil price [36]. Due to these major risks to social, economic, and environmental vulnerability, there is an incentive to increase the share of RES on the island.

At the same time, the climate on the island offers many opportunities for the generation of wind and solar energy. As a result, Bonaire is aiming for higher penetration of RES in the energy system to be

able to provide reliable, affordable, and sustainable energy. First, since the island's location is near the equator and the tropical climate, there is a constant and abundant irradiance. Building on the success of the solar park pilot at Barcadera, the solar park has expanded its capacity to a 6MW [104]. Moreover, in July 2023 a BESS was installed in addition to the solar park [11].

Besides the installed solar park, Bonaire is planning to upgrade the 0.9MW wind turbines placed at Morotin. According to the plans, these wind turbines will be replaced by 2.3MW wind turbines, since it was earlier not possible to transport wind turbines of this size [36]. Currently, the permits are prepared for the deployment of these capacity upgrades of wind turbines.

1.2.3. Electricity Tariffs Bonaire

The energy system's electricity rates in Bonaire are fixed and will be semi-annually updated. For 2023, the electricity rates are 0.43 USD/kWh for the first half-year. The fixed cost of the connection to the grid depends on the peak capacity of the connection [112]. The fee for feeding a surplus of electricity back into the grid was in 2022 only 0.05 USD/kWh for households [27] [25] and for large connections (larger than 13 kVA) this is 0.01 USD/kWh [27]. When less electricity is consumed compared to the electricity fed back there is no remuneration [35], however, a feed-in tariff can be agreed upon through a contract for ancillary services to the grid. In case the feed-in of energy to the grid is not used as a supplementary energy source for own consumption but for energy production purposes, a permit is required by law [114].

Besides, the energy is generated by a single producer named Contour Global, while in the Netherlands there are multiple electricity producers. The regulations between WEB and Contour Global are reported using a Power Purchase Agreement (PPA). Since there is only one energy producer at Bonaire, electricity pride is controlled by a regulator. This regulator is named Autoriteit Consument en Markt (ACM). There are several reasons for the control of the tariff by the ACM [61]. First, the ACM is controlling the electricity price for consumer protection purposes, as the consumer has no choice of energy producer on the island. Secondly, it protects investors from unstable and unpredictable energy prices thereby reducing the investment risk. Lastly, due to the lack of concurrence, it stimulates the operation of business efficiently and ensures the quality of work.

1.2.4. Bonaire International Airport (BIA)

The only airport at Bonaire is Bonaire International Airport, which is also known under the name 'Flamingo Airport'. BIA can be characterized as a small airport containing only one runway [63]. Nevertheless, the airport is larger than the airports of Saba and St. Eustatius, and smaller with respect to the airports of Curaçao and Aruba. Regarding passengers arriving and departing from BIA, the airport is recovering from the impact of Covid-19. Since the number of passengers is mainly determined by tourism, the impact on the airport was significant. In 2021, the total number of passengers arriving was 129,000 and departing 127,000. With respect to 2020, this is an increase of 62%, although it is still 49% less compared to 2019 [3]. Pre-covid, in 2019, BIA handled around 150,000 regional passengers from the surrounding islands, Aruba and Curaçao [63].

The aviation industry is actively evolving in the Dutch Caribbean, as this industry is of vital importance for the economy, the transport of goods and persons, tourism, and hospital transport [50]. Therefore the six islands in the Dutch Caribbean are cooperating in the Dutch Caribbean Cooperation of Airports (DCCA). The first project of DCCA will be about the electrification of inter-island aviation, where the ambition is to daily operate multiple reliable inter-island flights (Aruba-Bonaire-Curacao and Saba-St.Maarten-St.Eustatius) within 2030 [3].
Also, the Dutch State is closely cooperating in the development of the airports. In the *Luchtvaart Nota* of the Ministry of Infrastructure and Water Management the long-term vision, policy, and guidance of the future of aviation in the Netherlands is stated, where it is mentioned that the State will invest in the aviation industry of the Caribbean [50].
Bonaire International Airport is comparable to WEB in its fundamental function of facilitating a service. WEB has to facilitate the distribution of electricity and BIA has to facilitate the air transport of passengers and goods. Because of this reason, the core values of BIA are comparable to WEB. BIA has the ambition to realize reliable, sustainable, affordable, and safe aviation at Bonaire according to the *Luchtvaart nota* and the DCCA cooperation [63] [3] [50].

With the objective of introducing EA at Bonaire, BIA is taking significant steps towards a sustainable aviation industry on the island. The sustainable impact of these aircraft is most effective when the aircraft are charged by RES. To align with this goal, BIA plans to install a solar park to cover a significant share of its own energy consumption, including the charging of electric aircraft. With this solar installation, BIA aims to reduce grid reliance. More sustainable developments of BIA at the land side are the implementation of EV chargers for car rentals and electric buses at the airport [3].
As aviation is of both economic and social relevance for Bonaire, maintaining the flight schedule with reliable electrified aircraft is essential. Therefore, to meet turnaround times and maintain the flight schedule, it is necessary to have a reliable supply of electricity to charge the aircraft. A BESS is considered by BIA for more effective use of solar energy, a more consistent energy supply, and reduced grid reliance. Additionally, BIA has an intention to feed electricity into the grid as this would be beneficial for the business case of the BESS as well as lowering its peak load costs. However, it is not favored by WEB to feed substantial amounts of excess electricity into the grid. Nevertheless, there can be opportunities to provide services by the BIA's BESS to the grid [50].
Third, the affordability of the flights is crucial for the local communities on the islands. Regional flights are of daily use for the working and social life of the Bonairian citizen. The DCCA is working on electric aviation between the islands as a public transport-like system [63] [3].
Lastly, the shift to electric aircraft would also need extra safety. Specific considerations include revised safety certification of electric aircraft, proper charging infrastructure, and the safe and efficient operation of aircraft at the airport. In addition, new staff should be educated to perform maintenance and operations on the aircraft and airport-related operations [63].
The core values of the BIA are summarized in table 1.3

Table 1.3: The core values obtained from the annual report, *Luchtvaart nota*, and DCCA of Bonaire International Airport summarized [3] [50] [63].

Core Values of BIA	
1. Sustainability	Both on land as well as on the airside BIA is actively developing sustainable projects. These sustainable developments are supported by both the Caribbean airports the cooperation DCCA, as well as the Dutch State.
2. Reliability	As the economy and the daily life of the people of the Caribbean depend on the aviation industry, a reliable inter-island air connection is necessary. In particular, for EA a reliable energy supply is needed to charge electric aircraft and maintain the flight schedule.
3. Affordability	Regional flights are of importance for the local community at Bonaire for working or social life.
4. Safety	For the introduction of EA at airports revised certification of aircraft, proper charging infrastructure, and educated staff for maintenance and other airport operations are needed.

BIA is actively engaged in the development of the airport and the expansion of the airport infrastructure, as has been formulated in Masterplan 2040 [3]. To finance this project, the Ministry of Infrastructure and Waterways has provided 15 million euros, and Bonaire financed 6.6 million euros. The total investment is estimated at 50 million euros for the project, taking into account the transition to electric aviation [88].
Key components of the Masterplan are the expansion of the current terminal building with a dedicated area increasing the capacity for arriving and departing international passengers at the airport. Secondly, new aprons will be constructed for handling international flights and large business jets, and current aprons will be reconstructed to meet the international requirements of the ICAO [3].
In addition to expanding international connectivity, BIA is also committing to the regional connectivity of the island with reliable and affordable flights. In April 2021, the six airports of the Caribbean Netherlands signed a cooperation agreement under the name Dutch Caribbean Cooperation of Airports (DCCA). This agreement aims to lead to benefits in terms of regulation, safety, innovation, and sustainability. One of the primary projects of the six islands is the introduction of electric aviation between the islands. The objective was to achieve these electric air connections within 10 years of the agreement. The electric air connections will be between Aruba, Bonaire, and Curaçao (the ABC-liner) and between St. Maarten, Saba, and St. Eustatius (SSS-liner) [3].

Lastly, as part of its commitment to sustainability and in alignment with the transition towards electric aviation, the airport is planning to install a solar park on-site [3]. A feasibility study of the 0.5 MWp-1.0 MWp solar park conducted by BIA and WEB will provide insight into the operation of the solar park. Potentially, in the future, this solar park will be scaled up and possibly can be used as an energy power plant with the possibility of assisting as an electricity generation plant for the grid.

1.3. Literature Review

This section discusses existing literature that is related to the academic field of BESS for electric aviation charging (EA) purposes.

First of all, a noteworthy contrast in the operational characteristics of energy systems for EV charging and EA charging was indicated by the studies of [41] and [54]. In these studies, it was argued that the EA needs a considerably larger power for charging to accommodate the short turnaround time of the current flight schedules. Furthermore, aviation is highly scheduled and centrally managed, hence the charging pattern is known more deterministically, while EVs have a custom-driver operation behavior. For these reasons, aviation experiences less uncertainty in demand and provides less flexibility compared to EVs. Therefore, studies on EVs can not be directly applied to EA.

The electrification of aviation is accompanied by an increased electricity demand profile due to the fuel shift from kerosene to electricity. When the electricity for EA charging purposes is all drawn from the grid, costly grid reinforcements are needed as emphasized by the study of [45]. In particular, this study focused on the future aviation electricity demand for a case study at O'Hare Airport Chicago to analyze whether the grid capacity is capable of handling the peak-power demand associated with hybrid electric aviation. The study concluded that significant grid upgrades are needed to handle the transition toward hybrid aviation.

The charging of electric aircraft will give rise to substantially higher peak power demand. As a consequence, several studies have focused on deploying a BESS to minimize the peak power demand related to aircraft battery charging. This is either done directly in [79], [54], and [46] by performing an optimization minimizing for the charging power. Conversely, other studies, such as [53], [108], [40], [91], and [12] approached this indirectly by minimizing the operational or total investment cost. In these cost-based optimizations, the price of peak demand of electricity or emissions fees of grid electricity usage were included. This penalizes the use of grid electricity or the magnitude of the peak load of your grid connection.

To minimize the power for charging, two strategies are being discussed widely in literature, the battery-swapping model and the plug-in recharge model for aircraft charging. The effect of these models on the needed infrastructure, costs, and peak power is compared by [53], [54], [108], [40], [91], and [12]. The research conducted by [40] proposed the battery-swapping model in combination with a solar park as an alternative to conventional plug-in charging. This concept relies on the ability to disconnect the aircraft's battery and replace it with a fully charged battery to ensure a short turnaround time resulting in lower charging powers required [54]. The disconnected spare batteries serve as a BESS, and as a result, no permanent stationary BESS is needed to cope with the peak powers [108]. However, due to the relatively novel technology of battery-swapping, the battery-swap charging strategy requires extra complexity in battery replacement and charging schedule. Besides, with battery swap more standardization and extra constraints are imposed on battery and aircraft design [58] [108] and the implementation involves substantial investments [12]. It was concluded by the study of [40] that the battery-swapping charging method was only cost-effective for an electric aircraft penetration of less than 10%.

The feasibility of on-site generation of solar energy to enable charging aircraft with sustainable energy has been analyzed in [79], [40], and [41].
The research of [79] identifies the available area for a solar park for multiple airports to supply energy for charging electric aircraft at the airport. It was concluded that a standalone solar park was not capable of supplying energy during the entire day and providing the needed peak power. Therefore the research

recommended exploring other renewable energy sources or directly drawing from the grid. Moreover, according to this research, one may also consider the storage of the excess energy produced by the solar park to time-shift the electricity. This will result in an effective use of solar energy for EA to ensure an environmental impact will be made with the transition to EA.

As stated by [79] on-site PV generation and a BESS could be a promising combination for enabling EA. Therefore, the research by [40] considers the integration of a solar park and a BESS to power the batteries of electric aircraft. The least-cost solution was examined, where the energy system has the ability to feed electricity into the grid. The grid interaction generates extra revenue by arbitrage due to fluctuating electricity prices during the day.

Furthermore, a study by [41] delved into the interaction of aircraft batteries and the grid. Ancillary services to the grid are provided by the battery energy system through real-time balancing of the grid with primary and secondary frequency responses. However, the energy is provided for 15% by a solar park, for 50% by a gas turbine, and the remainder is drawn from the grid. This study also incorporated the swapped batteries of aircraft.

Article	Optimization	BESS	Solar	Conclusion and Comments
[45]	No	No	No	Hybrid aircraft increases electricity demand significantly Substantial grid upgrades needed at O'Hare Airport
[79]	No	No	Yes	A solar park to reduce grid impact, but does not suffice for increased electricity demand BESS recommended
[54]	Cost of electricity and capital expenditures	Swapped batteries	No	Significant reduction in power and cost with battery swapping compared to plug-in for electric aircraft charging
[46]	Peak power	No	No	By rescheduling flights significant power reductions can be achieved. Hybrid aircraft used
[53]	Energy expenditures	Swapped batteries	No	Cost reduced with optimization of charging schedule as well as power demand. Also compared to fossil-fueled aircraft cost reductions.
[108]	Capital and operational cost	Swapped batteries	No	Simultaneous use of swapped batteries and plug-in chargers for hybrid recreational aircraft in Milan and for large airport at Athens Degradation based on cycle life included
[40]	Capital and operational cost	Swapped batteries/ stationary battery	Yes	Assesed for different penetration levels of EA High penetration level plug-in more economic Neglecting aircraft type and distance A fixed electricity demand Generate revenue by feed-in electricity.
[91]	Capital and operational cost	Swapped batteries	No	Simultaneous use of plug-in and battery swap Higher charger power leads to higher grid peak but lower cost. Grid interconnection of batteries recommended
[41]	Operational cost and revenue	Swapped batteries	Yes	Revenue primary and secondary frequency response Hybrid 180 passenger with battery swap Electricity supply of PV and gas turbine
[12]	Investment infrastructure aircraft and operational cost	Swapped batteries	No	Hybrid aircraft for recreational aircraft Implementation cost recovered by fuel savings Aircraft, batteries and electricity main cost drivers

1.4. Knowledge Gap

Evaluating the previous work done in the academic field of BESS used for EA, extensive work has predominantly focused on BESSs used for the minimization of the electrical power on the grid or the cost-optimal solution of a BESS.
Secondly, comparatively little research has been done on stationary on-ground BESS, while much research was concentrated on battery swapping for charging purposes. Therefore, this study focuses on:

- Much research was done on either a BESS controlled for power minimization or cost minimization

for EA charging purposes. However, a study evaluating and comparing the optimization of different control strategies of stationary BESSs for EA charging purposes is lacking.
- While prior research focused on results in terms of either the costs or grid impact of a single BESS control strategy, this study will explicitly analyze for each control strategy multiple performance indicators: the impact on the local grid in terms of voltage fluctuations, distribution grid cable load, and the transformer (over)load. Moreover, the change in CO_2 emissions from grid electricity, and the LCOE of the airport's system are determined.
- As there is a lot of uncertainty in the future of EA, this study will include scenarios that will be analyzed on the threefold performance indicators. This identifies the sensitivity of each control strategy for input data and parameters that will potentially change in the future.
- Lastly, this study will use data from the particular case study of Bonaire. Bonaire International Airport distinguished itself by having a flight schedule predominantly covered by small regional aircraft. As this type is expected to be the first aircraft to be electrified, the charging power of these electric aircraft will dominate the total load profile of the airport. Conversely, prior research focused on large airports such as London Gatwick and O'Hare Airport which typically have a more diverse aircraft fleet.

1.5. Research Aim

This research is performed for the particular case of Bonaire. The primary objective of this report is to gain insight into how Bonaire International Airport can effectively control its BESS to be able to cope with the increased electricity demand profile resulting from the adoption of electric aircraft. This objective is evaluated by considering the main interests of the WEB and BIA: the impact on the grid infrastructure, the CO_2 emissions, and the LCOE of the airport's system.

Specifically, the impact on the grid is of major concern for the grid operator Water- en Energiebedrijf Bonaire (WEB). WEB has the challenge of maintaining grid stability at the islanded microgrid of Bonaire. This is of interest to WEB as costly grid infrastructure upgrades can lead to substantial increases in electricity costs for the Bonairain citizens. Also, WEB stands benevolent to work on the energy transition and reduce the CO_2 emissions.
On the other hand, Bonaire International Airport will install an on-site solar park to reduce its CO_2 emissions. This study aims to gain insight into the effect of different BESS control strategies in combination with the solar park on the reduction in LCOE and CO_2 emissions compared to the Business-as-Usual case.
Ultimately, this study ends with a conclusion in terms of the three performance indicators that can be used to assess to what extent the interests of both stakeholders are met.

1.6. Research Question

'What is the effect of different control strategies of a BESS on the technical, economic, and environmental performance so that it can facilitate both the grid operator and the airport to enable electric aviation?'

The following sub-questions are supportive of answering the main research question.

1. *How can the electric aircraft charging demand be computed and incorporated into the energy demand profile of the airport?*

2. *What is the effect of the electricity demand profile including electric aircraft charging of the airport on the voltage fluctuations, the distribution grid cable load, and the transformer overloading without a BESS?*

3. *What is the contribution of a BESS to the technical performance, the LCOE, and the CO_2 emissions from grid electricity of the system compared to the case without a BESS?*

4. *How sensitive are the results of the performance indicators to changes in input parameters and data for future scenarios?*

2

Theoretical Background

This Chapter discusses background theory regarding the relevant topics of the academic field of electric aviation 2.1, the renewable energy in the energy system and the grid 2.2, the BESS control strategies 2.3.

2.1. Electric Aviation

This section aims to set out the main challenges of electric aviation. Subsequently, small electric aircraft designs are reviewed.

2.1.1. Challenges of Battery Electric Aviation

Currently, electric and hybrid aircraft technology is evolving and multiple projections and timelines are proposed for the commercialization of electric aviation [8]. However, for the realization of commercial electric aviation, critical battery specification developments have to be made regarding the battery-specific energy (BSE), battery-specific power (BSP), the cycle life of the battery, cost, and safety [111]. Furthermore, the source of electricity used to power electric aircraft is of importance to ensure that the electrically powered aircraft have an environmental impact [1]. In this section, these challenges will be discussed.

A major share of an aircraft's energy consumption is attributed to the mass of the aircraft. The energy density (kWh/kg) of the state-of-art batteries is significantly lower than the energy density of kerosene [30]. Consequently, the aircraft's mass and therefore the required energy is substantially higher for battery-powered aircraft. For this reason, the energy density of batteries is the limiting factor of the passenger load and the operating range of the aircraft [43]. The relation between those parameters is defined by the Breguet range equation which is shown in equation 2.2 for electric aircraft, and in equation 2.1 for the conventional kerosene-fuelled aircraft [43] [14].

$$R_{\mathrm{f}} = \frac{\mathrm{L}}{\mathrm{D}} \eta_{\mathrm{p}} \eta_{\mathrm{tr}} \eta_{\mathrm{ther}} \frac{\mathrm{SE}_{\mathrm{fuel}}}{\mathrm{g}} \ln\left(\frac{1}{1 - \frac{\mathrm{m}_{\mathrm{fuel}}}{\mathrm{m}_{\mathrm{TO}}}}\right) \tag{2.1}$$

where, $\frac{\mathrm{L}}{\mathrm{D}}$ denoted the lift-to-drag ratio, η_{p} is the propulsion system efficiency, η_{tr} is the transmission efficiency, and η_{ther} represents the thermal efficiency of the engine. $\mathrm{SE}_{\mathrm{fuel}}$ is defined as the SE (Specific Energy or energy density) of the fuel and g is the gravitational acceleration. $\frac{\mathrm{m}_{\mathrm{fuel}}}{\mathrm{m}_{\mathrm{TO}}}$ represents the ratio of the fuel weight to the take-off gross weight, which is the total weight at which the aircraft is permitted to take off. This includes both the payload mass and the fuel mass.
For the electric aircraft, the Breguet range equation is slightly modified to incorporate the electric energy supply of batteries [14].

$$R_{\mathrm{electric}} = \frac{\mathrm{L}}{\mathrm{D}} \eta_{\mathrm{p}} \eta_{\mathrm{tr}} \eta_{\mathrm{ther}} \frac{\mathrm{SE}_{\mathrm{fuel}}}{\mathrm{g}} \frac{\mathrm{m}_{\mathrm{battery}}}{\mathrm{m}_{\mathrm{TO}}} \tag{2.2}$$

in this equation, the stack-up battery's efficiency is represented by η_{el}. $SE_{battery}$ is defined by the battery energy density. $m_{battery}$ is the mass of the battery.

Clearly, one of the most deciding specifications of a battery to enable the breakthrough of electric aviation is the energy density (or battery specific energy (BSE)). As became evident from the Breguet range equation, the BSE directly dictates the range and passenger load [14]. Currently, the electric vehicle (EV) market is dominated by lithium-ion batteries, which typically have a BSE of 250-300 [8]. While state-of-art lithium-sulfur batteries already achieved higher BSEs up to 600 Wh/kg [120]. For comparison the specific energy of current jet engine fuel is 12000 Wh/kg, so the effective specific energy including an assumed engine efficiency of 50% is 6000 Wh/kg [30]. Therefore, significant improvements are required in specific battery energy for all-electric aircraft to compete with conventional jet engines for long-haul flights and heavy payloads.
Since the BSE is a critical technological bottleneck for electric aviation, the development and future prospects of this battery specification are summarized in table 2.1. The key takeaway from the table is that there is an increase in energy density expected, although according to these predictions, it is unlikely that the battery energy density will compete with the energy density level of kerosene.

The second challenge as introduced by the Breguet range equation in 2.1 and 2.2 is the aircraft weight. The weight of the aircraft can result in significant load differences during flights, in particular for long-range [14].
First, batteries for electric and hybrid-fuelled aircraft are designed for a fixed distance and so the required battery weight is tied to this design range. Consequently, electric aircraft operating on distances shorter than the design range carry unused battery mass, while a conventional aircraft can be fuelled optimally based on the distance [43].
Moreover, depending on the range, the weight of a fuelled aircraft can decrease between 5-40% during a flight due to fuel consumption [111]. This weight reduction is not applicable to electric aircraft using batteries [14]. Therefore, the second part of the equation 2.2 is different from the second part in equation 2.1 to include the mass reduction during flight for fuel-burning aircraft.
Another weight challenge is the unfavorable reserve capacity requirements for short-range flights as this decreases with increasing range [14]. Lastly, the mass of the electric drives is much heavier when scaled to large planes, therefore this also creates a challenge for larger aircraft to develop low-mass electric drive trains at this scale [111].

The third and last main challenge in developing all-electric aircraft is the Battery Specific Power (or power density, BSP). An all-electric aircraft relies on batteries and electric motors to power the aircraft during all phases of flight. High power is mainly used during takeoff and climbing to flight altitude [105]. The power in different flight phases of a 150-passenger aircraft is depicted in figure 2.1.
The necessity for high BSP can be mitigated when using a hybrid configuration. This configuration will significantly lower the required BSP as in hybrid configuration the power of the fuel is an additional power source and therefore the battery does not need to take up all the required power [72].
BSP of state-of-art lithium-ion batteries ranges between 0.5-2 kW/kg [121] as can be seen in table 2.1. The BSP is constrained by the surface area, therefore it is not likely that the BSP will scale with BSE since the energy is more related to the volume of the battery [39].

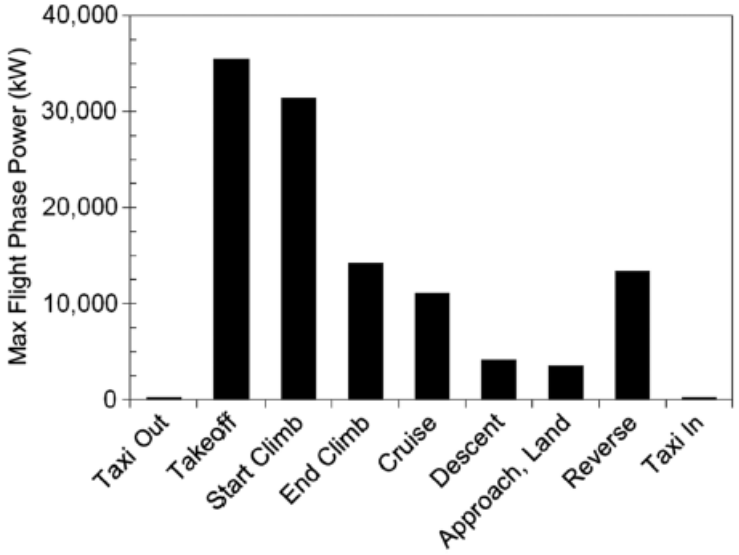

Figure 2.1: Power required for 150-passenger single-aisle aircraft during the different flight phases in the trajectory of an 1850 km mission [30].

The state-of-the-art Li-ion batteries have a minimum cycle life of 1000 cycles, and depending on the usage this could be up to 10000 [4] [33]. If it is assumed that the battery will be discharged to the maximum allowed depth of discharge for a flight, and an average of five flights a day, the lifetime of the battery of the aircraft would be 200 days, which makes it a costly operation [65].

The replacement of kerosene with electrically powered aircraft does not necessarily result in reductions in GHG emissions [1]. The environmental impact of the electrification of aircraft depends on the source of electricity, and so determines if carbon emissions are reduced with electric aviation. The exact reduction depends on the energy sources, the emissions regarding fuel production, transmission- and grid losses, and the lifetime assessment of the battery production and disposal [14]. In case the electricity for charging electric aircraft is not generated from renewable energy sources, the emissions are shifted to the power plant and the objective to reduce emissions in aviation will be risked [119].

Lastly, there are more challenges regarding the enabling of electric aviation. For example, the behavior of batteries in a different environment (temperature and pressure at flight altitude) [111], the inclusion of high voltage systems in aircraft, and requirements related to the thermal management [16]. Moreover, on-ground services like the airport and the electricity grid operator should prepare for the transition to electric aviation. The airport needs charging infrastructure and a renewed flight schedule due to the imposed charging times. Moreover, these electric aircraft increase the electricity demand of the airport and possibly this would require a significant capacity improvement of the grid connection [46] [53].

As the breakthrough of EA faces some challenges regarding the batteries used in the aircraft, a table is provided with the state-of-art and future prospects of the challenging battery specifications. It should be noted that BSE and BSP are often expressed on the battery cell level or on the battery pack level and are not always clearly mentioned. This can significantly influence the value of the density [78].

Table 2.1: This table provides the state-of-art battery technology and future prospects among batteries possibly used for electric aircraft [43]. The specific energy, power, and cycle life are included in this table. In the footnotes, the explicitly mentioned time horizon of the prospect is added.

Technology	Specific energy (Wh/kg)		Specific power (MW/kg)		Cycle life (cycles)	
	State-of-Art	Future	State-of-Art	Future	State-of-Art	Future
Li-ion	150-200 [97] 160 [95] 80-200 [121] [26] 100-265 [5] 200 [43] [98] 140-240 [115] 250 [47] 250-300 [8]	400[b] [26] 450[d] [26] 300 [66] 400-450[a] [5] 350 [a] [47] 500[b] [47] 400[c] [9]	1.8 [95] 2 [105] 1.2 [39] 0.5-2 [121] 0.25-0.34 [22]		300-1000 [97] 1000 [65] 3000 [121]	
Li-S	350-600 [22] 250-300 [26] 160-350 [115] 500 [71] [98] 300-600 [120]	200-700 [97] 500-650[b] [26] 800-950[d] [26] 600-700 [66] 500-1250[a] [43] 500-600 [115]	1 [71]		<200 [97] 100 [22] <300 [66] 100 [120]	1000 [98]
Li-air	300-350 [26]	600-750[b] [26] 1200-1400[d] [26] 900-1000 [66] 750-2000 [102] 1700 [37] 800-1750[a] [43] 2000 [52]		400-640 [52]	50 [26] [57] limited [66]	500 [52]

[a] = prospect for 2025, [b] = prospect for 2030, [c] = prospect for 2035, [d] = prospect for 2045. The prospect differs from each other since the sources are published in different years, nevertheless, it indicates the trends of battery development. Lastly, the future values with no footnote represent general future forecasts with no explicitly mentioned year.

2.1.2. Electric Aircraft Designs

This section reviews small electric aircraft designs. These aircraft designs can potentially be aircraft suitable to replace flights in the current flight schedule of BIA. The expectation is that small regional aviation is the first type of aircraft on which the electrification of aircraft can be realized [43]. All the all-electric and hybrid aircraft are turboprop aircraft as electric jet engines are still in the first stage of development [83]. Therefore, the focus here is on aircraft operating on a regional scale and are propeller-driven.

Alice by Eviation

The aircraft named Alice is in development by the Israeli company Eviation. Alice is able to transfer 9 passengers excluding the crew over a distance of 815 km without payload, a 30-minute reserve, and no headwind [69]. When considering this, the aircraft range is 460 km (250 nm). The aircraft will be able to cover this distance with a cruising speed of 410 km/h, and a maximum operating speed of nearly 480 km/h (260 knots) [31]. The Maximum Takeoff Weight (MTOW) or Gross Takeoff Weight (GTOW) of Alice is around 8,350 kg (18,400 lbs) of which almost 1,134 kg (2,500 lbs) is accounted for payload. The two electric-propelled engines of 700 kW are powered by a lithium-ion battery with a usable capacity of 920 kWh [5] [31]. Eviation expects to receive certification from the United States' Federal Aviation Administration (FAA) by 2025 and enter the commercial market in 2027 [32]. Cape Air and the Germain air operator Evia Aero ordered Alice aircraft as DHL did for a cargo variant [32] [69].

P-VOLT by Tecnam

Another nine-seater aircraft is the P-Volt designed by Italian aircraft manufacturer Tecnam. As stated by [82], although unofficially published, the range of the P-Volt with the current battery technology is 157 km (85 nm), and with improved battery technologies by 2030 this range increases to 269 km (145 nm) accounting for an 1100 kg battery pack. The MTOW of P-Volt is 4086 kg where 809 kg is taken up by usable payload. Lastly, the aircraft is powered by two 320 kW electric motors.
P-VOLT also experiences interest from orders by airliners. Tecnam received orders for the P-Volt of the

Norwegian regional carrier Widerøe. Since nearly three-quarters of the flights operated by Widerøe is less than 275 km, the P-VOLT will be used [5].

ERA by Aura Aero
The design of Aura Aero is the 19-passenger ERA, which is an electric regional aircraft. According to the expectation the first flight will be in 2026, and it is aimed to enter into service by 2028. The MTOW is 8,600 kg, where it is allowed to board 19 passengers accounting for 1,710 kg. Without a payload boarded, the maximum range of ERA is 1482 km (800 nm), while with payload this significantly reduces to 370 km (200 nm) [7].

ES-19 by Heart Aerospace
The ES-19 is developed by a Swedish start-up named Heart Aerospace with the objective to get all needed aircraft certifications and commercialize the all-electric 19-passenger aircraft by 2026 [32]. This aircraft has a Maximum Takeoff Weight (MTOW) of 8618 kg with the battery weight accounting for 3000 kg [15]. The ES-19 will not have any operational emissions, have lower operational costs compared to similar-sized conventional aircraft, and will also produce less noise. The operation range of the aircraft is 400 km and is able to fly with a cruise speed of 300 km/h. This will be powered by 4 electric motors of 400 kW each and 4 batteries of 180 kWh each [5]. The ES-19 provides favorable opportunities for small regional airports due to the obtained STOL (Short takeoff and landing) certification, which states that the aircraft is able to operate on runways of 750 m or longer [32]. The ES-19 has been ordered several times, including by Finnair for 20 aircraft, and by Mes Airlines for a fleet of 100 aircraft [69].

ES-30 by Heart Aerospace
Heart Aerospace is also testing a 30-passenger aircraft which is claimed to be operational in 2028. The all-electric configuration of the aircraft is able to operate on a 200 km range which is expected to increase to 300 km and 400 km in the mid and late 2030s. The hybrid configuration is able to operate on a 400 km range. The ambition of the manufacturer is to operate the aircraft with a turnaround time of 30 minutes with a fast charger [2]. The total mass of the aircraft will increase to about 20-21 tons and the battery pack will have a mass of approximately 5 tons. The total battery capacity of the aircraft in full electric configuration is expected to be 2000 kWh [42]. Lastly, Heart Aerospace also claims to be working on a 50-passenger configuration [80].

2.2. BESS and the Energy System

The adoption of renewable energy sources (RES) in the energy system plays an essential role in the energy transition. This section describes the challenges involved with the increased adoption of RES in the energy system, the role of a BESS in combination with RES, and the effect of control strategies on the grid, associated costs, and environmental impact.

2.2.1. Renewable Energy Sources in the Energy System

One of the primary challenges with RES is the intermittency and non-controllability in the generation of electricity [29]. Since RES relies on weather conditions the energy output can not be predicted accurately for long-term periods [4]. Due to abrupt and unforeseen changes in energy output, the real-time generation of electricity based on RES can complicate the real-time balancing of supply and demand, especially with a growing share of RES [29].
Grid congestion forms another effect of the increasing share of RES. Grid congestion is the event of reaching or exceeding the transmission capacity of the local grid, restricting the electricity transmittable. This challenge arises as renewable energy is generated more decentralized, unlike conventional power plants that are typically centralized [92]. With the decentralized energy generation, the local grid is not designed for a high capacity resulting from the variable renewable energy power output. Grid congestion can occur on both the supply side as excess electricity is fed into the grid as well as on the demand side as a consequence of increased electricity demand. A conventional approach to avoid grid congestion was by upgrading the grid capacity. However, grid capacity expansion is a time-consuming project, with high capital expenditures involved, and faces land and resources restrictions [119].

A third challenge arising from the growing share of RES is the fluctuations of voltages due to variable feed-in of electricity generated by RES [93]. A sudden peak of electricity feed-in into the grid increases the voltage while sudden peak loads in electricity demand decrease the voltage. The voltage fluctuations are caused by imbalances of supply and demand and can affect equipment.

2.2.2. BESS and Renewable Energy Sources

A suitable solution for the challenges of real-time supply and demand balancing, grid congestion [92] [13], and voltage fluctuations [93] is a battery. The use of a BESS as a solution for these challenges is addressed in this section. However, first, the working principle of a BESS is explained.

Batteries are a relatively mature energy storage technology [4], and are one of the oldest forms of electricity storage [19]. A simplified illustration of a battery setup is depicted in figure 2.2. A battery consists of one or multiple electrochemical cells, each of which is composed of electrolytes (or separators), either in a liquid, solid, or paste form. The electrolyte of the battery separates positive and negative electrodes from each other. When discharging a battery, an oxidation-reduction reaction occurs at the electrodes resulting in a flow of free electrons through an external circuit.
The basic working principle of a battery during discharge is as follows. At the anode lithium ions and free electrons are formed by an oxidation reaction. Positively charged lithium ions flow through the electrolyte (in figure 2.2 the separator) while free electrons flow through an external circuit and recombine at the cathode in a reduction reaction. During the discharge period, free electrons flow from the negative electrode (anode) to the positive electrode (cathode) through the external circuit causing an electric current [60].

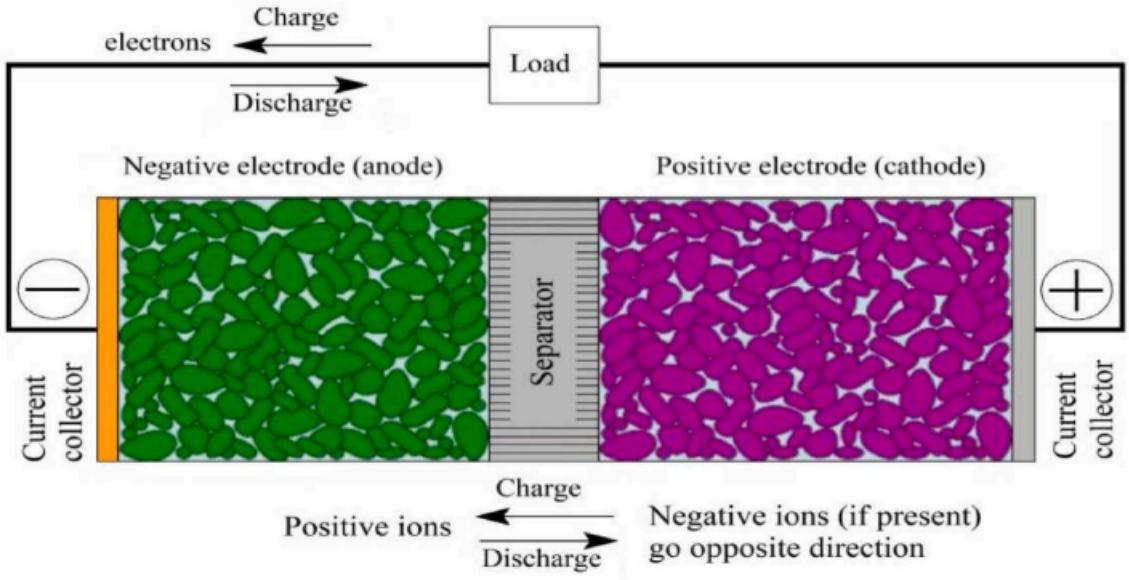

Figure 2.2: Battery setup of a Li-ion battery. During discharge, at the anode, the reduction occurs, while at the cathode, and positive electrode, the oxidizing reaction occurs. The electrons flow through an external circuit from the anode to the cathode [60].

The first addressed problem, the real-time balancing of the grid, requires rapidly responding power sources [33]. The conventional approach to meet electricity demand and to ensure the reliability of real-time balancing is the use of diesel generators or other fossil-fuelled-powerplants which are controllable power plants, in contrast to RES. These power plants are capable of responding to mismatches in supply and demand. A BESS can act as a suitable substitution for these conventional power plants since a BESS is able to rapidly response to mismatches in supply and demand, even more rapidly than the conventional power plants [13] [33]. In case of a deficit in the supply of renewable energy to meet demand a BESS can discharge, or in case of an excess of generated renewable energy a BESS can charge. In the absence of a

battery, the excess generated energy of RES would be curtailed, leading to the waste of sustainable energy.

The second challenge involves the risk of grid congestion. During periods of grid congestion, a BESS is able to shift the production of electricity in time to periods of more available grid capacity. This results in a more flat grid capacity occupation, and is also known as *peak shaving* or *peak shifting* [21]. Traditionally, the transmission and distribution grid must be sized according to the highest peaks in the year, which only occur several times a year. The use of batteries can significantly lower the needed peak capacity of the transmission and distribution grid [13], thereby reducing the risk of energy losses by curtailment and over-investments of grid infrastructure [55].
The principle of peak shaving is shown in figure 2.3, where peak-hour electricity can be shifted to the off-peak periods. The use of a BESS can therefore facilitate the efficient use of the grid capacity and the generation of sustainable energy.

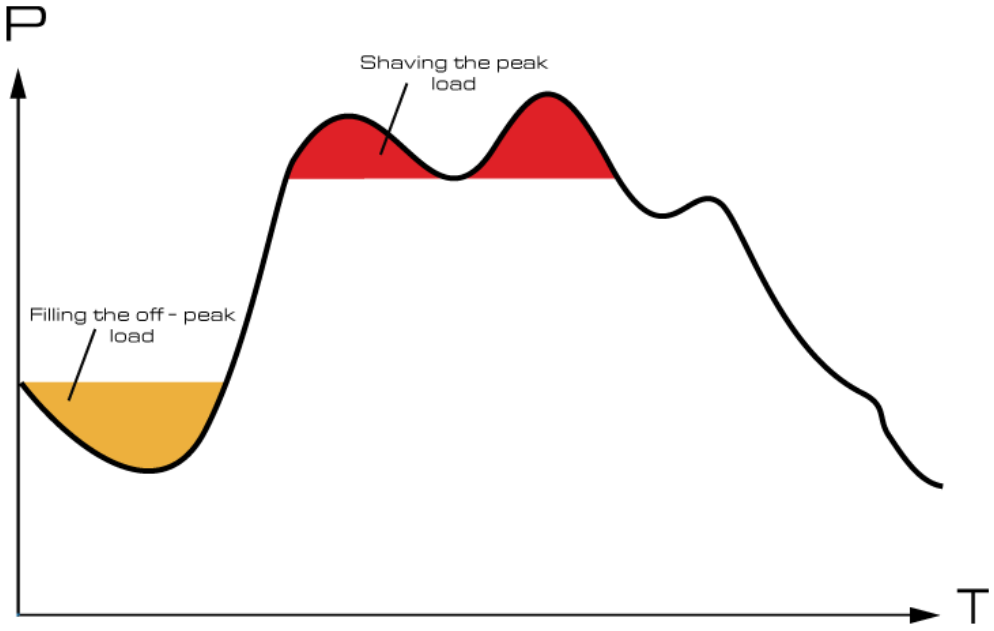

Figure 2.3: The principle of peak shaving, where the shaded areas correspond to electricity volume. The red area is stored to reduce strain on the grid. With the storage of electricity, a BESS is able to shift the peak in time to the off-peak hours. The energy released during off-peak hours is shown by the orange area [96].

Moreover, the last issue with RES is the voltage fluctuations due to the peaks of electricity feed-in. As a BESS is able to rapidly respond to fluctuations of the RES, the BESS is capable of performing voltage and frequency regulation [33]. The mismatch of supply and demand balancing is strongly reflected in the voltage of the grid. A BESS can be an effective solution for real-time balancing of the grid and thereby regulating the voltage of the grid [33].

2.3. Control Strategies BESS

Three key control strategies are discussed in this section: Self-Consumption, Peak-Shaving, and Cost-Optimal. Each of the control strategies has an impact on the technical, economic, and environmental effects.

Self-Consumption

The first control strategy under consideration is Self-Consumption, which seeks to maximize the on-site consumption of PV electricity. The Self-consumption is defined by 2.3 [64][44]:

$$\text{Self-consumption} = \frac{\text{On-site consumed PV electricity}}{\text{Total generated PV electricity}} \tag{2.3}$$

Interpreting this definition, the Self-Consumption of PV electricity without a BESS is determined by the instantaneous overlap of PV generation and demand. The deployment of a BESS allows temporary storing and shifting of PV electricity to obtain a higher fraction of on-site consumed PV electricity thereby increasing the fraction of Self-Consumption [44]. In the context of electric aircraft charging, a high Self-Consumption ratio potentially leads to charging electric aircraft with a higher proportion of sustainable energy causing a more effective usage of electric aircraft with a sustainability standpoint.
However, it should be noted that the capacity of the solar park should be compared relative to the total demand to interpret the Self-Consumption ratio correctly. In cases where a solar park's capacity is relatively small compared to the total energy demand, the Self-Consumption tends to be higher. Conversely, an oversized park where the excess of renewable energy is fed into the grid or discarded, results in lower Self-Consumption ratios. Nevertheless, this can be assessed with another ratio as defined in equation 2.4, the Self-Sufficiency ratio:

$$\text{Self-Sufficiency} = \frac{\text{On-site consumed PV electricity}}{\text{Total load demand}} \tag{2.4}$$

The Self-Consumption control strategy offers several advantages in economic, technical, and environmental terms. The on-site utilization and storage of PV electricity are economically attractive in case of a large price gap between the electricity purchase price and the feed-in tariff [59] [67].
From a technical perspective, the Self-Consumption control strategy of a battery leads to more independence of grid electricity [44]. With a high Self-Consumption, less electricity is taken from the grid which translates to a reduced reliance on grid electricity [103]. Consequently, an environmental impact is achieved as this reduced grid reliance results in diminished CO_2 emissions originating from grid electricity [59].
However, a downside of the Self-Consumption control strategy is that commonly batteries reach full capacity before noon, which coincides with the PV peak-power generation, providing no advantage regarding the peak power injection into the grid. Nevertheless, the integration of intelligent forecast algorithms batteries enables BESS to reduce the peak power injection by charging the battery during peak power generation periods [67].

Peak Shaving

The second considered control strategy is Peak Shaving, where the BESS actively manages to mitigate high peaks on the grid. In the context of EA, these peaks are primarily related to the charging of electric aircraft, and the BESS supports to cope with the high power demand for aircraft charging. Numerous studies [109] [103] [86] highlighted several technical, economic, and environmental advantages associated with Peak Shaving.

Peak Shaving can contribute to maintaining the balance between electricity generation and demand. In scenarios where this is not perfectly matched, the imbalance can lead to problems such as grid instability, voltage fluctuations, and even complete blackouts [109].
Moreover, efficient utilization of the existing grid capacity is achieved. A commonly used metric for the grid capacity utilization is the load factor: $LF = P_{avg}/P_{peak}$. This results in postponing costly grid infrastructure upgrades [86]. A low load factor represents a highly variable load profile. A high load factor is essential for the economic feasibility of the asset as this results in lower cost [109].
Furthermore, peak loads are a threat to the system's efficiency. High peak loads are associated with high currents. The grid efficiency is affected by the high currents as the power losses are nonlinearly related to the current. Reduction of peak power contributes to an increasing system efficiency [109].

In addition to the technical contribution of Peak Shaving, a BESS can yield economic advantages. The conventional approach for handling peaks was increasing the capacity of the system components [109]. This often leads to underused reserve capacity resulting in higher capital investment costs for the grid operator. Peak Shaving offers a more cost-effective usage of the grid capacity by effectively using

the existing infrastructure [86] [109]. Additionally, peak loads accelerate the degradation of the system components thereby increasing the maintenance costs [86]. Therefore, Peak Shaving is advantageous for delaying grid infrastructure upgrades and the associated costs [103]
The economic benefit of Peak Shaving extends to the generation of electricity as well. Diesel generators are often used during peak hour demand in isolated electricity grids. These power plants typically possess expensive operation and maintenance costs [109]. Secondly, the cost of electricity of the peak hour plants tends to be more expensive than the baseload plants to be able to recoup the investment costs during the limited active hours [109].

Lastly, from an environmental perspective, Peak Shaving can lead to less utilization of peak generators [109]. While peak shaving, a more constant load on the grid is maintained, and thereby there is less reliance on diesel generators needed during peak hours, resulting in diminished CO_2 emissions [86].

Cost-Optimal

The final control strategy is the Cost-optimal BESS strategy which aims to optimize the operational costs associated with the system.

The BESS is capable of shifting the intermittent PV electricity in time by alternately charging and discharging electricity. This allows a BESS to benefit from fluctuating energy prices, which potentially enhances the economic performance of the BESS through energy arbitrage [87].
However, it is essential to note that with a constant feed-in tariff and electricity purchase price the energy arbitrage opportunities are eliminated. As a result, a constant purchase price and feed-in tariff of electricity cause higher lifetime costs of a PV-BESS combination in comparison to a fluctuating or a time-of-use electricity pricing scheme [118].
Nevertheless, the electricity surplus can be sold to the grid generating revenue. In case the electricity market is limited by a constant pricing scheme, the BESS acts by increasing its Self-Consumption due to the price incentive of the low feed-in tariff compared to the electricity purchase price [70].
Moreover, with the costs associated with PV electricity generation often being lower than grid electricity costs, Self-Consumption is even more economically attractive. Consequently, with increased Self-Consumption the stress on the electricity grid lightens [118], thereby enhancing the technical performance as was explained previously.

Lastly, the Cost-Optimal strategy of the BESS can contribute in terms of technical performance. As the costs of the peak price can cover a significant share of the total electricity costs, the monthly price paid for the maximum peak load on the grid at Bonaire is included in the optimization. Including the price for the peak power in the optimization creates a financial incentive to reduce the peak on the grid, thereby reducing the associated issues with high peaks on the grid [91].

2.3.1. Battery Performance and Degradation

Battery aging is the irreversible degradation of the battery's usable capacity and power. The degradation is caused by complex interactions at the cell level, therefore accurately predicting and determining the aging of a battery is very complex [23]. Although, battery degradation can roughly be divided into two parts. Calendar aging occurs when the battery is idling (inactive) and cycling aging occurs during operations (charging or discharging) [100]. The degradation when idling is affected by the operating temperature of the battery, at the state-of-charge (SOC) level, and the elapsed time. While for cycling degradation the power, depth of discharge (DoD), and heat generation are also of importance [23]. However, in the study of [100] it is assumed that the temperature is kept constant at 25 C°as this is beneficial for the lifetime and ensures the optimal performance of the battery.

3
Methodology

This chapter aims to explain the methodology of the research. First, in section 3.1 the method to approximate the electricity demand of electric aircraft will be presented. Subsequently, in section 3.2 the impact on the grid of the total load profile of the airport is discussed. In section the method for the third sub-question is explained where battery control strategies are modeled. These control strategies will be analyzed for performance indicators that are relevant for both stakeholders, which are presented in sections 3.3.4, 3.3.5, and 3.3.6. Lastly, in section 3.4 the sensitivity of the control strategies of batteries to changes in data and input parameters of future scenarios is analyzed.

3.1. Electricity Demand Profile Electric Aviation

First of all, the electricity demand for electric aircraft at BIA is approximated. Some assumptions or approximations of parameters have to be made based on other aircraft as some parameters are not public for electric aircraft designs. However, some aircraft have already made a testing flight [31]. Therefore, these parameters will be more realistic. In Chapter 2 a pre-study as background information was done for electric aircraft design.

3.1.1. General Assumptions on Electric Aviation

To be able to calculate the electricity demand for electric aircraft and construct the charging load profile for BIA, some assumptions are made regarding electric aviation:

- In the current flight schedule, only conventional aircraft that have similar passenger capacity to the electric aircraft designs are replaced.
- The claimed parameters of the electric aircraft by companies are used for calculations. In case a parameter is not known, a general assumption is made based on comparable aircraft or assumptions from the literature.
- The current flight schedule will be used and maintained. This means that the number of flights, the destinations, the time of arrival and departure (and so the charging time), and the passenger capacity are maintained in this research.
- The studied electric aircraft are designed for a specific operating range and thereby for a specific battery capacity and weight. However, the aircraft in this research will be charged according to the energy needed for the distance of the trip. Therefore, it is not necessary to use all of the battery capacity for the trip of the aircraft. This can lead to redundant transported battery mass and inefficient energy consumption.
- The departure time of the current flight schedule is rounded to the nearest 15 min as the model runs on 15 min-base. This results in a turnaround time for the aircraft of 30 minutes which is the available charging time.

3.1.2. Current Flight Schedule

The current flight schedule is obtained from `flightrader24.com` [34]. A typical departure schedule on Tuesday is seen in figure 3.1 for different aircraft types. From the current flight schedule, small aircraft that are feasible to be replaced by an electric aircraft will be filtered. In this case, the Boeing 787-8 and the Airbus are too large for electrification and are discarded from the flight schedule.

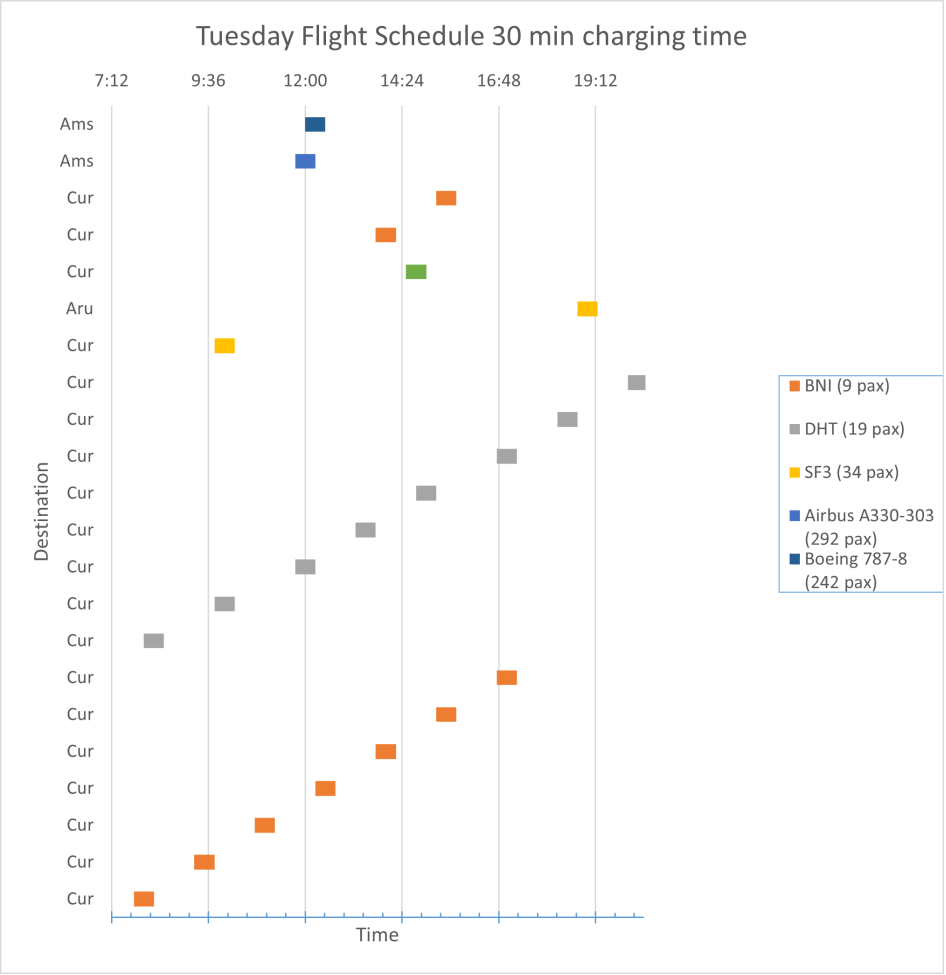

Figure 3.1: Schedule of BIA on a typical Tuesday with on the y-axis the destination and on the x-axis the time of the day. The charging time is assumed to be 30 minutes. So this table provides the charging time and the departure time for each aircraft on Monday.

3.1.3. Electricity Demand Aircraft

This subsection will approximate the electricity consumption of each type of electric aircraft for specific destinations. The energy for specific destinations is computed by two equations. First, the Breguet range equation as already discussed in the literature review will be used. However, this equation assumes a constant cruise speed and does not take the energy consumption during the take-off and climb phases into account. For short-range flights, this assumption can not be made, as the take-off energy accounts for a significant share of the total energy needed [106]. To compensate for this, also a take-off energy equation will be used to approximate the trip energy.

For the energy consumption during the cruise phase at altitude, the Breguet range equation for battery-powered aircraft is recalled in 3.1. In this equation, $E_{electric}$ is the energy demand of the aircraft for the operating range $R_{electric}$. m_{TO} is the total weight of the aircraft, $mathrm\eta$ represents the total efficiency, and (L/D) is the lift-drag ratio.

$$R_{electric} = \frac{L}{D}\eta_p\eta_{tr}\eta_{ther}\frac{SE_{fuel}}{g}\frac{m_{battery}}{m_{TO}},$$

Rearranged and rewritten, (3.1)

$$E_{electric} = \frac{R_{electric}m_{TO}g}{(L/D)\eta_{total}}$$

The Breguet range equation assumes a constant cruise speed and altitude. Also, it does not include the energy during the take-off and climb phases. For long-range flights, this can be assumed, however, for short-range flights the energy consumption in these phases is significant. In figure 3.2 the actual range is compared to the range according to the Breguet range equation. It can be concluded that the calculated range is higher compared to the actual range. Specifically, for the short-range flights, the take-off and climb energy consumption should be considered as the actual stage length is significantly lower compared to the stage length calculated with the Breguet range equation [106]. As the electric flights are operating on short-range, the take-off and climb energy consumption is included.

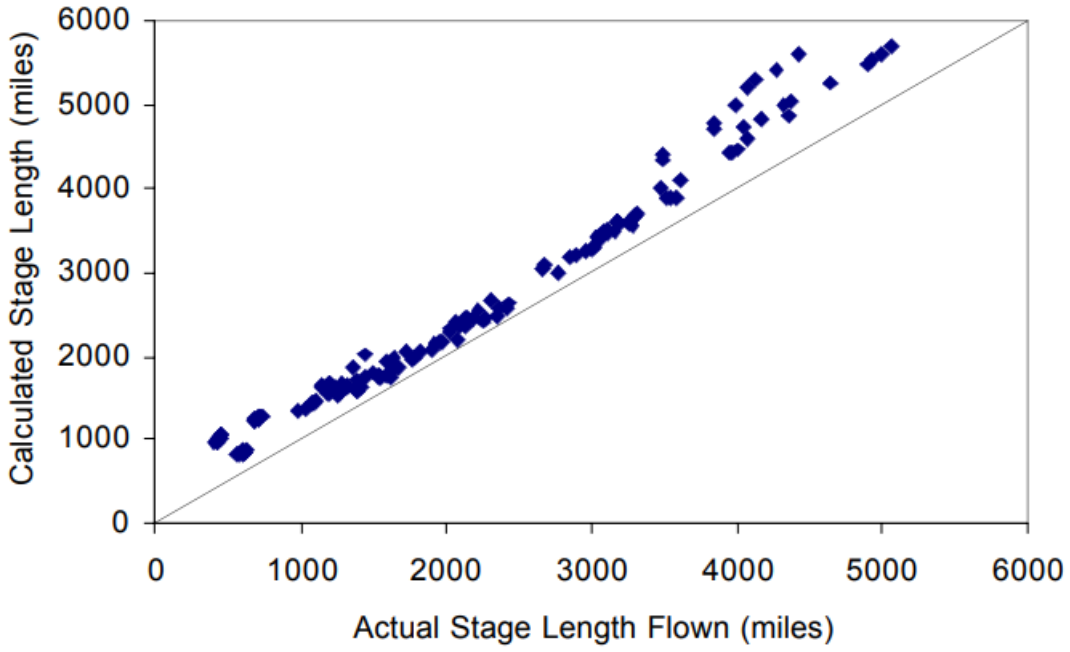

Figure 3.2: Deviation of actual stage length compared to calculated stage length is for short-range flights more significant compared to long-range flights. The Range equation provides an optimistic range and so concludes that less energy is needed for the range [106].

The approximation of energy consumption during the takeoff and climbing phase can be explained with a free-body diagram. A free-body diagram is a simplified schematic figure of the forces acting on a body. In figure 3.3, a free-body diagram is seen of the aircraft during the cruise phase at altitude.
Four forces are acting on an aircraft. In the vertical plane, the gravity and the lift force are acting on the aircraft, while in the horizontal plane, the drag force and the thrust force from the propeller are acting on the aircraft. In figure 3.3, all the forces acting on the aircraft are in equilibrium and the acceleration is zero. So, the lift is equal to the weight and the thrust from the propeller has to overcome the drag force. The thrust and drag force are along the flight path while the lift is always perpendicular to the flight path. As the drag and lift force are both aerodynamic forces, the lift-drag ratio is a measure of the aerodynamic efficiency of the aircraft [38].

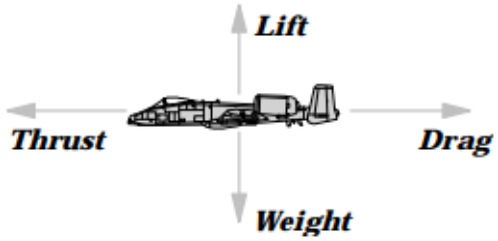

Figure 3.3: Balance of forces acting on an aircraft during steady state phase. Aircraft stays at the altitude due to the equilibrium of forces in the y-direction [77].

However, during the climb phase of the aircraft, the balance of forces will be relocated as can be seen in figure 3.4. The aircraft will point its nose upwards. The angle between the flight path line and the horizontal is called the angle of attack (θ) [51].

From figure 3.4, it can be seen that the force equilibrium in the direction of the flight path and perpendicular to the flight path is changed. When decomposing the force originating from the weight, one component of the weight exerts a force in the direction of the drag force, which the thrust force has to overcome. The cosine component of the weight is now equal to the lift force [116]. The lift-drag ratio is changed with respect to the steady-state flight and can be increased by using flaps in the wings. However, this lift-drag ratio will be smaller than the max lift-drag ratio. The lift-drag ratio varies for different aircraft types, however, typically lies between 12 and 20 during steady state. Therefore a lift-drag ratio of 16 is assumed during steady-state flight [69].

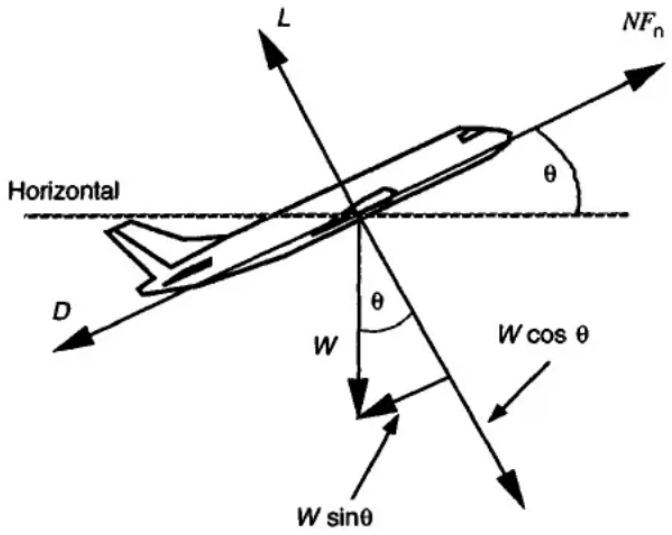

Figure 3.4: Free body diagram of an aircraft during climb phase. The lift-drag ratio is smaller compared to the steady-state phase. With the flaps of the wings, the lift can be somewhat increased but it also causes an increased drag [51].

The energy needed for climbing can be split up into three components. The potential energy needed to reach a certain altitude h, and the kinetic energy to obtain a certain cruise speed v_{cruise}. Lastly, the energy to overcome the drag force exerted on the aircraft during ascension is included in equation 3.2 [84].

$$E_{0,t} = \frac{1}{2} m {v_{cruise}}^2 + mgh + F_D s, \tag{3.2}$$

where F_D is the drag force, and s is the distance covered during ascent. In the climb phase, the aircraft will ascent with a climb angle with the horizontal axis θ as can be seen in figure 3.4. The climb angle can be approximated using the flight trajectory provided by [34]. Based on this trajectory the climb angle is assumed to be equal to 5°. Rewriting the equation in 3.2 in terms of the free-body diagram,

the total energy during the take-off and climb phase can be approximated with the following equation [84]:

$$E_{total} = \frac{mg}{\eta}\left(\frac{{v_{cruise}}^2}{2g} + h + \frac{s}{(L/D)}\right) = \frac{mg}{\eta}\left(\frac{{v_{cruise}}^2}{2g} + h\left(1 + \frac{1}{\sin(\theta)(L/D)}\right)\right) \tag{3.3}$$

where θ is the climb angle of the aircraft and the efficiency η of the aircraft is included. v_{cruise} and h are the cruise speed and the altitude the aircraft will ultimately reach, respectively.
Lastly, it is assumed that the battery charging efficiency is 95% and 10% additional losses in the system operation.

3.2. Grid Impact Electric Aviation without BESS

This section aims to explain how the voltage fluctuations and distribution grid cable load can be analyzed for the electricity demand for electric aircraft charging for the Business-as-Usual case. The Business-as-Ususal case (BaU) represents the current situation at BIA without a solar park and BESS. From the previous analysis, the aircraft charging profile is obtained on a 15-min base.

The total electricity demand of the airport is the summed load profile of the charging load profile of electric aircraft and the current baseload profile of the airport. Therefore, a 15-min data set of the current electricity demand of the airport is obtained. A measurement of the electricity consumption at BIA is done for two consecutive months. This will be repetitively used throughout the year. Ultimately, the total electricity demand profile is used for the grid impact analysis.

Four analyses are done for the impact on the grid, which are done in Vision and Python. Vision is a tool that can be used for grid network analysis [81]. In Vision, the microgrid of Bonaire is modeled where the electricity consumers and producers are nodes that are linked by the cables on the medium-voltage level (12.2 kV). Moreover, specifications and dimensions of grid cables, transformers, and sub-stations are included. Transformers connect the medium-voltage level to the low-voltage level. At the transformer node of the airport, the load profile of the airport can be uploaded and a dynamic load-flow analysis can be run. This dynamic load flow analysis takes the time-based load profiles of other nodes within the grid network of Bonaire into account.
The dynamic load-flow analysis is done for the worst week in terms of solar irradiation on a 15-minute basis. In Vision, a week profile is created by providing the electricity demand profile of a typical weekday, a Saturday, and a Sunday. Ultimately, this analysis provides three results:

- Overloading of the transformer capacity in hours and its maximum duration from the Python model.
- Load on cables the cables of the grid, presented in % of the maximum capacity of the cable from Vision.
- Voltage fluctuations presented in % of the grid voltage which is 12.2 kV for Bonaire. The acceptable range of the voltage fluctuations is 95%-105%.
- Peak on the grid of both load demand and feed-in obtained from the Python model.

The outcomes act as the results of the grid impact of electric aviation in the Business-as-Usual case. The same analysis is also done in case the 1000 kWp solar park is installed at BIA.

Figure 3.5 shows the location of the airport transformer in the grid. The line going upward from the airport transformer in the figure is disconnected. Therefore, it can be seen that the transformer of the airport is located at the end of a single grid line. At the airport's node, the voltage fluctuations and the distribution cable load are analyzed. In the appendix A.2.2, a figure of the whole Vision model is included.

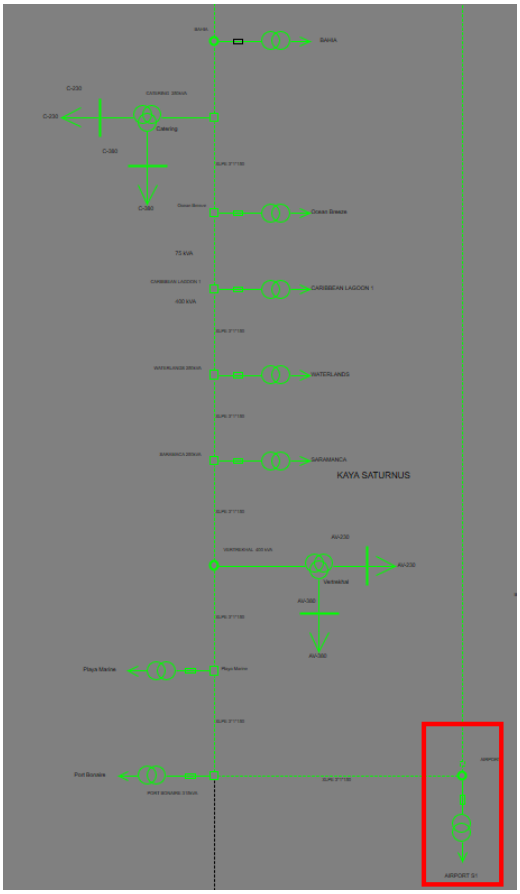

Figure 3.5: Electricity grid medium voltage level (12.2 kV) of Bonaire in Vision near the airport [81].

3.3. Model Battery Control Strategies and Performance Indicators

This section explains the methodology of the model that optimizes the battery according to its control strategy using Mixed-integer linear programming (MILP) in Python, where Pyomo is used as the optimization modeling language. Pyomo is a free optimization modeling language, however, Pyomo cannot solve the optimization problem. Therefore, the used optimization solver tool for this model is Gurobi 10.0.1 Optimization, which is free for academic use.

The model is made to obtain output data and parameters that can be used for further analysis in this research where the contribution of a BESS with different control strategies in technical, economic, and environmental terms will be investigated. The BESS is used to handle the electricity demand profile of electric aircraft charging at the airport given a 1000 kWp PV solar park. The BESS provides additional power during aircraft charging. Therefore, the power of the BESS is based on the peak power of aircraft charging. With this model, insight is gained into the load flow within the system, the load profile on the grid, and the associated costs. The load profile on the grid will be used for further analysis in the grid analysis program Vision and for CO_2 emissions analysis. The optimal sizing of the infrastructure is outside the model's scope.

3.3.1. System Set Up

A Python optimization model is made of the following system setup. This system is made based on the current infrastructure at the airport as the optimal infrastructure configuration at the airport is out of the scope of this research. Different electrical system configurations at the airport will not impact the battery and energy costs of the system. In addition, the voltage fluctuations, cable load, and peak load will be assessed at the grid connection (which was discussed in section 3.2). Therefore, this is independent of the electrical system configuration behind the grid connection.

As can be seen in 3.6, the system consists of a PV solar park and a BESS. If needed, the grid can be used to meet demand. The PV solar park is able to feed excess electricity into the grid. The BESS can be charged with electricity from the grid and electricity from the solar park. The BESS can discharge to the grid and discharge to meet the demand of the airport. The BESS is not able to simultaneously charge and discharge.

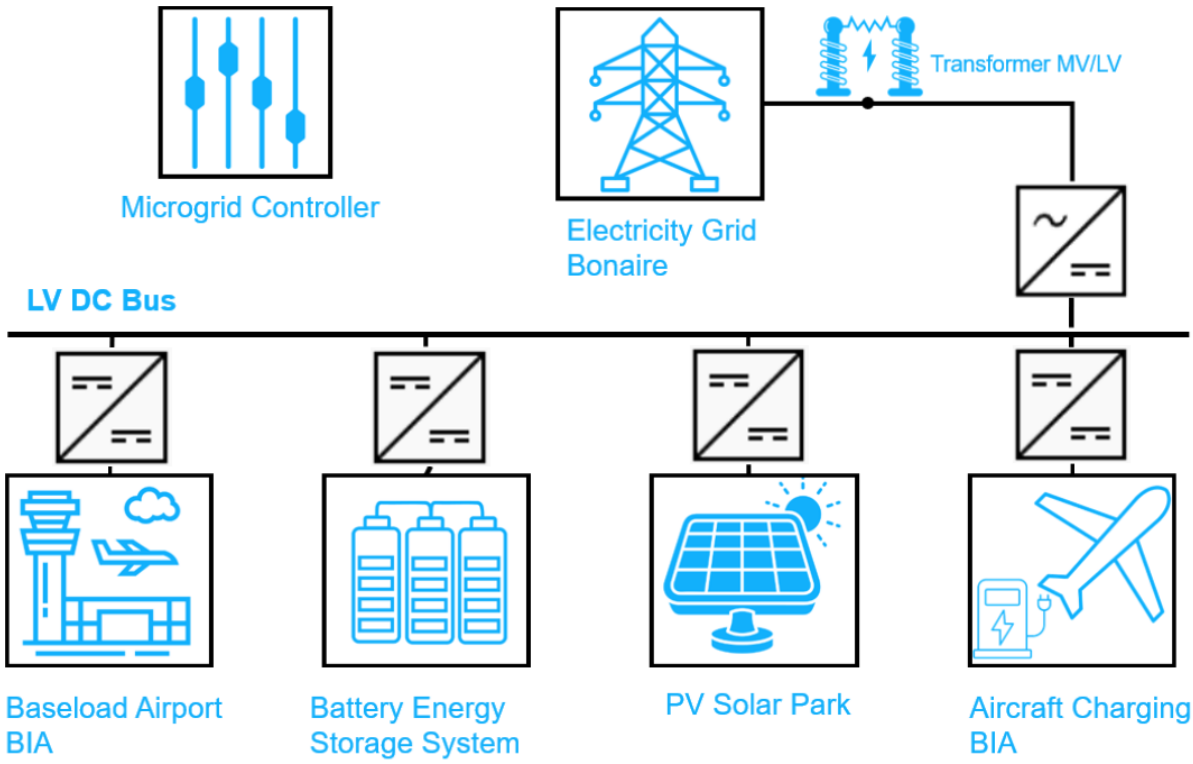

Figure 3.6: System setup at Bonaire International Airport.

3.3.2. General BESS Model Formulation

The optimization model of the BESS made in Python is presented in this section. The variables, parameters, and constraints are discussed. Ultimately, the objective functions of the control strategies with additional constraints for specific control strategies are discussed at the end of the section.

Input Parameters

For the model, multiple data sets are used, as well as single input parameters. These input parameters are listed below.

Data sets

The model is programmed for an entire year on a 15-min base, therefore, the total time set T = 35040 for time steps t. The following data sets are used in the model.

- P_t^{solar} is the total power output of the solar park for each time step t. The data of the PV output is obtained from Photovoltaic Geographical Information System (PVGIS) [24]. The time scale is 15 minutes in kW.
- $P_t^{load,airport}$ is the measured baseload of the airport for two months. These two months are used throughout the year on a time scale of 15-min.
- $P_t^{load,EA}$ is the power that is needed to charge the electric aircraft. This calculation of electric aircraft charging power is performed in section 4.1 and used for the load profile of the electric aircraft.

The yearly load profile of the PV output of a 1 kWp PV crystalline silicon solar park is depicted on a 15-min base in figure 3.7 for 2020. The profile is scaled to a 1MWp solar park. The orientation of the system is optimized by PVGIS [24], where the Azimuth angle is 20°. and the slope of the PV panel is 12°, and a system loss of 14% is assumed.

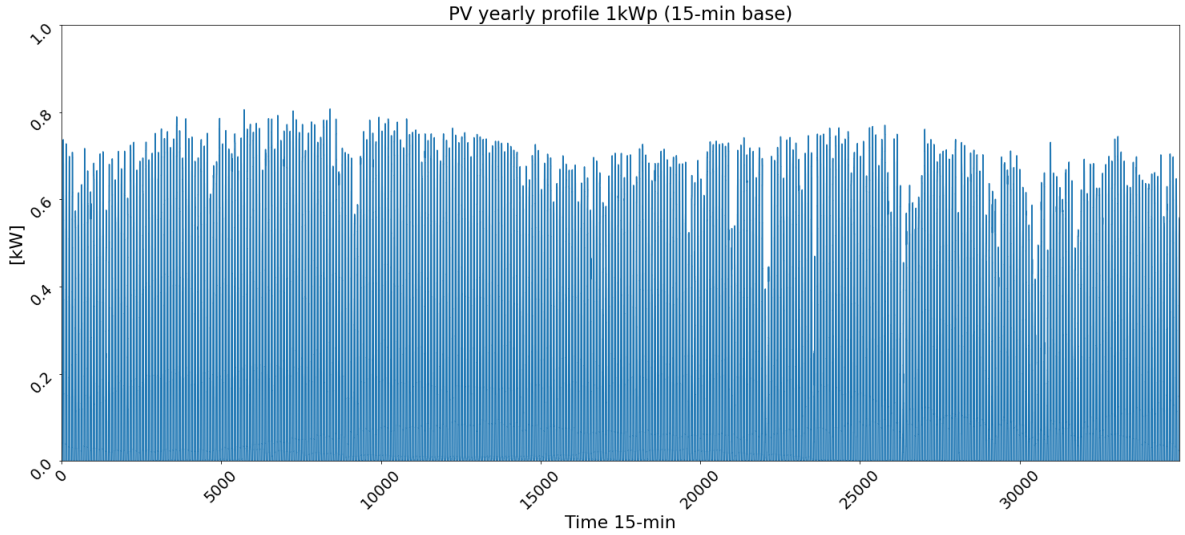

Figure 3.7: Solar PV output of a 1 kWp solar park assuming 14% system losses. 2020 yearly profile on a 15-min base. The data is obtained from [24].

The load of the airport was acquired through measurements at the airport for 2 consecutive months (June-July 2022). Due to this data limitation, these months are assumed to be repeating the whole year. Nevertheless, these two months give an indication of the base load profile pattern. Figure 3.8 illustrates a two-week profile of the load of the airport. The horizontal blue line represents the current transformer capacity.

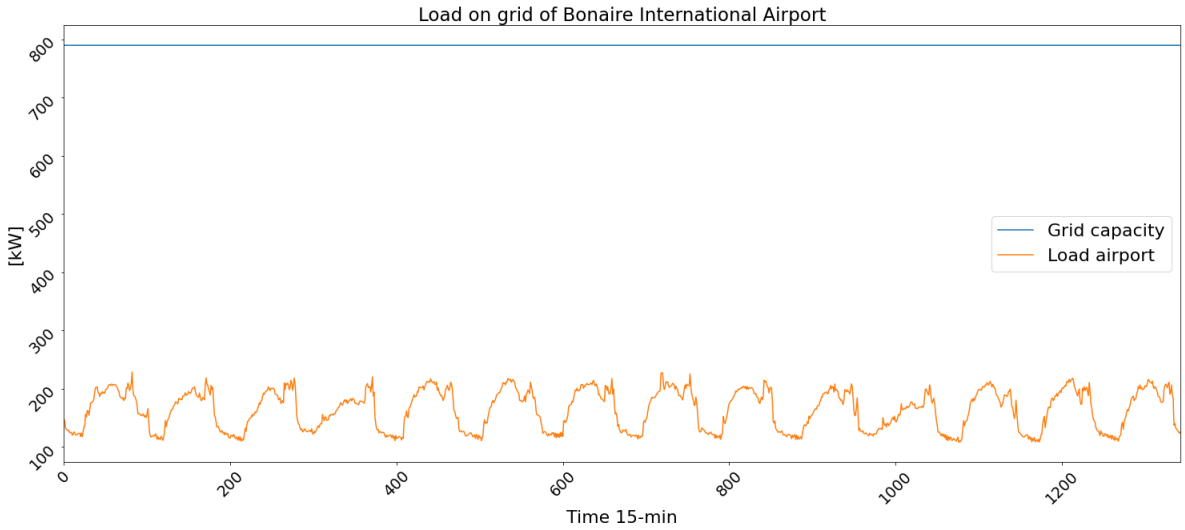

Figure 3.8: Measurement of load of the airport of two weeks in the period of June-July 2022.

Single input parameters

- $C_{gridelec}$ is the cost of electricity purchased from the grid [$/kWh]. The electricity purchase cost at Bonaire is 0.425 $/kWh.

- C_{feedin} is the remuneration of electricity fed back into the grid [$/kWh]. The electricity feed-in remuneration at Bonaire is 0.01 $/kWh as BIA is a large consumer.
- C_{peak} is the cost related to the peak on the grid of the grid connection [$/kVA/month]. The peak cost is 11.48 $/kVa/month.
- P^{max} is the max power of the BESS [kW]. This power is taken equal to the peak power of aircraft charging. Although BIA will install a PV park, the worst-case scenario is assumed that there is no PV. The peak power of aircraft charging for 9 pax is 978.95 kW, which for simplicity is assumed to be taken as 1 MW for the BESS power.
- $P^{gridcap}$ is the capacity of the transformer and determines the size of the grid connection which is currently between (-790 kW, 790 kW).
- $B_{capacity}$ is the capacity of the BESS [kWh]. The capacity of the BESS is based on the power capacity of the BESS. The BESS is assumed to be operated with a 0.5C rate as this is beneficial for the lifetime of the BESS [20]. Therefore, the capacity of the BESS is 2MWh.
- η is the charge and discharge efficiency of the BESS[%], which is taken as 95% for both.
- $CAPEX_{solar}$ is the capital expenditure of the solar park [$/kW]. This value is equal to 1448 $/kW for the year 2023 according to [76]
- $OPEX_{solar}$ is the operational expenditure of the solar park and is equal to 16.5 [$/kW/year] according to NREL [76].
- $CAPEX_{BESS}$ is the capital expenditure of the BESS for a 2-hour battery [$/kW]. The CAPEX of the BESS is equal to 1216 $/kW according to a report of NREL [75].
- $OPEX_{BESS}$ is the operational expenditure of the BESS for a 2-hour battery [$/kW/year]. The OPEX of the BESS is equal to 30.4 $/kW/year according to a report of NREL [75].
- kWp is the size of the solar park [kWp].
- SOC_{min} is the minimum of the BESS SOC of 20% [%].
- SOC_{max} is the maximum of the BESS SOC of 80% [%].
- dt is the conversion factor of kW to kWh as the model runs on a 15-min base for the SOC calculation [0.25].

Decision Variables
The optimization variables included in the MILP are defined as follows:

- $P_t^{solar,load}$ is the power generated by the solar park that will be used to meet load demand.
- $P_t^{solar,bat}$ is the power generated by the solar park which charges the battery. This variable is limited by P^{max} of the BESS.
- $P_t^{solar,grid}$ is the excess electricity that will be fed into the grid for remuneration.
- P_t^{curt} is the last term of the solar energy flow. Which is the curtailed solar energy.
- P_t^{charge} is the power at which the BESS is charged limited by the P^{max} either with solar or grid energy.
- $P_t^{charge,grid}$ is the power at which the BESS is charged from the grid limited by the P^{max}.
- $P_t^{discharge}$ is the power at which the BESS is discharged limited by the P^{max}.
- $P_t^{discharge,load}$ is the power at which the BESS is discharged to the load limited by the P^{max}.
- $P_t^{discharge,grid}$is the power at which the BESS is discharged to the grid limited by the P^{max}.
- $P_t^{gridelec}$ is the electricity power taken from the grid.
- SOC is the state of charge of the battery.
- $P_t^{load,grid}$ is the net load on the grid which.
- P^{peak} is the peak load demand on the grid.
- u_t^{b1} is a binary variable to prevent simultaneous charge and discharge of the BESS.
- u_t^{b2} is a binary variable to prevent simultaneous use of grid electricity and PV electricity feed into the grid. This would result in an uneconomic use of electricity due to the difference in the purchase price and feed in remuneration.
- u_t^{b3} is a binary variable to prevent simultaneous charge from the grid and PV electricity feed into the grid. The introduction of this binary variable is for the same reason as binary variable two.
- u_t^{b4} is a binary variable to prevent simultaneous discharge to the grid and use grid electricity to meet the airport demand.

Set of Constraint

Here the set of constraints on the system is explained. These can roughly be divided into the load flow and the battery operation constraints. First, the set of load flow constraints is considered.

Load flow constraints

The first constraint 4.4a states that the total supply must meet the demand for all t. The total supply consists of the PV power used for the load, the grid electricity used, and the discharge of the BESS to the load. The demand is represented by the total load of the airport.
The second constraint 4.4b is the load flow constraint of the output of the PV-solar park. The PV output is scaled by the kWp-term and can either transmit its energy to the load, the BESS, or the grid. The last option is to curtail this solar park.

$$P_t^{\text{solar,load}} + P_t^{\text{gridelec}} + P_t^{\text{discharge,load}} = P_t^{\text{load,EA}} + P_t^{\text{load,airport}} \quad \forall t \in T \tag{4.4a}$$

$$P_t^{\text{solar}} * kWp = P_t^{\text{solar,load}} + P_t^{\text{solar,bat}} + P_t^{\text{solar,grid}} + P_t^{\text{curt}} \quad \forall t \in T \tag{4.4b}$$

The next set of constraints determines the load on the grid which is represented by constraint 4.5a, where electricity feed-in reduces the load on the grid while charging the BESS and using grid electricity increases the total load on the grid. The peak load is given by constraint 4.5b, where P^{peak} is an auxiliary variable and is equal to the highest absolute peak of the load on the grid in T. In constraint 4.5c, the same applies to the negative peaks on the grid due to electricity feed-in. These peak load statements are necessary for the minimization of the peak load costs in the objective function of the Cost-Optimal strategy.

$$P_t^{\text{load,grid}} = P_t^{\text{gridelec}} + P_t^{\text{charge, grid}} - P_t^{\text{solar,grid}} - P_t^{\text{discharge,grid}} \quad \forall t \in T \tag{4.5a}$$

$$P^{\text{peak}} \geq P_t^{\text{load,grid}} \quad \forall t \in T \tag{4.5b}$$

$$-P^{\text{peak}} \leq P_t^{\text{load,grid}} \quad \forall t \in T \tag{4.5c}$$

Lastly, binary variables are introduced to prevent the system from operating uneconomically. Consuming grid electricity to meet demand or charging the BESS while at the same time feeding electricity into the grid results in an uneconomical operation. The purchase price of grid electricity is higher compared to the feed-in remuneration. If an equal amount of electricity is exchanged with the grid, this results in a net zero exchange on the grid. To prevent this event from happening, the binaries are incorporated by the following constraints in 4.6a, 4.6c, 4.6b, 4.6d, 4.6e, and 4.6f.

$$P_t^{\text{gridelec}} \leq P_t^{\text{gridelec}} * u_t^{\text{b2}} \quad \forall t \in T \tag{4.6a}$$

$$P_t^{\text{solar,grid}} \leq P_t^{\text{solar,grid}} * (1 - u_t^{\text{b2}}) \quad \forall t \in T \tag{4.6b}$$

$$P_t^{\text{charge,grid}} \leq P_t^{\text{charge,grid}} * u_t^{\text{b3}} \quad \forall t \in T \tag{4.6c}$$

$$P_t^{\text{solar,grid}} \leq P_t^{\text{solar,grid}} * (1 - u_t^{\text{b3}}) \quad \forall t \in T \tag{4.6d}$$

$$P_t^{\text{gridelec}} \leq P_t^{\text{gridelec}} * u_t^{\text{b4}} \quad \forall t \in T \tag{4.6e}$$

$$P_t^{\text{discharge,grid}} \leq P_t^{\text{discharge,grid}} * (1 - u_t^{\text{b4}}) \quad \forall t \in T \tag{4.6f}$$

Battery operation constraints

In addition to the set of constraints regarding the load flow, the battery operational constraints are presented here. These include charging, discharge, and state of charge constraints. To start with the charge constraints in 4.7a. The BESS can be charged with grid electricity or electricity from the solar park. Moreover, the power at which the BESS is charged is constrained by P^{max} as in 4.7b. In this constraint, a binary variable is added to prevent simultaneous charging and discharging of the BESS (see also constraint 4.8b).

$$P_t^{\text{charge}} = P_t^{\text{charge,grid}} + P_t^{\text{solar,bat}} \quad \forall t \in T \tag{4.7a}$$

$$P_t^{charge} \leq P^{max} * u_t^{b1} \quad \forall t \in T \tag{4.7b}$$

For the discharge of the BESS, almost the same constraints hold.

$$P_t^{disharge} = P_t^{discharge,load} + P_t^{discharge,grid} \quad \forall t \in T \tag{4.8a}$$

$$P_t^{discharge} \leq P^{max} * (1 - u_t^{b1}) \quad \forall t \in T \tag{4.8b}$$

Lastly, the charge and discharge behavior of the BESS determines the *SOC* level of the BESS which is incorporated in the following constraint. Where the *SOC* is in kWh and the charging and discharging power in kW on a 15-min base. Therefore, the charge and discharge power is multiplied by dt which is equal to 0.25 to convert the kW to kWh.
Moreover, the *SOC* starts at 50% of the battery capacity and can cycle between 20% and 80% of the $B_{capacity}$.

$$SOC_t = SOC_{t-1} + P_t^{charge} * \eta * dt - P_t^{discharge} / \eta * dt \quad \forall t \in T \tag{4.9}$$

3.3.3. BESS Control Strategies Model Formulation

In this section, the modeling of the three considered control strategies with their objective function and additional constraints are discussed.

Control Strategy I: Self-consumption

The first considered control strategy is self-consumption, where the on-site consumption of PV electricity is maximized. The self-consumption is defined by 4.10 [64][44]:

$$\text{Self-consumption} = \frac{\text{Self-consumed PV-power}}{\text{Generated PV-power}} \tag{4.10}$$

The self-consumed PV power comprises two components: directly consumed solar energy by the load and the contribution of the BESS to the self-consumption of solar energy. The sum of these two components relative to the total generated PV power is called self-consumption.

The total generated PV power in terms of the model variables is equal to the sum of the energy output P_t^{solar} of the solar park scaled by the size of the solar park kWp. In the numerator in equation 4.11 the on-site energy usage of the solar park is optimized.
The first term is the solar energy directly used to meet load demand. Secondly, the BESS is able to enhance the self-consumption ratio by storing the surplus of solar energy and using the stored solar energy when there is a deficit. To obtain a high self-consumption the discharge of the BESS to the load is maximized [17]. Additionally, the interaction of the BESS with the grid is minimized in order to prevent the discharged energy to the load from being maximized due to grid energy. This stimulates to use of the BESS capacity for self-consumption and obtains a high fraction of solar energy in the discharged energy volume that is supplied to the load. In particular $P_t^{discharge,load}$ is used to be maximized as this includes the efficiency of the BESS (see equation 4.9) and therefore there is an incentive to first use the solar energy directly. The self-consumed energy is higher if energy is used directly instead of via the BESS due to its efficiency.
Lastly, the curtailment of solar energy reduces the self-consumption therefore this also needs to be minimized. Moreover, in case of an energy surplus and a full battery the solar energy will be transmitted to the grid instead of being curtailed.

Self-Consumption =

$$Maximize \left(\frac{\sum_{t=1}^{T} (P_t^{solar,load} + P_t^{discharge,load} - P_t^{charge,grid}) - P_t^{discharge,grid})}{\sum_{t=1}^{T} (P_t^{solar} * kWp)} - \sum_{t=1}^{T} P_t^{curt} \right) \quad \forall t \in T \tag{4.11}$$

Control Strategy II: Peak Shaving
The second control strategy is Peak Shaving. A BESS can be used to reduce the peak load on the grid. The same objective is set for Peak Shaving as was set for the Self-Consumption control strategy. However, for Peak Shaving a threshold is set to the maximum absolute peak load on the grid. Therefore, the variable $P_t^{load,grid}$ has imposed a minimum and maximum value in the model as defined by the equation 4.12. The threshold for the minimum counteracts peaks in the feed-in of electricity, while the maximum threshold counteracts the peaks of peak load demand. The threshold is set at 50% of the maximum peak load of the total demand profile.

$$\begin{aligned} & P_t^{load,grid} = P_t^{gridelec} + P_t^{charge,\,grid} - P_t^{solar,grid} - P_t^{discharge,grid} \quad \forall t \in T \\ & \text{with:} \quad Threshold_{min} \leq P_t^{load,grid} \leq Threshold_{max} \end{aligned} \tag{4.12}$$

Control Strategy III: Cost-optimal Operation
The last control strategy is the Cost-optimal operation where the operational costs are minimized. The corresponding objective function is given in equation 4.13.

$$\text{Cost-optimal Operation} = \textit{Minimize}\ (\text{OPEX cost}) \tag{4.13}$$

The parameters for the OPEX costs are previously provided. The objective function for the minimization of the cost in a year is given by:

$$\begin{aligned} \text{OPEX cost} = & \sum_{t=1}^{T} (P_t^{gridelec} + P_t^{charge,\,grid}) \cdot C_{gridelec} - \sum_{t=1}^{T} (P_t^{solar,grid} + P_t^{discharge,grid}) \\ & \cdot C_{feedin} + P^{peak} \cdot 1.73 \cdot 12 \cdot C_{peak} + OPEX^{PV} + OPEX^{BESS} \quad \forall t \in T \end{aligned} \tag{4.14}$$

Where the total cost of electricity purchase is given by the first term of the equation. Remuneration is received for feeding electricity into the grid, represented by the second term. The cost for the maximum peak on the grid is paid monthly. 1.73 is the conversion factor for kW to kVa in this electrical system.

3.3.4. Technical Performance Indicator
The impact on the grid analysis is done with Vision and will be the same as was done on the impact on the grid in the Business-as-Usual case as explained in 3.2. The total grid load profile of the airport can be obtained from the Python optimization model and a week on a 15 minute-base can be uploaded in Vision. The results of the three distinct battery control strategies are compared to the Business-as-Usual case with and without the PV system. Ultimately four results are provided by the Vision and Python model

- Overloading of transformer capacity in hours.
- Range of loads on distribution grid cables in % of its capacity.
- The range of voltage fluctuations in % of the 12.2 kV grid voltage.
- The demand peak load and the feed-in peak in kW.

3.3.5. Economic Performance Indicator
The second performance indicator is obtained from the economic analysis, where the Levelized Cost of Electricity (LCOE) is calculated for the airport for the Business-as-Usual cases and for the BESS control strategies.

$$LCOE = \frac{\sum_{t=1}^{\text{Lifetime}} \frac{CAPEX+OPEX+E+P+F}{(1+WACC)^t}}{\sum_{t=1}^{\text{Lifetime}} \frac{D}{(1+WACC)^t}} \quad \forall t \in \text{Lifetime} \tag{4.15}$$

Where the costs consist of the CAPEX and OPEX of the BESS and the PV system. The electricity purchase costs, subtracted by the feed-in revenue, are represented by E. P is defined as the costs for the peak load on the grid, and F are the financing costs using a WACC of 10%. D is the total airport demand for one year. The considered costs are:

- Total costs of electricity over a year. The total cost of electricity purchased is reduced by the total remuneration for the electricity fed into the grid. The electricity purchase price is 0.425 $/kWh and the feed-in tariff is 0.01 $/kWh.
- A cost for the grid connection is paid monthly to WEB. These costs are based on the highest peak load on the grid and are equal to 11.48 $/kVa/month.
- Operational and maintenance cost of the PV solar park. These OPEX costs are obtained from NREL [76] and include all the fixed costs such as insurance and operating labor, but also the replacement costs, and (un)scheduled maintenance costs. The OPEX cost for PV is equal to 16.9 $/kW/year.
- Operational and maintenance cost of the BESS. These OPEX costs are also obtained from NREL and are equal to 27.7 $/kW/year [75].
- CAPEX costs of PV solar park, which include installation, material costs, and electrical infrastructure [76]. The CAPEX costs are equal to 1109 $/kW.
- CAPEX costs for are 2-hour BESS, which are equal to 1488 $/kW according to NREL [75].

The time horizon of the LCOE is calculated over the shortest lifetime of the BESS or the PV system. There is a remaining asset value in case the PV or the BESS has not reached its lifetime. A depreciation of the PV solar park and the BESS are evenly distributed over their lifetimes. Financial costs are included over the remaining asset value for each year, where a WACC of 10% is assumed on Bonaire for the airport. Over the time horizon of the LCOE, an annual electricity demand growth of four percent is assumed. To include the effect of the electricity demand growth and the degradation of the battery on the change in the electricity purchase costs and the peak load costs, the annual change (%) of these costs components are approximated by calculating the first year costs, and the last year costs in which a degraded battery and grown electricity demand is included.
The lifetime of the PV solar park is assumed to be 20 years. However, the BESS lifetime depends on the intensity of the BESS usage. Therefore, a capacity degradation formula is used, where the end of life of a BESS is often set at 80% of the initial capacity.

As was mentioned in chapter 2 the BESS lifetime in terms of battery capacity depends on both the cycling and the idling. In the study [101], the cycle lifetime and the calendar lifetime due to idling are determined using the empirical equations for BESS capacity degradation as shown in 4.16 [101].

$$\begin{aligned} C_{cal} &= 1.9775 \cdot 10^{-11} \cdot \mathrm{e}^{0.07511 \cdot T} \cdot 1.639 \cdot \ \mathrm{e}^{0.007388 \cdot SoC \cdot t^{0.8}} \\ C_{cyc} &= 0.021 \cdot \mathrm{e}^{-0.01943 \cdot SoC_{avg} \cdot cd^{0.7612} \cdot n_c^{0.5}} \end{aligned} \tag{4.16}$$

In the equation of calendar aging, t is the time in months of idling, T is the temperature in Kelvin, and SoC is the state of charge level during idling. In the equation for cycling aging, SoC_{avg} is the average state of charge of a cycle, cd is the cycle depth, and nc is the number of cycles [101] [100]. However, in the study of [100] the temperature is kept constant at 25C°. Although the temperature heavily influences the degradation, the study assumed that BESS are deployed with air conditioning [100] and kept at a constant temperature. Where 25 C°is advantageous for the performance and for the lifetime [100].
The model in this thesis is on a 15-minute base instead of months. Therefore, the equation is corrected for the time scale and the constant temperature as stated in 4.17. The capacity fade due to cycling and idling together contribute to the total capacity fade.

$$\begin{aligned} C_{cal} &= 0.1723 \cdot \mathrm{e}^{0.007388 \cdot SoC} \cdot (t/2880)^{0.8} \\ C_{cyc} &= 0.021 \cdot \mathrm{e}^{-0.01943 \cdot SoC_{avg} \cdot cd^{0.7612} \cdot n_c^{0.5}} \end{aligned} \tag{4.17}$$

To calculate the total capacity degradation using the previously mentioned equations, the SoC profile is needed as an input, from which the average SoC, the number of cycles, and cycle depth can be determined. Secondly, the SoC level for the idling capacity degradation and the number of time steps of idling can be obtained. A commonly used tool for this purpose is the rainflow counting method. The rainflow counting method is often used for counting stress fluctuations on materials for fatigue analysis [94] but is also used for battery cycling [100] [94] [68]. The rainflow counting method that is used for the BESS SoC profile in this thesis is obtained from [85]. The SoC profile from the

model restricts the degradation assessment over one year. Therefore, it is assumed that the BESS undergoes a degradation of such a year consecutively until the BESS is degraded to 80% of its initial capacity.

In figure 3.9 an example of the rainflow counting is depicted. From left to right water flows from the 'roof' of the profile. When the water falls off a roof and drops on another roof a full cycle is counted, if not a half cycle is counted. The absolute difference between the start and the end is the depth of discharge [18]. In the figure, E-F-E' is counted as a full cycle, where a full cycle is only counted if the length of the stage in the middle (E-F) is smaller than the previous (D-E) and next stage length (F-G). Otherwise, it will be counted as a half cycle.

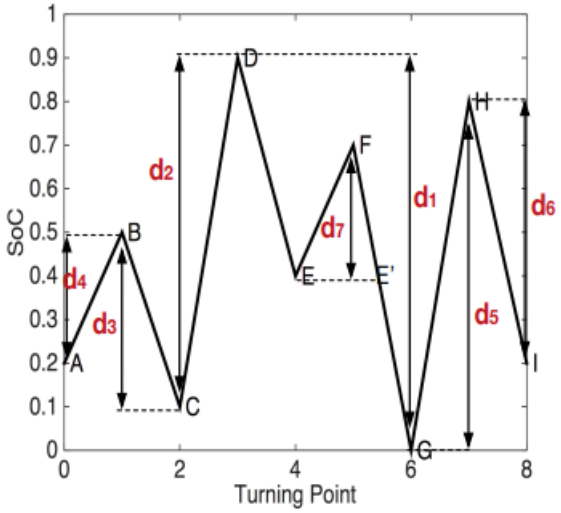

Figure 3.9: An example of a rainflow counting. Raindrops are falling from left to right from the 'roofs' of the profile. Half cycles are counted when the drop is not falling on another roof. A full cycle is counted at E-F-E', where the raindrop falls on another roof. Full cycles are only counted when E-F is smaller than the previous and next lengths of D-E and F-G, respectively [94].

3.3.6. Environmental Performance Indicator

The last performance indicator is the sustainable performance indicator which consists of two factors: Self-sufficiency and CO_2-emissions.
First, Self-sufficiency is used as the performance indicator as described by the ratio in 4.19. Self-Sufficiency is the ratio of the sum of self-consumed PV over the total energy consumption. The rest of the electricity is taken from the grid. Therefore, the ratio can be interpreted as a ratio that reflects the independence of the grid.

$$\text{Self-sufficiency [\%]} = \frac{\text{Self-consumed PV-power}}{\text{Total energy consumption}} \cdot 100\% \tag{4.18}$$

Secondly, the residual share of the consumed electricity by the airport comes from the grid. The change in CO_2 emissions from the electricity production at Bonaire is calculated and represents the environmental performance indicator. The change is measured as the difference between the CO_2 emissions with electric aviation and the installed system at the airport and the currently emitted CO_2 of the baseload of the airport.

$$\text{Change } CO_2 \text{ Emissions Electricity Grid [\%]} = \frac{(CO_2 \text{ Emissions with EA}) - (\text{Current } CO_2 \text{ Emissions})}{\text{Current } CO_2 \text{ Emissions}} \cdot 100\% \tag{4.19}$$

A model is made that computes the CO_2 emissions from the electricity production at Bonaire. This model considers the whole electricity demand on a one-hour basis of Bonaire as well as the production of electricity by wind, PV, and diesel generators. In addition, it considers the charging and discharging

of the BESS and the curtailment of wind and PV. The PV data is taken from PVGIS [24] for the year 2019, and the 10-minute wind data is obtained from KNMI [56] of 2019 (the worst year of the available data). With the log law to correct for wind speeds at rotor height and the power curve, the energy output of the turbines is determined.

The model consists of the assets tabulated in 3.1 and the decision scheme for the electricity supply of the model is depicted in figure 3.10.
The total load profile of BIA is added to the total demand of Bonaire in the model. The total load profile of BIA from the optimization model is on a 15-min base. Therefore the 15-min values of the optimization model are translated to kWh and are used on an hourly base. The model of Bonaire identifies if the new load profile caused by the adoption EA increases diesel-generated electricity production. Ultimately, the added diesel usage can be translated into CO_2 emissions.

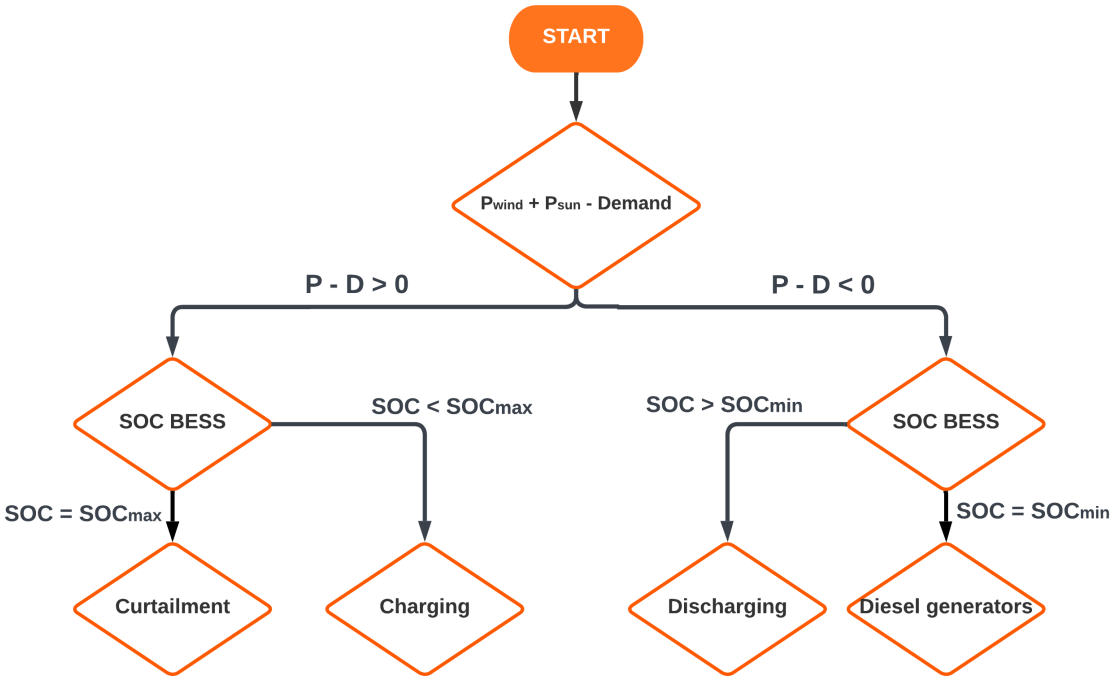

Figure 3.10: Decision scheme of Electricity Production Model of Bonaire.

In figure 3.10, the decision scheme for electricity supply is depicted. First, the model uses the RES comprising the solar and wind energy production, subsequently the BESS is used if it has available capacity. In case the BESS is empty Diesel generator I, followed by Diesel generator II is used. These generators run on Heavy Fuel Oil (HFO). Lastly, there are reserve Diesel generators owned by WEB in case of emergency, which are running on Light Fuel Oil (LFO).

Table 3.1: Current energy production assets on Bonaire (System Expansion 0)

Bonaire Energy System	Number	Available Capacity	Total Available Capacity
Wind Turbine I	1	330 kW	330 kW
Wind Turbine II	12	900 kW	10.8 MW
PV solar park	1	200 kWp	200 kWp
Diesel I (P nominal 2.85 MW)	5	2.50 MW	12.5 MW
Diesel II (P nominal 1.8 MW)	5	1.7 MW	8.5 MW
Diesel Reserve (P nominal 1.8 MW)	4	1.75 MW	7 MW
BESS	1	6 MWh/6MW	6 MWh/6MW

3.4. Scenarios Future Bonaire

The last performed analysis is on future scenarios for the year 2030. First, parameters that influence the technical, economic, and sustainability performance indicators are identified and used to differentiate scenarios among them. The adoption level of electric aircraft is assumed to be the most uncertain parameter with the highest impact among the input parameters. Therefore this is taken as the distinguishing parameter for three scenarios. The other influential parameters are used to differentiate sub-scenarios. The parameters are taken as conservative, moderate, and optimistic values and are sub-scenarios of the scenarios with different adoption levels of EA.

The adoption level of electric aviation is an uncertain and influential parameter that dominates and determines the electricity demand profile and peak demand of BIA, thereby being of concern for the technical performance indicator. Therefore, three adoption levels of electric aviation are considered for future scenarios as thee scenarios.

- Adoption level 1: 9-pax aircraft
- Adoption level 2: 9-, and 19-pax aircraft
- Adoption level 3: 9-, 19-, and 30-pax aircraft

Three scenarios are distinguished based on the adoption level of EA. As there are multiple other input parameters and data that are influential on the three performance indicators, sub-scenarios are drafted. These sub-scenarios are differentiated for conservative, moderate, and optimistic values. Each adoption level is tested for these sub-scenarios.

In addition to the adoption of EA, the electricity demand growth of Bonaire and BIA impacts the load on the grid and thereby the technical performance indicator. Therefore, three different electricity demand growth rates are considered for the sub-scenarios. Since there is no grid connection with surrounding grids, it is assumed that historical electricity production data reflects the historical electricity demand on Bonaire. For the electricity growth, the minimum, average, and maximum growth rate of electricity production at Bonaire for the period 2012-2021 (graph in Appendix A.4) is taken for the conservative, moderate, and optimistic scenarios, respectively.

The second performance indicator is the economic performance indicator. The CAPEX and OPEX costs of the BESS and PV are considered for the sub-scenarios. These cost predictions for 2030 are obtained from NREL forecasts. Secondly, the electricity purchase costs of the grid are based on the historic electricity purchase rates of the period 2016-2030 (graph in Appendix A.3), where the maximum, average, and minimum electricity price is taken for the conservative, moderate, and optimistic scenarios, respectively.
Also, the feed-in tariff is changed for the scenarios. As decentralized energy production is relatively new for Bonaire the impact of widespread decentralized energy production is unknown. Therefore forecasts face a lot of uncertainty and historic trends of the feed-in tariff are absent. The current feed-in tariff of 0.01 $/kWh is taken as the conservative scenario. It is assumed that 0.075 $/kWh is taken as the moderate scenario and the optimistic scenario uses a feed-in tariff of 0.15 $/kWh. The costs for the different scenarios are included in table 3.2.

Table 3.2: Sub-Scenarios with associated costs[76] [75], electricity prices, growth rates, and system expansions.

Sub-Scenarios	Conservative	Moderate	Optimistic
Economic Parameters			
CAPEX PV	1488 $/kW	923 $/kW	709 $/kW
OPEX PV	16.9 $/kW/year	11.6 $/kW/year	9.6 $/kW/year
CAPEX BESS	1109 $/kW	897 $/kW	643 $/kW
OPEX BESS	27.7 $/kW/year	22.4 $/kW/year	16.0 $/kW/year
Electricity Purchase Price	0.425 $/kWh	0.314 $/kWh	0.223 $/kWh
Electricity Feed-in Tariff	0.01 $/kWh	0.075 $/kWh	0.15 $/kWh
Technical Parameter			
Electricity Demand Growth	0%	4%	8%
Sustainable Parameter			
System Expansion	System Expansion 0 No Expansion	Expansion I	Expansion II

Lastly, the sustainability performance indicator is assessed based on the change in CO_2 emissions of grid electricity due to the demand load profile of the airport. With an increasing share of RES in the energy system of Bonaire, the CO_2 emissions related to grid electricity usage decrease. Therefore, different considered system expansions of the electricity production of Bonaire are included. These energy systems expansions are considered and analyzed by WEB for future energy system expansions. In the conservative scenario, there is no expansion (System Expansion 0) and development of the energy system at Bonaire until 2030. Therefore the same energy system is used as was tabulated in 3.1. In the Moderate Scenario, the sustainable energy production changes according to the energy mix tabulated in 3.3 (System Expansion I).

Table 3.3: System Expansion I: New sustainable energy production mix Bonaire for Moderate Scenario

Moderate Scenario	Number	Available Capacity	Total Available Capacity
Wind Turbine I	1	330 kW	330 kW
Wind Turbine II	7	3450 kW	24.15 MW
PV solar park pilot	1	200 kWp	200 kWp
PV solar park II	1	6 MWp	6 MWp
BESS	1	14 MWh/14 MW	14 MWh/14 MW

In the optimistic scenario, the sustainable energy mix on the island changes according to the energy mix tabulated in 3.4 (System Expansion II).

Table 3.4: System Expansion II: New sustainable energy production mix Bonaire Optimistic Scenario

Optimistic Scenario	Number	Available Capacity	Total Available Capacity
Wind Turbine I	1	330 kW	330 kW
Wind Turbine II	13	3450 kW	44.85 MW
PV solar park pilot	1	200 kWp	200 kWp
PV solar park II	1	6 MWp	6 MWp
BESS	1	22 MWh/22 MW	22 MWh/22 MW

As there are 3 control strategies, 3 adoption levels of EA, and 3 sub-scenarios, this ultimately results in 27 scenarios that are evaluated on the three performance indicators. This can be seen in figure 3.11 in the appendix.

The capacity of the system changes with the load profile. Therefore, the capacity power of the BESS is assumed to be scaled to the highest peak power demand of electric aircraft charging. In the case of the 9- and 19-pax, it is 1000 kW, for the 30-pax it is 2500 kW.
The capacity of the solar farm is scaled to the total electricity demand of aircraft charging. As a baseline situation, a solar park of 1000 kWp was considered by the airport. This is used for the 9-pax situation. For the 19-pax, 1300 kWp is used, and for the 30-pax 1600 kWp, scaled to the total electricity demand of the airport. The system sizing is tabulated in 3.5.

Table 3.5: System Sizing for the different scenarios of EA adoption.

System Sizing Scenarios			
	9-pax	9-, 19-pax	9-, 19-, 30-pax
PV	1000 kWp	1300 kWp	1600 kWp
BESS	2000 kWh/1000 kW	2000 kWh/1000 kW	5000 kWh/2500 kW

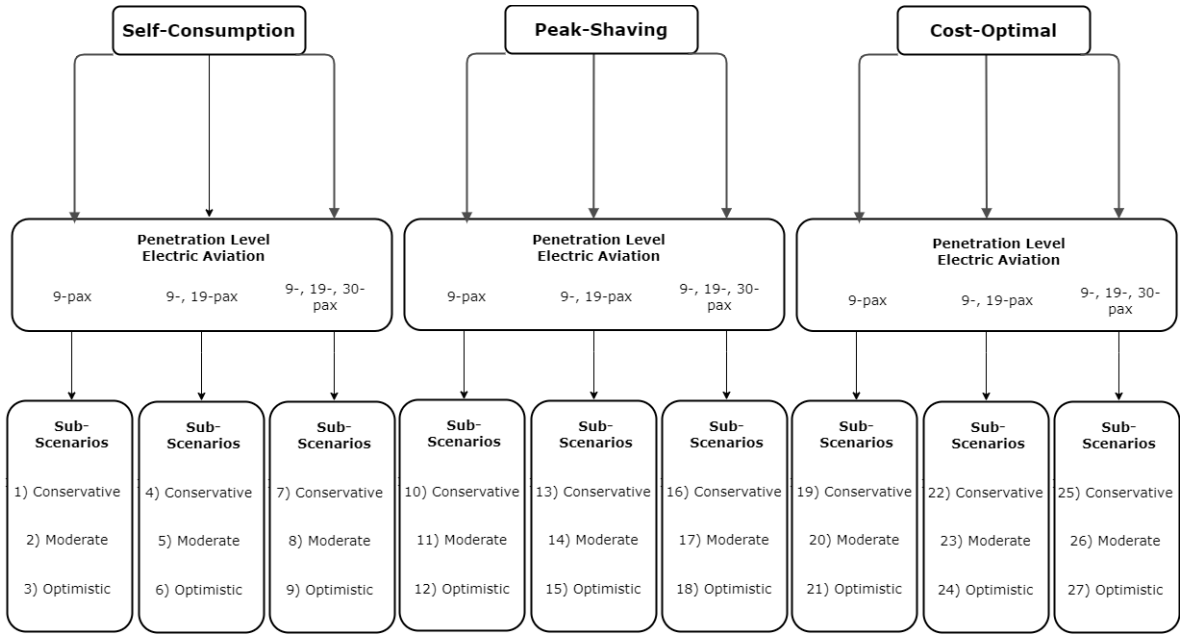

Figure 3.11: Overview of the considered scenarios. 3 control strategies, 3 adoption levels of EA, 3 sub-scenarios results in 3x3x3 = 27 scenarios.

4

Results

This chapter aims to provide the results of the research. First the for the electricity demand profile of charging electric aircraft at BIA is discussed in section 4.1. In section 4.2, the impact on the grid of electric aircraft charging is presented. The third section 4.4 provides the battery profiles resulting from the model and the performance indicators. The last section 4.5, provides the results of the sensitivity of the performance indicators to future scenarios.

4.1. Results Electricity Demand Profile Electric Aviation

Considering the whole flight schedule, at BIA the largest share of flights is covered by the short-range types of flights as can be seen in table 4.1, these include the flights to Aruba and Curaçao. The large distance flights and the large aircraft are not considered further.

In Chapter 2 the electric aircraft was discussed. The currently operating small aircraft at BIA feasible to be replaced are the DHC-6 Twin Otter (DHC-6), the Britten-Norman Islander (BNI), and Saab 340 (S340), which are all turboprop aircraft. Table 4.2 summarizes the aircraft replacements and their electric alternatives as well as their route- and passenger specifications.

Table 4.1: The most used routes of flights at BIA [34]

#	Destination	Flights/week
1	Curaçao	156
2	Amsterdam	14
3	Aruba	5
4	Miami	3
5	Atlanta	2
6	New York	1
7	Santo Domingo	1
8	Houston	1

Flights between Curaçao and Bonaire are operated on an approximately two-hour basis using a DHC-6 Twin Otter to carry 20 passengers between the islands or using the 9-passenger Britten-Norman Islander [34]. The DHC-6 is substituted with the ES-19 electric aircraft, and the BNI is replaced with the 9-seater Alice. The larger aircraft is the Saab 340 (S340), which is a turboprop aircraft with a 34-passenger capacity operating between Bonaire, Aruba, and Curaçao [34]. The S340 will be replaced by the ES-30 which has a seating capacity of 30 passengers.

Table 4.2: Summary of considered aircraft for electrification at BIA and feasible aircraft designs with comparable pax that are claimed to be commercially operated within the period until 2030.

Current Aircraft	Destination	Distance (km)	Pax	Frequency	Electric Aircraft	Pax
DHC-6	Curacao	79	20	Every 2 hours	**ES-19**	19
BNI	Curacao	79	9	Every 2 hours	**Alice**	9
S340	Curacao	79	34	2-3/day	**ES-30**	30
S340	Aruba	190	34	Weekly	**ES-30**	30

The energy consumption approximated using both the Breguet range equation and the take-off and climb equation for electric aircraft Alice, ES-19, and ES-30 and their destinations are summarized in table 4.3. The input parameters for the Breguet range equation and for the take-off and climbing equation are tabulated in A.1 in Appendix A.2.1. The charging power will be twice the value of the total electricity demand for each trip of the electric aircraft as the turnaround time is 30 minutes. The resulting charging profiles are seen in Chapter 4.2 in figures 4.1, 4.2, and 4.3 by the green curves.

Table 4.3: Energy consumption for commercially operating electric aircraft for Curacao and Aruba.

	Alice (9 pax)	**ES-19 (19 pax)**	**ES-30 (30 pax)**
Curacao (76 km)	245 kWh	241 kWh	588 kWh
Charging Power (30 Min)	489 kW	482 kW	1176 kW
Aruba (194 km)	529 kWh	535 kWh	1334 kWh
Charging Power (30 Min)	1059 kW	1070 kW	2667 kW

4.2. Results Grid Impact Electric Aviation no BESS

This section aims to construct the total load of the airport BIA, which includes the load of the baseload of the airport itself and the additional load of charging the electric aircraft. Ultimately, this load profile will be used to analyze the impact on the grid. In this case, there is no BESS included, and is referred to hereafter as the Business-as-usual case (BaU).

4.2.1. Electricity Demand Profile without PV

In Chapter 4.1, the approximation of energy consumption of electric aircraft capable of replacing the conventional aircraft in the current flight schedule is provided. Analyzing the current flight schedule reveals that a turnaround time of 25 minutes is common. As the model runs on a 15-minute base, the turnaround times are assumed to be 30 minutes and the departure times are rounded to the nearest quarter of the hour.
The charging of the batteries of the electric aircraft is executed with a 2C rate (30 minutes), taking into account the battery charging efficiency of 95% and additional system losses which are assumed to be 90%. The resulting charging profiles are depicted in figures 4.1, 4.2, and 4.3 by the green curves. The yellow curves represent the total load of the airport consisting of the baseload (red) of the airport and the charging profile.

Figure 4.1: Charging load profile of electric aircraft for one week (Monday - Sunday) on a 15-minute basis for 9-passenger aircraft.

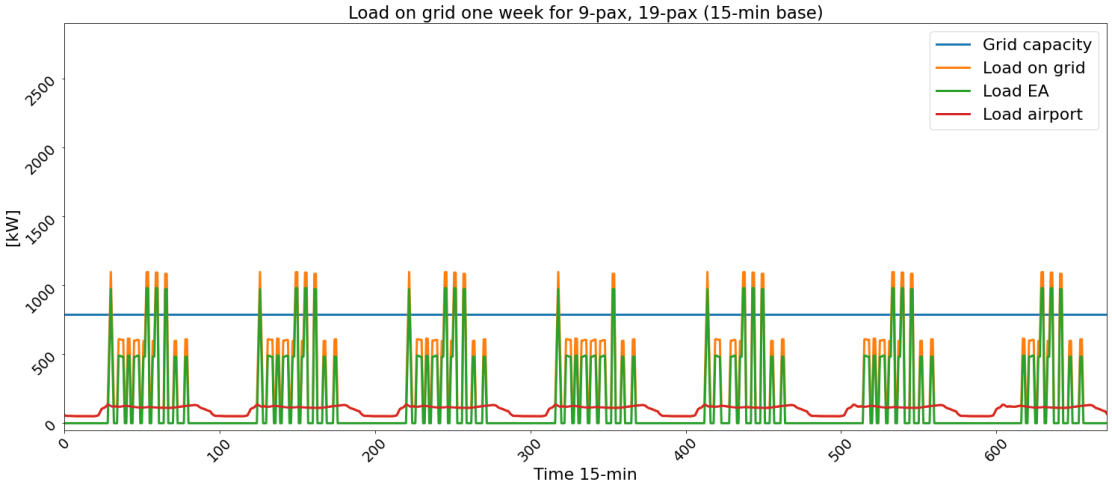

Figure 4.2: Charging load profile of electric aircraft for one week (Monday - Sunday) on a 15-minute basis for 9- and 19-passenger aircraft.

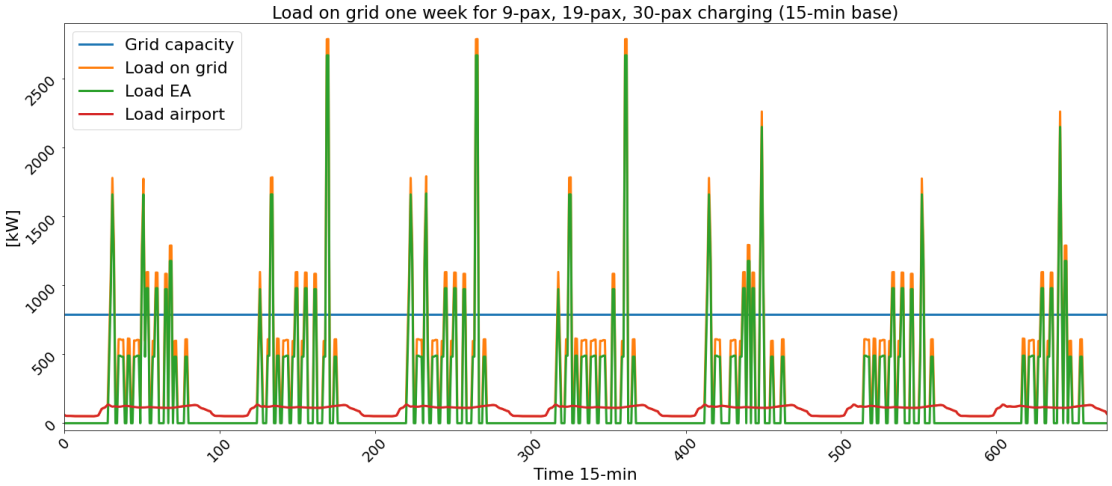

Figure 4.3: Charging load profile of electric aircraft for one week (Monday - Sunday) on a 15-minute basis for 9- and 19- and 30-passenger aircraft.

4.2.2. Electricity Demand Profile with PV

The previous electricity demand profiles of BIA are the Business-as-Usual case. In the context of future developments, BIA will install an on-site PV solar park. Considering a 1.0 MWp PV solar park without the deployment of a BESS, the resulting electricity demand profile for one week is depicted in figure 4.4. The lowest graph is the PV system output and the middle graph is the total electricity demand of the airport for the 9-pax aircraft charging. The top graph is derived from the summation of the two lower graphs. The negative load sign indicates that BIA is feeding electricity back to the grid.
The same graphical representations of these profiles for the expanded adoption of electric aircraft are provided in Appendix A.3.1.

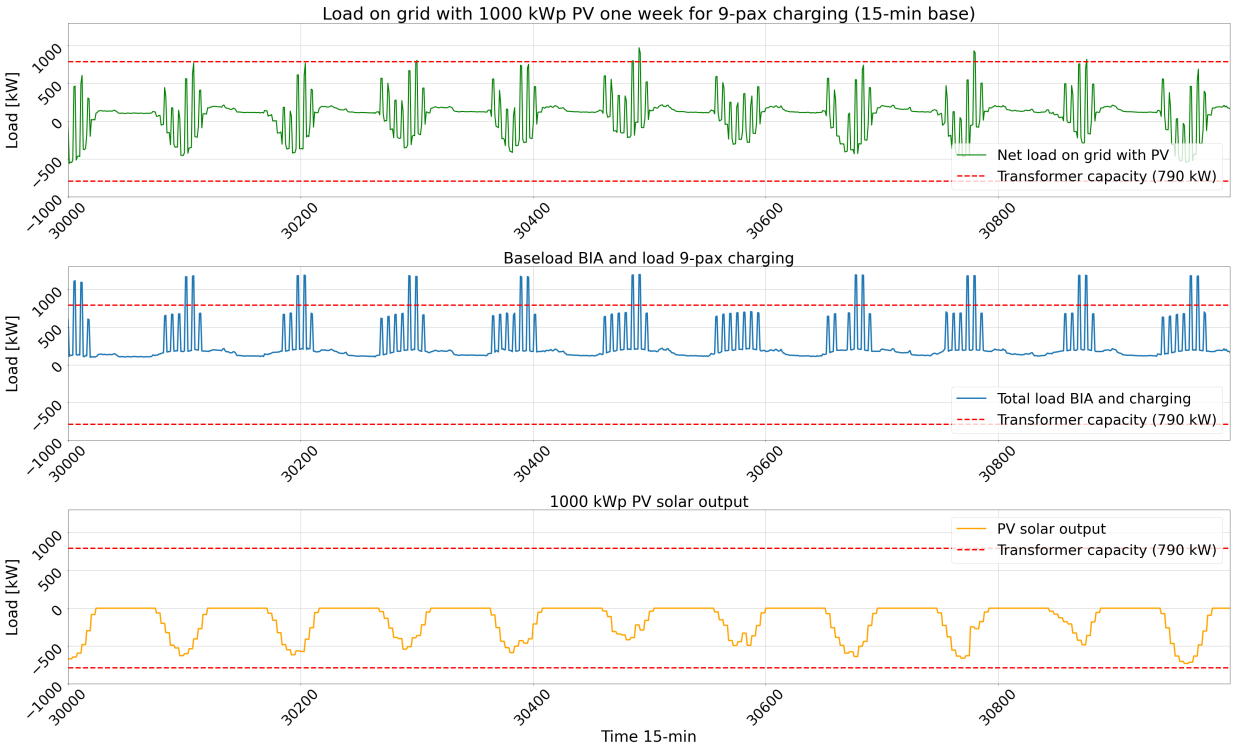

Figure 4.4: Demand profile of BIA for 9-pax aircraft charging and 1 MWp PV solar park installed.

4.3. Impact on the Grid

In this section, the following results regarding the impact on the grid infrastructure are presented: the transformer overloading and duration (hours), the grid cable load (%), and the voltage fluctuations (%). This is done for the Business-as-Usual situation (BaU) and for the case with a 1 MWp installed solar park. A summary of the grid impact for those cases is tabulated in table 4.4 at the end of the section.

From the presented figures 4.1, 4.2, and 4.3, it can be seen that the transformer capacity (-790 kW,790 kW) that connects BIA to the grid is overloaded. In the Business-as-Usual situation, the transformer is overloaded for 313 hours, 560.75 hours, and 952.25 hours during one year with increasing electric aircraft adoption. Transformer overloadings are seen when two aircraft need to be charged simultaneously for the 9-, and 19-pax adoption level. When the 30-passenger aircraft is adopted into the flight schedule, more and heavier overloads of the transformer are observed as aircraft are charged outside the solar irradiation time window.
However, the installation of a 1 MWp solar park considerably lowers the hours of transformer overloading. In figure 4.4, it is evident that the 1000 kWp PV solar park reduces the peak loads. Nevertheless, the charging of electric aircraft still leads to instances of transformer overloading when aircraft are simultaneously charged during days of diminished availability of solar irradiance. In appendix A, the same figures can be seen for the expanded adoption of electric aircraft. In those figures A.5 and A.6 peaks exceeding the transformer capacity are seen more frequently due to aircraft charging outside the window of solar irradiance. Conversely, the surplus of electricity generated by the solar park is fed back into the grid, which is represented in the graphs by a negative grid load.

Figure 4.5 represents the span of loads on the cables of the grid. It is observed that a solar park slightly reduces the maximum load on the cables that connect the airport to the grid. This is also apparent from figure 4.4. The same trend remains with the adoption of electric aircraft as is depicted in figure 4.5. In all cases, the PV installation of 1000 Wp, reduces the minimum to 0% which states intermittent periods during which the airport is occasionally operating independently of the grid imposing no load on the cables of the distribution grid. This is possible as the transformer of the airport is located at the end of a grid cable line.

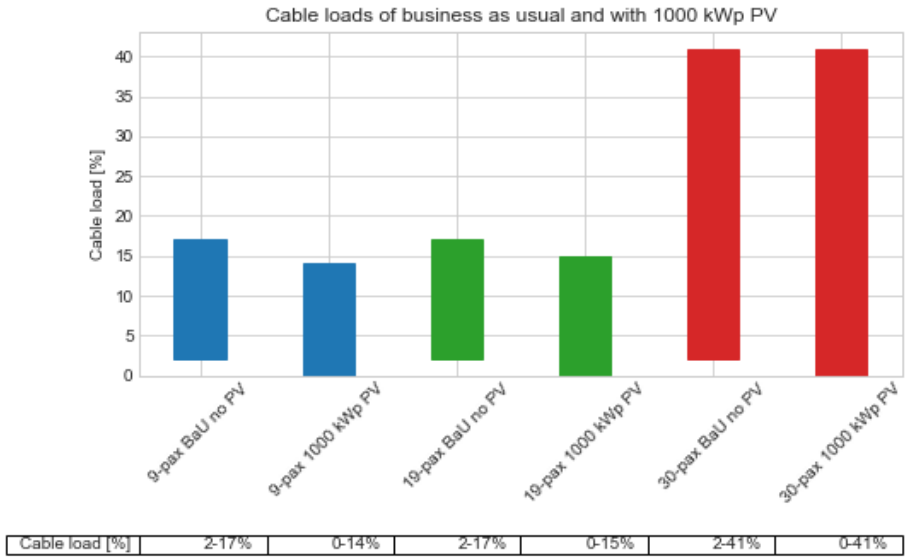

Figure 4.5: Cable load range for the business-as-usual case and with installed 1000 Wp solar park. This is done for an increased adoption of electric aircraft.

In the context of voltage fluctuations, depicted in figure 4.6, it is noticeable that with the increasing adoption of electric aircraft, the voltage dropped to 98% of 12.2kV. The deployment of a 1000 kWp solar park reduces sudden peak loads of power demand and consequently reduces the voltage drop. Considering all cases, the voltage fluctuations remain within the acceptable range of voltage fluctuations, which spans from 95% to 105%.

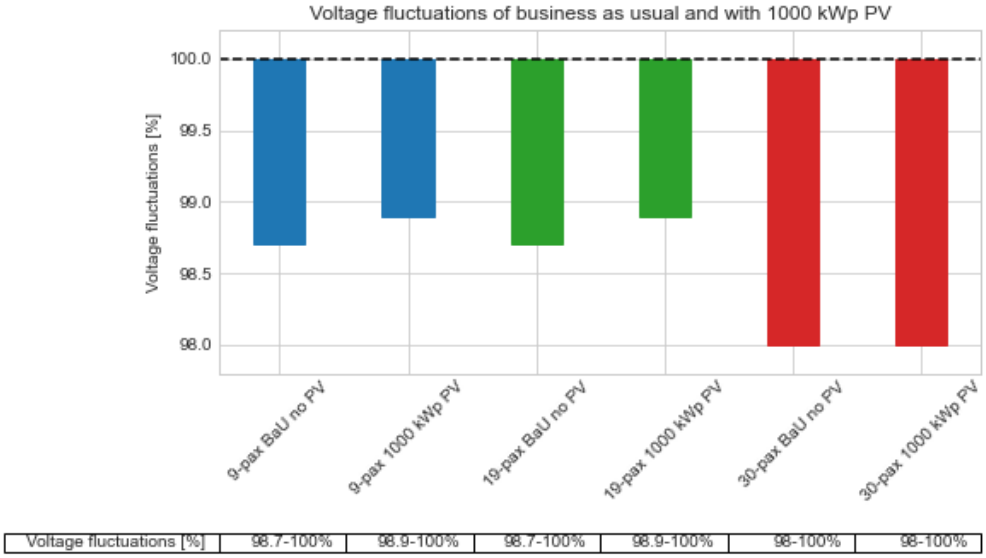

Figure 4.6: Voltage fluctuations range for the business-as-usual case and with installed 1000 Wp solar park. This is done for an increased adoption of electric aircraft. The acceptable range of voltage fluctuations is projected by the striped red lines.

Table 4.4: A summary of the impact on the grid for different adoption levels of EA. The overloading of the transformer and the maximum duration of the overloading are given in hours or minutes. The cable capacity is given as the % of the maximum cable capacity. The voltage fluctuations are given in %. The acceptable range of the voltage fluctuations is between 95%-105%.

	9-pax Load		**9-, 19-pax Load**		**9-. 19-, 30-pax Load**	
	no PV	1 MWp PV	no PV	1 MWp	no PV	1 MWp PV
Transformer Overload [Hour]	313 hours	7.5 hour	560.75 hours	142.5 hour	952.25 hours	512.75 hour
Max Duration Overload [min]	30 min	30 min	30 min	30 min	45 min	45 min
Cable Load [%]	2-17%	0-14%	2-17%	0-15%	2-41%	0-41%
Voltage Fluctuations [%]	98.7%-100%	98.8%-100%	98.7%-100%	98.9%-100%	98%-100%	98%-100%

4.4. Results Model Control Strategies BESS

This section presents the resulting load profile and the performance indicator of different BESS control strategies. Furthermore, a comparison is made between the control strategies and the business-as-usual cases. All the performance indicators are specifically given for the 9-pax electric aircraft charging and a 2000kWh/1000kW BESS and 1000 kWp PV. First, the resulting load profiles for a week are presented, Subsequently, the technical performance indicator and the economic performance indicator will be presented, and lastly, the results of the environmental performance indicator are provided.

4.4.1. Model Control Strategies

Self-Consumption

The load profile of the BESS over the course of one week (Friday-Thursday) under the Self-Consumption control strategy is depicted in figure 4.7, In this figure, the upper graph includes the PV power output (displayed in negative and red), together with the charging and discharging patterns. As the objective of this strategy is Self-Consumption, PV electricity is predominantly used for immediate consumption by the load. During intervals with no aircraft charging there is a surplus of PV electricity which is used for charging the BESS or grid injection in case the BESS reaches full capacity. However, when the PV power does not suffice to meet the load, the BESS is discharged which is primarily during aircraft charging which is associated with high power demand, or during the night.
The resulting charging and discharging behavior of the BESS results in the State of Charge (SOC) which is depicted in the middle graph, here it is evident that the BESS is charged during daylight hours. In the upper graph, the 6th day exhibits a low PV output which results in the highest peaks of this week (as shown in the bottom graph in orange). Conversely, the first day experiences a surplus of electricity. It can be seen that the battery reaches full capacity during the day and is therefore required to discharge immediately to free up capacity during the day. During those days, peaks can arise on the feed-in side. The bottom graph represents the total demand of the airport in blue and in orange the resultant load on the grid due to the BESS and the solar park activity. Although the BESS and the solar park effectively reduce the load on the grid, some peaks are recognized in load demand during low irradiation periods while there are power injections into the grid during periods of high irradiation.

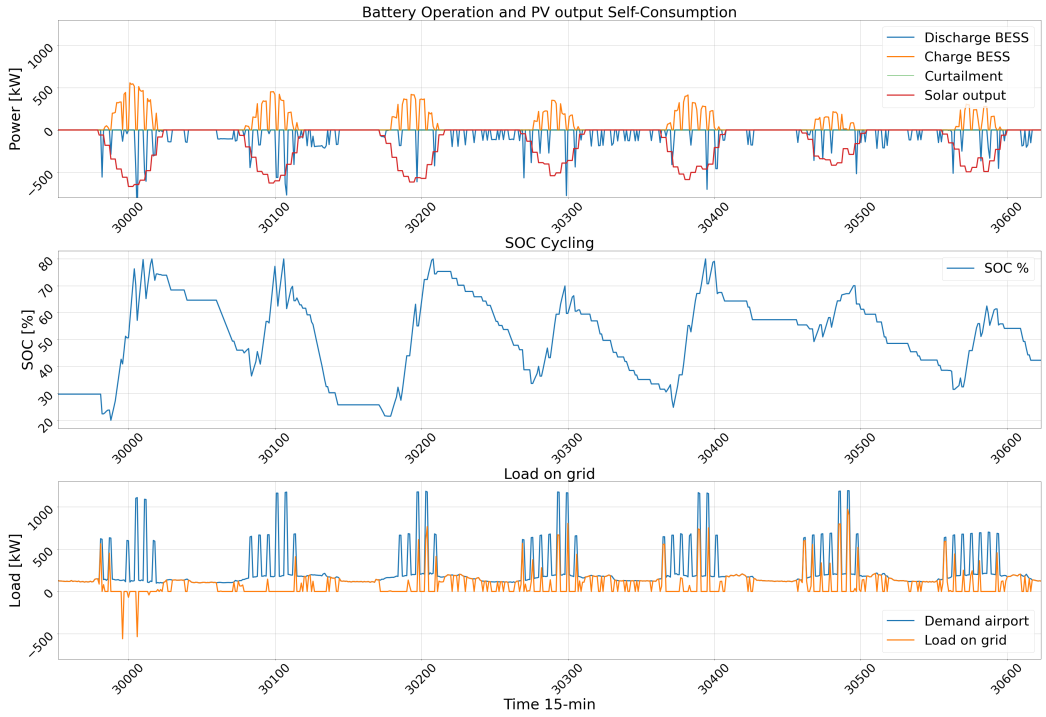

Figure 4.7: The battery charging profile of a 2000kWh/1000kW BESS in combination with a 1000 kWp solar park controlled by Self-Consumption. The upper graph represents the (dis)charging behavior of the battery and the PV electricity production (negative). The graph in the middle provides the resulting SOC-cycling of the BESS. Lastly, the total demand profile of the airport and the net grid load are given in the graph at the bottom.

Peak Shaving

Derived from the optimization model, the resultant load profile of the BESS controlled by Peak Shaving for the same week is depicted in figure 4.8.

From the graph in the middle of the figure, it can be noticed that the battery gradually discharged during the nighttime hours. However, the BESS maintains a reserve of about 50% SOC during the night from the 5th to the 6th day as on the 6th day there will be low irradiance. The peaks with Peak Shaving are lowered to 50% of the initial peak load.

In the bottom graph, the load on the grid is seen with the red-striped Peak Shaving thresholds. It is evident from this graph that the peak shaving is working through in both the demand side as well as in the electricity injection into the grid and cycles between the maximum and minimum peak shaving thresholds. In particular, the Peak Shave strategy successfully operates on the 6th day, where the peaks that were present with the Self-Consumption strategy are lowered to the maximum peak shaving threshold.

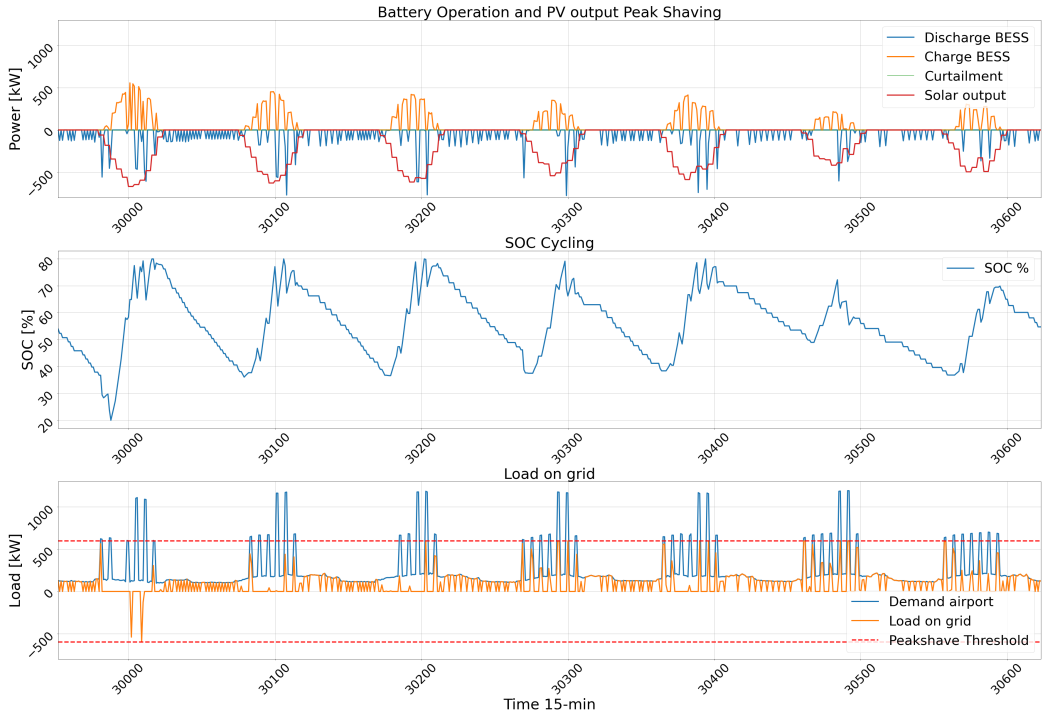

Figure 4.8: The battery charging profile of a 2000kWh/1000kW BESS in combination with a 1000 kWp solar park controlled by Peak Shaving.

Cost-Optimal

The BESS profile and the associated grid load resulting from the cost-optimal optimization model are graphically presented in figure 4.9.

The implementation of the Cost-Optimal strategy actively minimizes the peak load on the grid as there is a cost associated with the exerted peak load on the grid. As illustrated in the bottom graph, the peaks on the grid are relatively low to mitigate the associated peak load costs. Furthermore, it is seen that the energy in the battery is predominantly used for aircraft charging and the battery keeps a capacity reserve for forthcoming days of low irradiance.

Figure 4.9: The battery charging profile of a 2000kWh/1000kW BESS in combination with a 1000 kWp solar park controlled by Cost-Optimal.

4.4.2. Technical Performance Indicator

The total grid load profile for each BESS control strategy is given in figure 4.10. In this figure, the green curve represents the Self-Consumption strategy, the red curve the Peak Shaving strategy, and the blue curve the Cost-Optimal strategy. Furthermore, the purple lines depict the transformer capacity (-790kW,790kW). Lastly, the yellow curves represent the load on the grid in the Business-as-Usual where only a 1000 kWp PV park is installed and no BESS is deployed. This case is taken into account for comparison purposes.

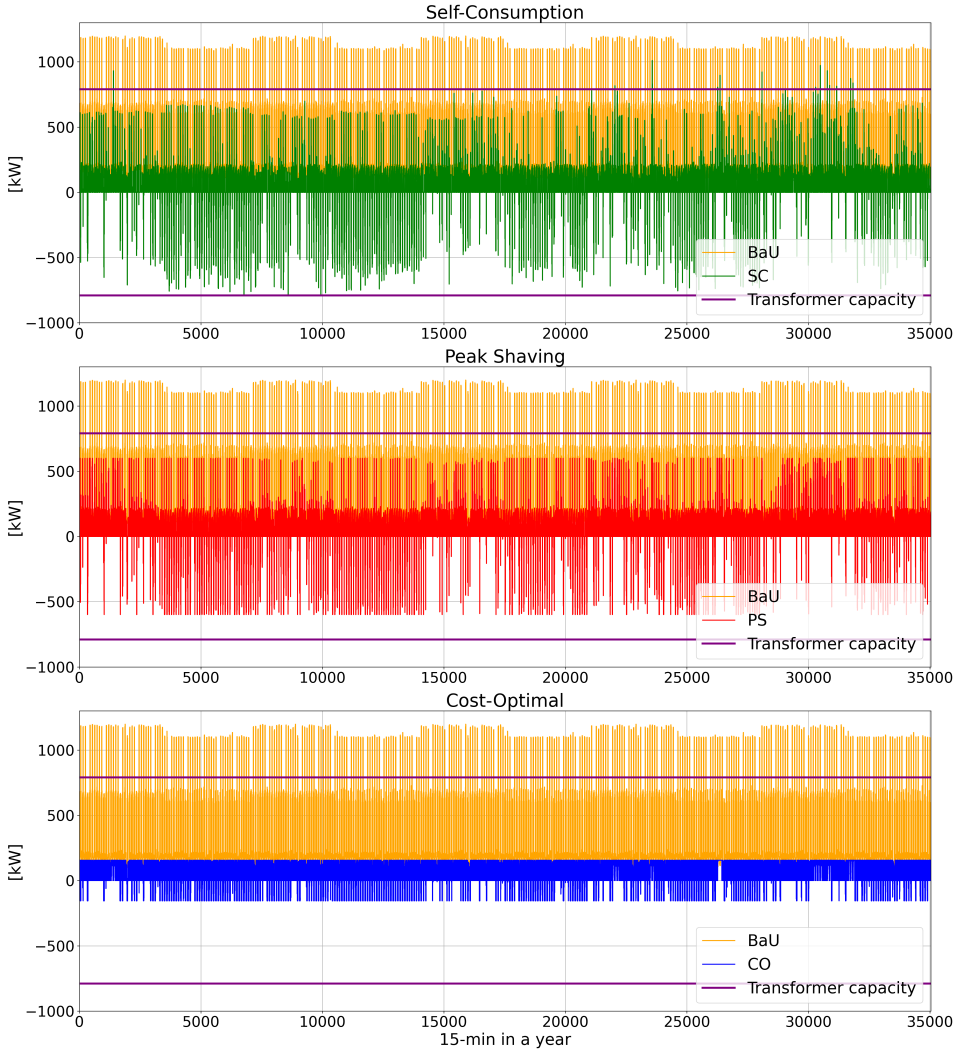

Figure 4.10: Comparison of the Business-as-Usual with PV (BaU) with a PV system of 1000 kWp, Self-consumption (SC), Peak shaving (PS), and Cost-optimal (CO) control strategies for the entire year with a BESS 2000kWh/1000kW and a PV system of 1000 kW.

From figure 4.10, it is observed that in the Business-as-Usual case with PV (yellow), peaks exceed the transformer capacity even though a 1000 kWp solar park is installed. Conversely, depending on the control strategy, a BESS manages to operate within the transformer capacity, both for grid electricity demand and grid feed-in. As previously found, the number of hours of transformer overloading for the adoption of 9-pax aircraft with a 1 MWp solar park was 7.5 hours. When operating a BESS with Self-Consumption this is reduced to 5.25 hours. With the other control strategies, no transformer overloads are observed. These results can be found in the summarizing table 4.5 at the end of the section. In the same table, the maximum feed-in and demand peaks are included for the different control strategies and the Business-as-usual situation for comparison purposes. The maximum peak demand is not reduced by controlling the BESS by Self-Consumption compared to a solar park without a BESS. In contrast to the Peak Shaving BESS, which is able to effectively reduce the peak load both in demand and feed-in to 50% of the initial peak demand. Lastly, the Cost-Optimal BESS is able to reduce the peaks both in demand and feed-in substantially to only 155 kW by actively minimizing the peak power costs.

For the grid analysis in Vision, the load profile during the worst week in terms of solar irradiation is taken which is the week of Monday 14th until Sunday 20th of November (t = 30242:30914). From Vision, the voltage fluctuations on the grid and the load on the cables on the grid are obtained. In figures 4.11 and 4.12, the results of the voltage fluctuations from the 12.2 kV of the grid and the load on the cables of the grid are depicted. As was observed earlier the Business-as-Usual case without PV

has the largest voltage drop, however, it is clear that the BESS does not cause a significant change in voltage drop. With the installation of 1000 kWp PV the voltage drop is reduced by 0.2% while adding a BESS the voltage drop is reduced by either 0.2% or 0.3% depending on the control strategy. Taking into account that the acceptable range of voltage fluctuations is in the range of 95%-105%, no unacceptable voltage fluctuations are observed in the case with and without a BESS or PV.

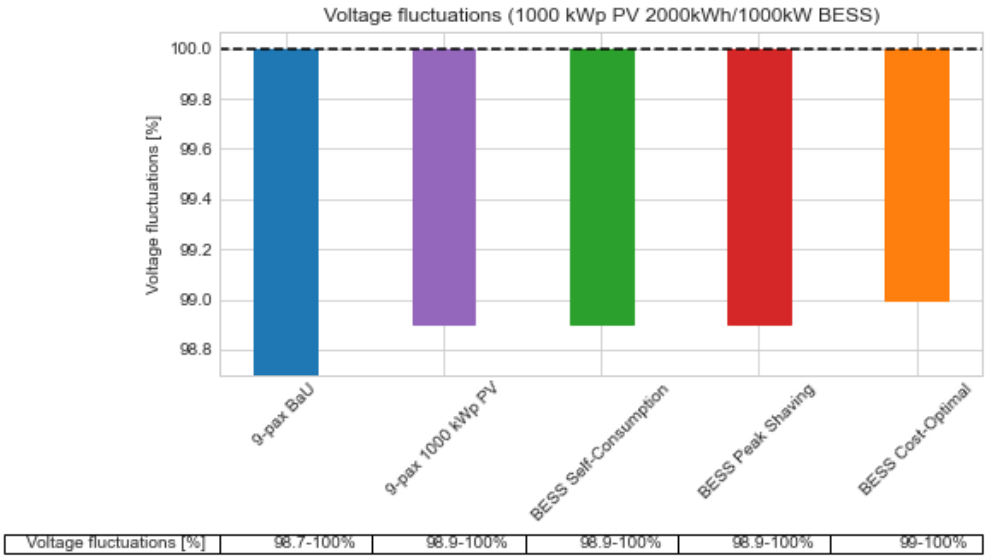

Figure 4.11: Voltage fluctuations range for the business-as-usual case and with installed 1000 Wp solar park. This is done for an increased penetration of electric aircraft.

The differences in the load on the grid cables are more significant among the different control strategies. The Self-Consumption reduces the maximum peak load on the grid cables to 14%. With the control strategy of 50% Peak Shaving the cable load is reduced even more to 8%. The lowest load on the cables of the grid is obtained by Cost-Optimal controlled BESS.
A summary of the technical performance indicator is given in table 4.5.

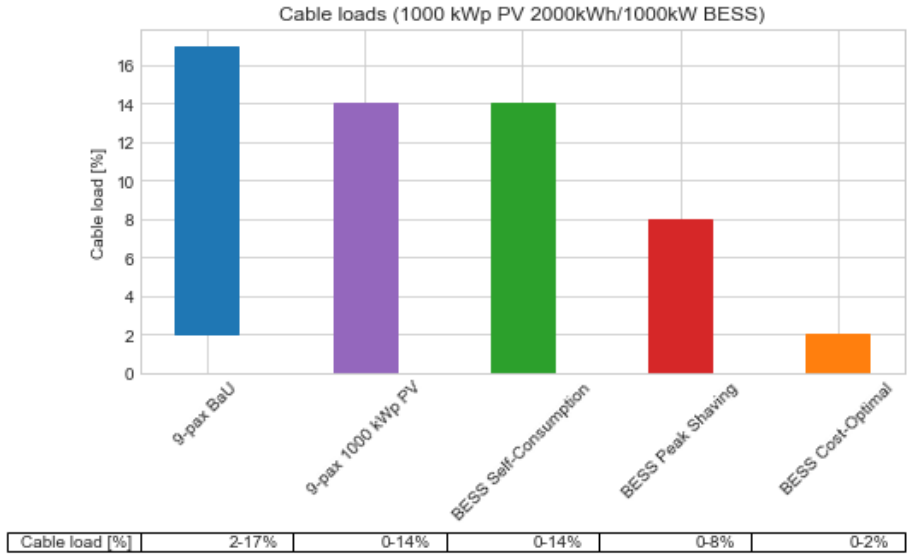

Figure 4.12: Cable load range for the business-as-usual case and with installed 1000 Wp solar park. This is done for an increased penetration of electric aircraft.

Table 4.5: A summary of the technical performance indicator for the different control strategies with the 9-pax electric aircraft adoption level. The results are compared to the previously presented results from the Business-as-usual case and the case with 1 MWp installed.

9-pax EA Charging	Business-as-Usual		Self-Consumption	Peak Shaving	Cost-Optimal
	no PV	1 MWp PV			
Transformer Overload [Hour]	313 hours	7.5 hours	5.25 hours	0 hours	0 hours
Max Duration Overload [min]	30 min	30 min	30 min	0 min	0 min
Cable Load [%]	2-17%	0-14%	0-14%	0-8%	0-2%
Voltage Fluctuations [%] of 12.2kV	98.7%-100%	98.8%-100%	98.9%-100%	98.9%-100%	99.0%-100%
Peak Load Demand [kW]	1198 kW	1010 kW	1010 kW	599 kW	155 kW
Peak Load Feed-in [kW]	99 kW	-690 kW	-788 kW	-599 kW	-155 kW

4.4.3. Economic Performance Indicator

This section provides the results of the economic analysis. The LCOE of the system at the airport and its cost components for the Business-as-Usual cases and for the different battery control strategies are obtained and presented in figure 4.13.

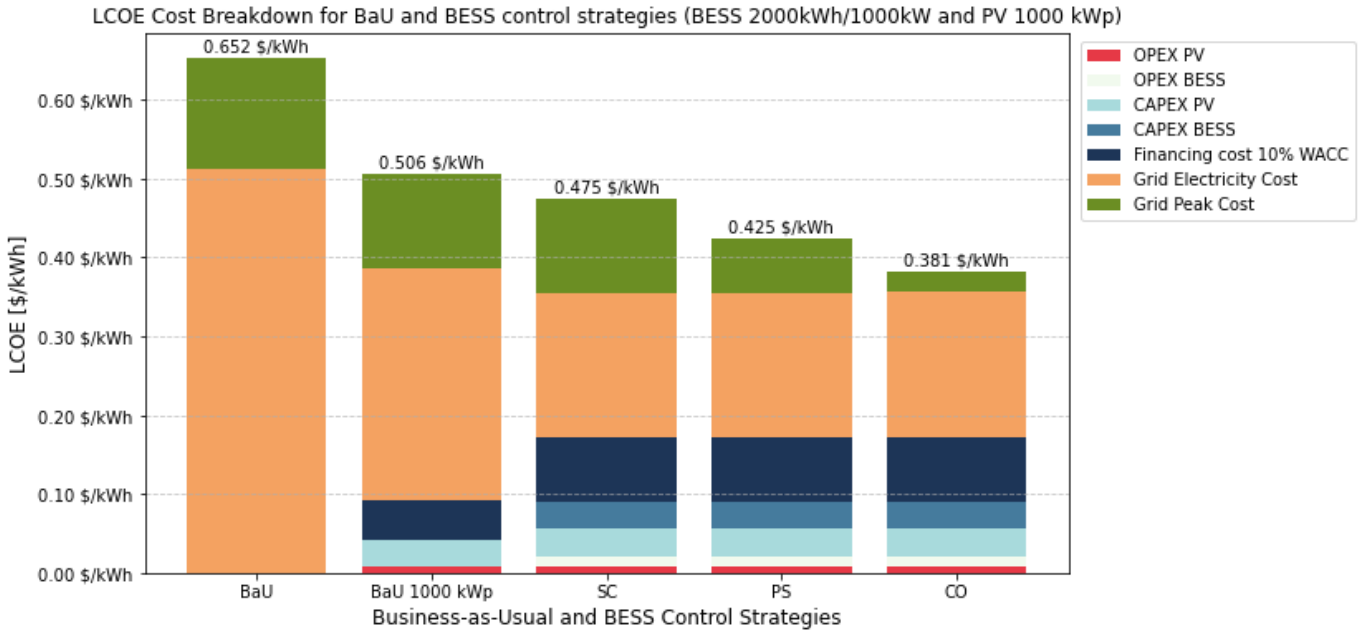

Figure 4.13: LCOE of airport's system for all cases

It is evident from the figure that for the Business-as-Usual case, the main cost is covered by the electricity purchase cost. Secondly, the cost related to the peak load on the grid covers the rest of the total costs. This results in an LCOE 0.652 $/kWh of the airport over a period of 15 years.
The installation of a 1000 kWp solar park leads to a lower LCOE for the airport. Even though the solar park induces CAPEX, OPEX, and financing costs, the reduction in peak load costs and the reduced costs of electricity purchase results in an LCOE of 0.506 $/kWh.

The deployment of the BESS induces extra CAPEX, OPEX, and financing costs to the total costs. The OPEX costs are paid annually. The lifetime is determined with the rainflow counting discussed in 3.3.5. For this system sizing each of the control strategies needs to replace the BESS after rounded 15 years.

A significant reduction in grid electricity purchase cost is seen due to the deployment of the BESS which managed to use PV electricity more efficiently. Moreover, it becomes clear from figure 4.13 that the costs associated with the peak load on the grid are lowered, however, this depends on the used control strategy. The costs of the deployment of the BESS are extinguished by the lower costs of electricity purchase and the corresponding peak load costs. Ultimately, the deployment of a BESS with Self-Consumption as an addition to the solar park leads to a relatively small reduction of 0.031 $/kWh in LCOE.
Utilizing the Peak Shaving controlled BESS effectively constrains the load on the grid not surpassing 50% of the peak load of the total demand profile. Consequently, this control strategy ensures that the costs related to the peak load on the grid are reduced too. The remaining cost components of the Peak Shaving controlled BESS are comparable to the cost components of the Self-Consumption controlled BESS. This yields an LCOE of 0.425 $/kWh.
Lastly, the lowest costs are achieved by the control strategy of the Cost-Optimal BESS, which results in a peak load cost reduction of 85% over the Business-as-Usual case. The LCOE is the lowest for the Cost-Optimal controlled BESS with 0.381 $/kWh.

From the graph in figure 4.6, it can be concluded that depending on the control strategy a BESS is able to reduce the LCOE by 27%-42% compared to the Business-as-Usual case. Compared to the solar-only case, the reduction in LCOE is significantly reduced. A major factor in reducing the cost with respect to the Business-as-Usual case was the effective use of electricity leading to lower purchase costs and the peak load price. Secondly, the cost of peak load creates differences in the total cost under the different BESS control strategies as can be seen from table 4.6, in which an overview of all the cost components is provided.

Table 4.6: Summary of the cost components of LCOE over a period of 15 years using a WACC of 10 %.

LCOE Cost Components [$/kWh] for the airport system: BESS 2000 kWh/1000kW, PV 1000 kWp						
		Business-as-Usual	**Business-as-Usual 1000 kWp**	**Self-Consumption**	**Peak-Shaving**	**Cost-Optimal**
Lifetime	PV system	-	20 years	20 years	20 years	20 years
	BESS	-	-	15.60 years	16.46 years	15.84 years
CAPEX	PV system	-	0.035 $/kWh	0.035 $/kWh	0.035 $/kWh	0.035 $/kWh
	BESS	-	-	0.034 $/kWh	0.034 $/kWh	0.034 $/kWh
Financing	System	-	0.049 $/kWh	0.081 $/kWh	0.081 $/kWh	0.081 $/kWh
OPEX	PV system	-	0.008 $/kWh	0.008 $/kWh	0.008 $/kWh	0.008 $/kWh
	BESS	-	-	0.013 $/kWh	0.013 $/kWh	0.013 $/kWh
Variable Cost	Peak Load	0.141 $/kWh	0.119 $/kWh	0.119 $/kWh	0.070 $/kWh	0.026 $/kWh
	Electricity	0.511 $/kWh	0.294 $/kWh	0.185 $/kWh	0.183 $/kWh	0.185 $/kWh
Total	**LCOE**	**0.652 $/kWh**	**0.506 $/kWh**	**0.475 $/kWh**	**0.412 $/kWh**	**0.382 $/kWh**

4.4.4. Environmental Performance Indicator

This section presents the environmental performance indicator of the airport for the Business-as-Usual cases. Moreover, the results of the performance indicator for each of the battery strategies are provided. First, the self-sufficiency of the airport is given. Subsequently, the change of CO_2 emissions originating from the grid electricity is given. The change is measured for each control strategy as the difference between the CO_2 emissions before EA was adopted and after EA was adopted. This change in CO_2 is considered as the environmental performance indicator.

As was discussed in Chapter 2 the energy system of Bonaire consists of diesel generators, wind turbines, a solar park, and a BESS. With the 9-pax aircraft, a 2000kWh/1000kW BESS, and 1000 kWp solar park, the self-sufficiency rates, and the change in CO_2 emissions from diesel generators are given in table 4.7 and depicted in figure 4.14.

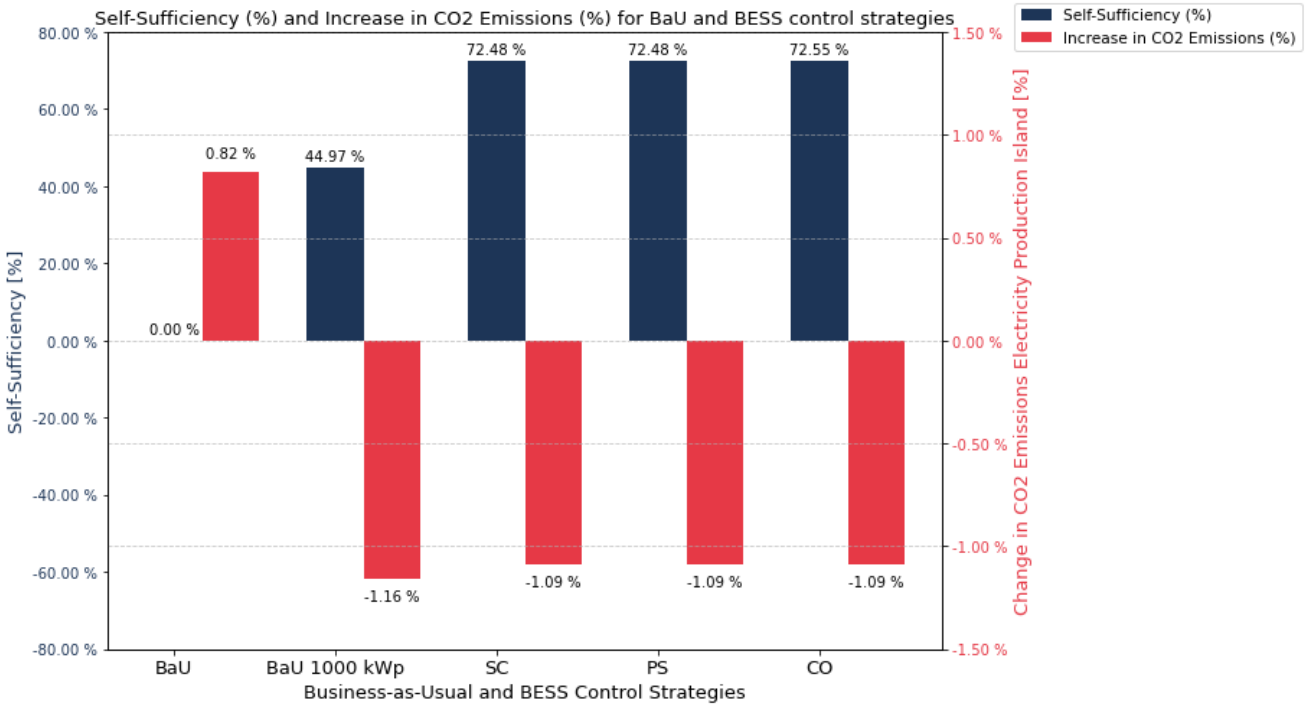

Figure 4.14: Sustainable Performance Indicator for Business-as-Usual cases and BESS control strategies. These are the results of the 9-pax aircraft charging.

First, from table 4.7 it is seen that the self-sufficiency of the BESS-included cases is significantly increased compared to the Business-as-Usual case without a BESS and with a 1000 kWp solar park. However, between the different control strategies, the differences in self-sufficiency are insignificant. The Self-Consumption is optimized to achieve a high self-consumption and thereby a high self-sufficiency. The Peak Shaving BESS is able to operate with the same self-sufficiency while halving the peak demand loads on the grid. However, for the sizing used, it is seen that the cost-optimal solution results in a higher self-sufficiency although very small.
In the appendix, figures A.7, A.8, A.9, show the sum of all load flows over the entire year for the different control strategies from which the self-sufficiency can be calculated.

The rest of the electricity is taken from the grid and affects the total CO_2 emissions originating from the grid electricity production of the island. In table 4.7, the change of the CO_2 emissions from grid electricity in case EA is adopted and the BESS and PV system are installed at the airport is given compared to the emissions before EA was adopted.
The Business-as-Usual scenario without a solar park results in an increase in CO_2 emissions of +0.82%, as all the extra aircraft charging load is taken from the grid. The addition of the solar park realizes a reduction of CO_2 emissions in the electricity production of -1.16%. For the BESS control strategies, the CO_2 emissions from the grid are reduced less, resulting in -1.09%.

Table 4.7: Sustainability performance of the Business-as-Usual with and without a solar park installed, and the BESS control strategies. These are the results of the 9-pax aircraft charging

	Self-Sufficiency	**% Total increased CO2**
BaU No PV	-	+0.82%
BaU 1000 PV	44.97%	-1.16%
Self-consumption	72.48%	-1.09%
Peak Shaving	72.48%	-1.09%
Cost-Optimal	72.55%	-1.09%

4.5. Results Future Scenarios Bonaire

This section presents the results of the sensitivity analysis of the performance indicators to changes in input parameters and data of future scenarios. As the development of the technology of electric aviation until 2030 is uncertain, this is chosen as the main parameter to change. Therefore, three distinctive scenarios for the three adoption levels of EA are drafted, with each scenario divided into three sub-scenario (conservative, moderate, and optimistic). These scenarios are all tested for each of the control strategies of the BESS.

In each figure, the same methodology has been followed where the blue colors denote the Self-Consumption control strategy, while the red colors correspond to the Peak Shave controlled BESS, and the green colors represent the Cost-Optimal controlled BESS. Secondly, the darkness of the colors indicates the sub-scenarios, where the light color corresponds to the conservative sub-scenario and the darkest color to the optimistic sub-scenario.

4.5.1. Sensitivity Technical Performance Indicator

The sensitivity of four parameters is presented: Airport peak load (figure 4.15), Grid cable load (figure 4.16), Voltage fluctuations of the airport (figure 4.18), and the Peak load of the island (figure 4.17).

In figure 4.15 the peaks of the electricity feed-in (negative) and demand (positive) are graphed. It is seen that Self-Consumption leads to the highest peaks both in electricity demand and feed-in at the airport. Furthermore, with a higher adoption level of electric aircraft, the peak loads of the airport increased accordingly, with the Self-Consumption strategy exhibiting the heaviest sensitivity. Additionally considering the sub-scenarios, different demand growth rates for the airport baseload cause an increase in the peak loads as seen from figure 4.15. However, with 50% Peak Shaving these growth rates can be effectively controlled. The peak loads, either in electricity demand or injection, can be recognized in figure 4.16, where the load on the grid cables is graphed.

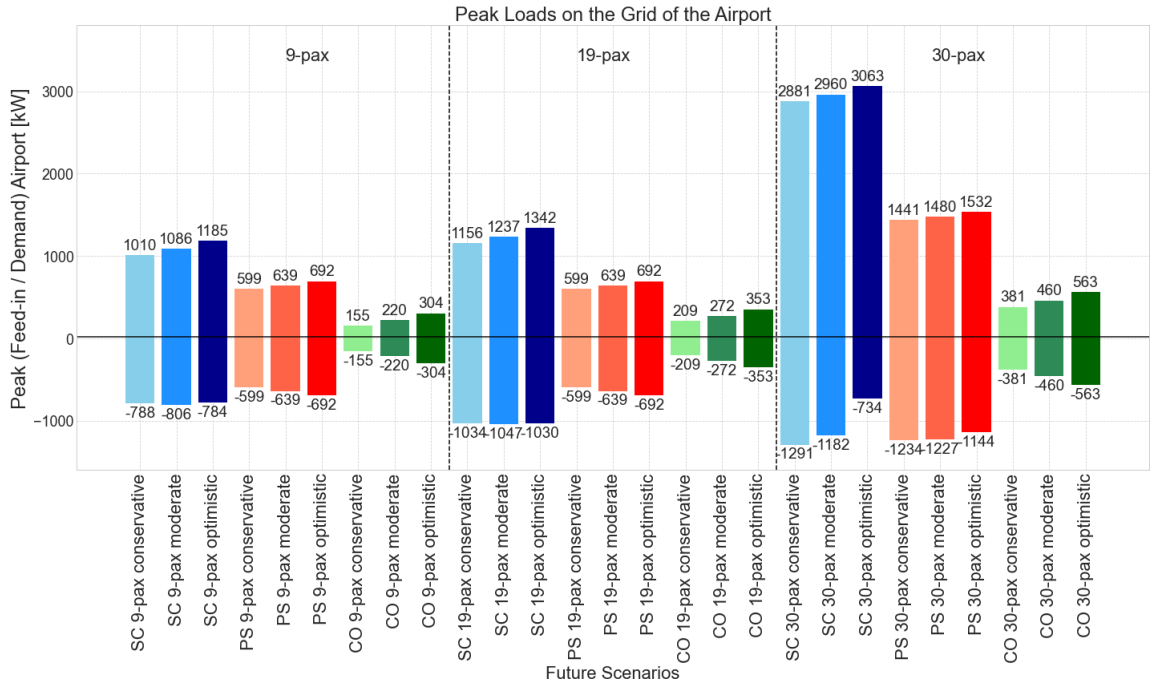

Figure 4.15: Sensitivity of peak loads in electricity feed-in and demand of the airport for different scenarios. The negative values are feed-in peaks, while positive values are the maximum peaks of demand.

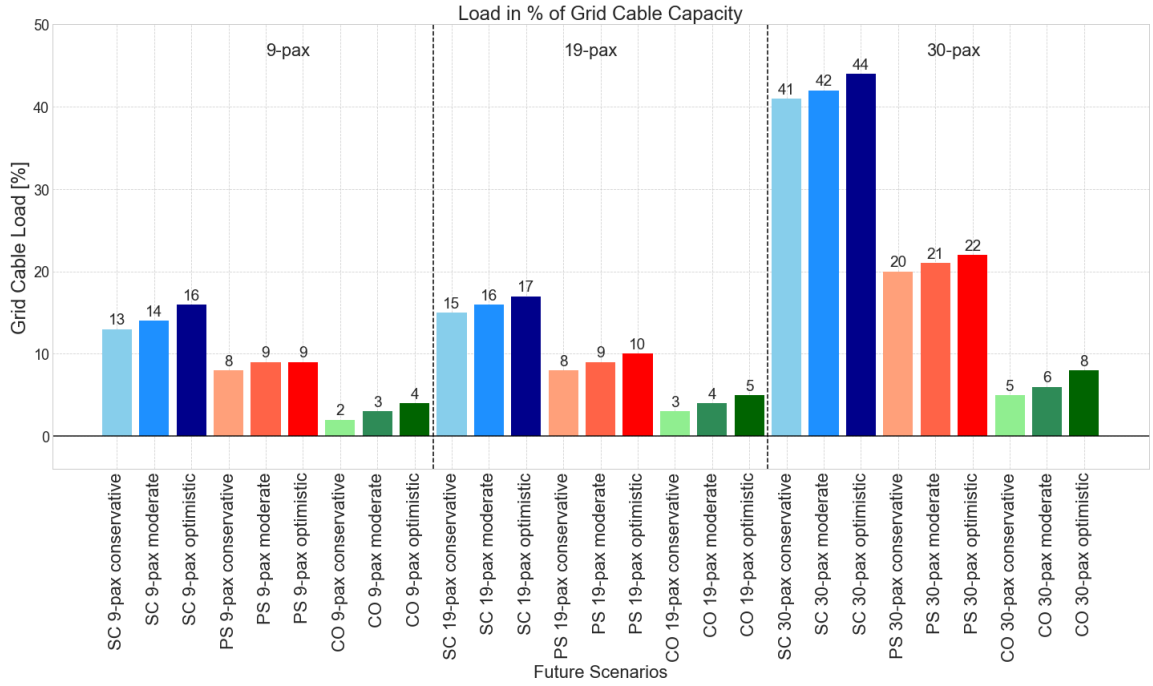

Figure 4.16: Sensitivity of the grid cable loads for the different future scenarios. The highest peak in either electricity demand or injection can be recognized as the highest peak load on the grid cables.

Figure 4.17 identifies the percent change in the overall island peak due to the change in the airport's load. The results are based on the Python optimization model which operates on a 15-minute base. Since the inputs of the model on the island level are on an hourly base, the load profile of the airport is converted from a 15-base to a one-hour-base. Therefore, figure 4.17 shows two bars for each scenario, the dark color uses the average of the four quarters in an hour, and the transparent color uses the maximum value within the hour.
The graph shows that taking the average results in an increase of less than 2% of the peak load of the island. Conversely, an analysis based on the maximum airport demand can lead to a substantial increase in the island's peak, specifically with the Self-Consumption control strategy at the highest EA adoption level. The Peak-Shaving control strategy limits the peak load on the grid to 50% of the peak load demand of the airport. The battery is able to control the maximum peak of the airport which demonstrates that the Peak-Shaving control strategy is the least sensitive control strategy. The increase of the peak load on the grid among the sub-scenarios of Peak-Shaving is due to the different growth rates used for the baseload of the airport.

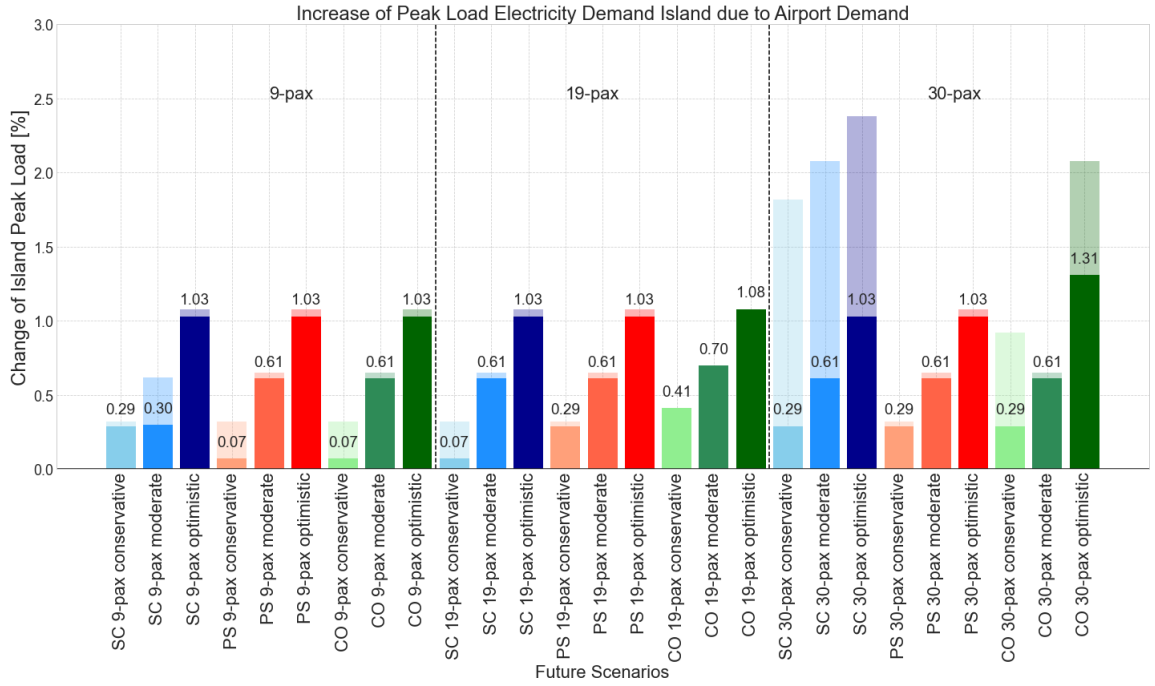

Figure 4.17: The sensitivity of the island peak for future scenarios. Two points are included for each scenario, where the highest point is using the maximum load of the airport within an hour, while the lower point indicates the average load of the airport on a one-hour-base.

The last technical performance indicator is the voltage fluctuations at the airport. Figure 4.18 presents the voltage fluctuations for each future scenario. The dark bar represents the minimum voltage and the transparent color represents the maximum voltage at the airport. It is evident that for each scenario and control strategy, the voltage fluctuations are approximately the same and follow the same trend among the sub-scenarios. However, it is seen that there is a significant voltage drop with the optimistic scenario. The lowest voltage level is observed for the Self-Consumption BESS with a 30-pax adoption level of EA and with the optimistic sub-scenario. In this scenario, the voltage fluctuations are risking to exceed the allowable threshold of 95% for the voltage fluctuations.

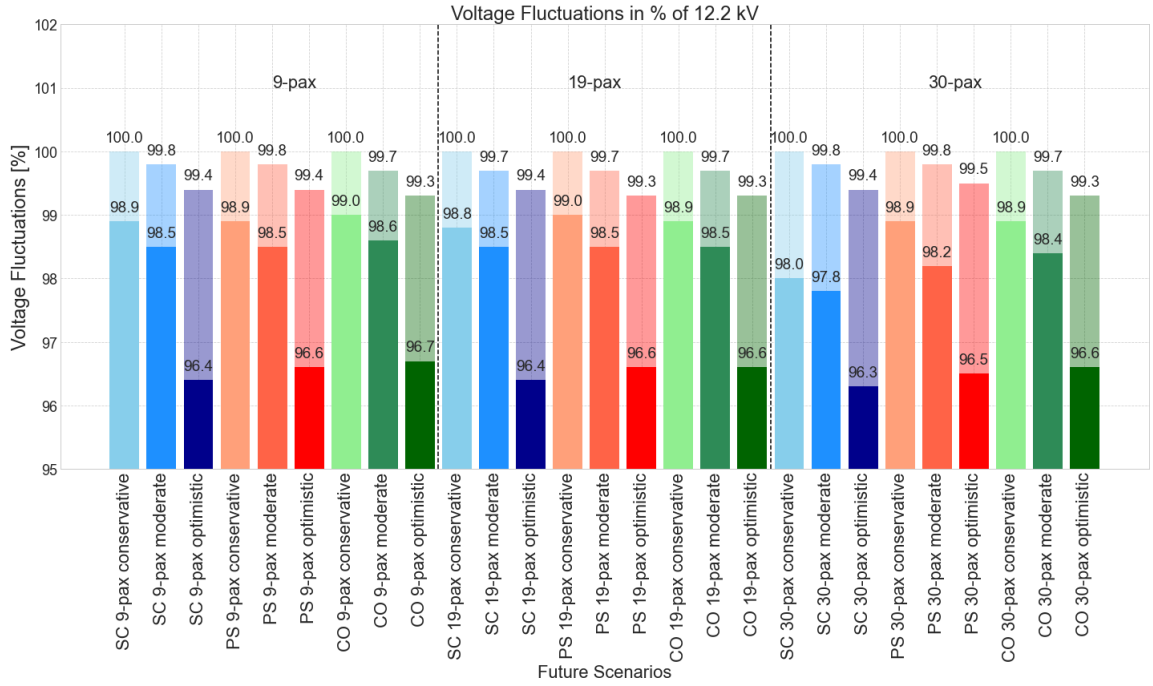

Figure 4.18: The sensitivity for future scenarios of the voltage fluctuations at the airport. The lower point is the minimum voltage level during a week, while the higher point indicates the maximum voltage level in the week.

4.5.2. Sensitivity Economic Performance Indicator

In figure 4.19 the LCOE is depicted for each scenario. The figure shows the impact of the adoption level on the LCOE, as well as the influence of the different sub-scenarios on the costs. The figure indicates that the Self-Consumption strategy is the most sensitive with an increasing adoption level of electric aircraft, while the Cost-Optimal control strategy shows the least change in LCOE. Whereas among the sub-scenarios the costs-optimal solution is relatively more sensitive compared to the Self-Consumption strategy. Furthermore, it is seen that for each control strategy, the 19-pax adoption level leads to the lowest costs. The BESS is sized according to the peak power needed for aircraft charging, which is the same for the 9-pax and 19-pax aircraft. The solar park is sized based on the total energy demand of charging, which increases with the adoption of 19-pax. This system sizing results in a lower LCOE compared to the 9-pax adoption level.

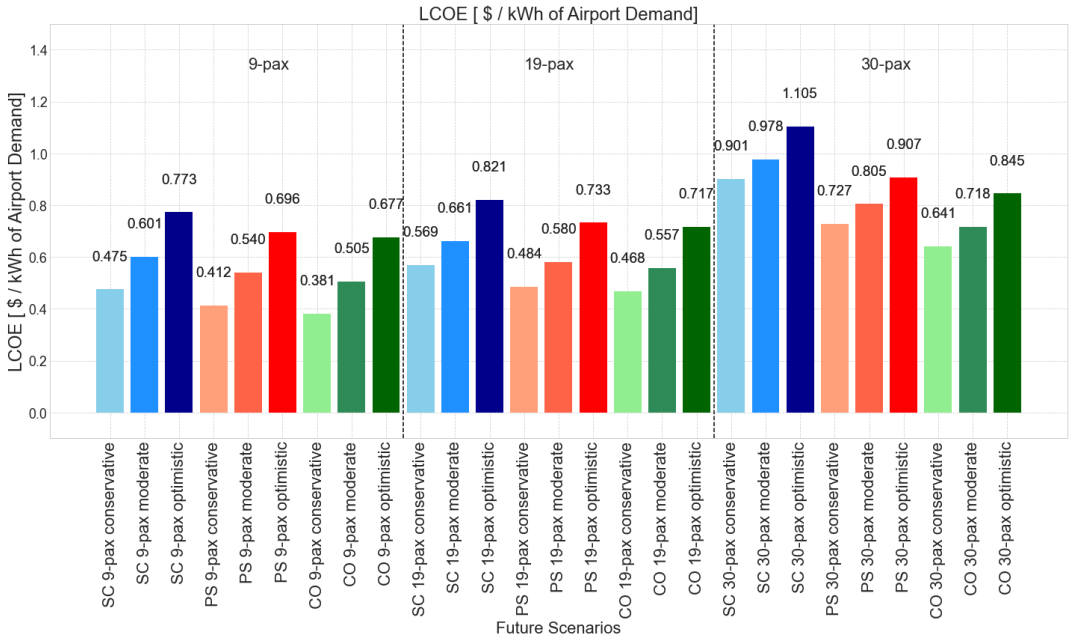

Figure 4.19: Results sensitivity for future scenarios of the economic performance indicator.

4.5.3. Sensitivity Environmental Performance Indicator

The last performance indicator for which the sensitivity is analyzed is the environmental performance indicator, where the change in CO_2 emissions from the electricity production at the island is calculated due to the energy demand and feed-in profile of the airport. It is evident from figure 4.20 that in the conservative and moderate sub-scenarios, the CO_2 emissions from grid electricity are reduced ranging from 0.14% to 1.09% considering all adoption levels of EA. Conversely, for the optimistic scenario, the CO_2 emissions are slightly increasing due to the grid load profile of the airport.
Lastly, with an increasing adoption level of electric aircraft, there is an increase in CO_2 emissions. This increase in emissions is relatively small as the capacity of the solar park and the BESS is scaled by the sum of the load for charging corresponding to the adoption level of EA.

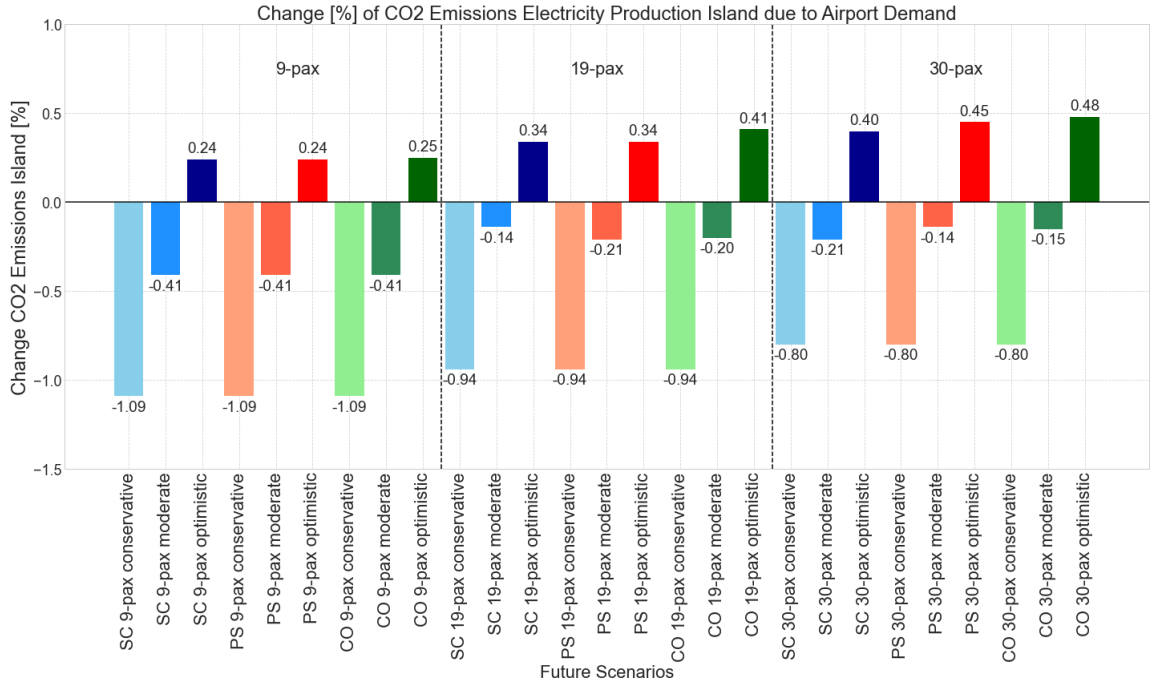

Figure 4.20: Sensitivity for future scenarios of the environmental performance indicator.

5

Discussion and Conclusion

5.1. Conclusion

This section provides the conclusion of the report. The sub-questions are answered here which are based on the findings of this research. Ultimately, the main research question is answered at the end.

1. How can the electric aircraft charging demand be computed and incorporated into the energy demand profile of the airport?

It was found that at Bonaire International Airport three distinct conventional aircraft types operate that are feasible to be replaced by electric aircraft by 2030. In Chapter 2 multiple electric aircraft designs were explored. Three electric aircraft were found to be suitable to replace the currently operating conventional aircraft based on comparable seat capacity and operating range. For the 9-pax aircraft, Alice is the most promising candidate. Secondly, Heart Aerospace's ES-19 and ES-30 are identified as well-suited alternatives for the 19-pax and 30-pax, respectively.
These aircraft operate on short-range to Curacao and Aruba, 79 km and 194 km, respectively. From a flight schedule analysis, the departure times in the current flight schedule at Bonaire International Airport are obtained for each aircraft. Moreover, it was observed that the aircraft had a turnaround time of 30 minutes which was used as the charging time. Using the flight schedule, turnaround time, the Breguet Range equation, and take-off equation, an electricity demand profile was constructed for electric aircraft charging.
The results showed that the 9-pax Alice, the 19-pax ES-19, and the 30-pax ES-30 require a peak power of 418-906 kW, 412-914 kW, and 1006-2280 kW for charging depending on the destination, respectively. From this, it is seen that for larger aircraft higher charging rates are needed. Moreover, the simultaneous charging of aircraft in the flight schedule caused high peak loads in the demand profile.
The summation of the charging load profile with the data of the baseload of the airport resulted in a total demand profile of the airport.

2. What is the effect of the electricity demand profile including electric aircraft charging of the airport on the voltage fluctuations, the distribution grid cable load, and the transformer overloading without a BESS?

The results for the second sub-question are provided in section 4.3 and are assessed under two scenarios: one with a 1000 kWp solar park and one without. These two scenarios are analyzed across an increasing adoption level of EA: 9-pax, 19-pax, and 30-pax.
In the absence of a solar park, transformer overloads are observed with the adoption of electric aircraft. The demand profiles of the 9-pax and 19-pax cause, respectively, 313 hours and 560.75 hours of transformer overload annually. The results showed that for these adoption levels of EA, the transformer is overloaded when two aircraft are simultaneously charged. Furthermore, the introduction of 30-pax aircraft and the required high charging power leads to substantial and more transformer overloads for a total of 952.25 hours annually.
The incorporation of a 1000 kWp solar park reduces peak load occurrences. For the 9-, and 19-pax

aircraft adoption levels, transformer overloads are reduced to 7.5 hours and 142.5 hours annually, predominantly during days of low solar irradiation. However, for the 30-pax adoption level of EA, a standalone solar park does not suffice to reduce the maximum peak load on the grid as it is constrained by the instantaneous overlap of demand for aircraft charging and produced solar energy. As a result, peak loads also arose outside the time window of solar irradiation.
Based on the results it was observed that the adoption of electric aviation, independent of the adoption level and the installation of a solar park, requires transformer capacity upgrades.

Subsequently, an analysis of the voltage fluctuations and load on the cable of the distribution grid revealed that the grid experiences amplified voltage drops and higher cable loads as the adoption of electric aircraft expands. However, in the context of voltage fluctuations no significant risks were noticed with a maximum voltage drop to 98% of 12.2 kV, while the allowable voltage fluctuation range is within 95-105%. The grid cable load for 9- and 19-pax adoption levels remained below 17% without a solar park and with a solar park below 14%. While for the 30-pax adoption level, it substantially elevated to 41%. The installation of a solar park reduces the voltage drops for all adoption levels, albeit only by a modest decrease. Regarding, the distribution grid cable load no reduction is seen for the 30-pax adoption level as there are aircraft charged outside the time window of solar irradiation.

3.What is the contribution of a BESS to the technical performance, the LCOE, and the CO_2 emissions from grid electricity of the system compared to the case without a BESS?

This research focused on three distinct charging control strategies: Self-Consumption, Peak-Shaving, and Cost-Optimal. The battery profiles resulting from the optimization model are presented in 4.4.1.

The Self-Consumption BESS aims to maximize the solar energy consumption on-site. Therefore, the BESS charges the excess solar energy. On days with high irradiance, the BESS reaches maximum capacity before the window of solar radiation ends resulting in electricity feed-in into the grid. Conversely, low irradiance days cause peaks in electricity demand. Those peaks can be counteracted by the Peak-Shaving control strategy. The battery profile showed that the BESS anticipates the forthcoming days of low irradiance by keeping a reserve capacity, effectively reducing the peaks that were present in the Self-Consumption control strategy. Lastly, the Cost-Optimal control strategy actively reduces peak loads as this induces a substantial share of the costs, but it was seen that this required a higher capacity reserve for days with low irradiance.

The technical performance indicator includes three parameters from the previous sub-question and the peak power both on the demand and the feed-in sides. The results can be found in section 4.4.2. The results revealed that the Self-consumption-controlled BESS was not capable of reducing the maximum peak load demand compared to the solar park-only case. Peak loads were -788 kW on the feed-in side and 1010 kW on the demand side, causing overloads of the transformer for 5.25 hours annually and resulting in a grid cable load of 0-14% of the cable capacity. The other control strategies managed to operate within the transformer capacity. The Peak-Shaving controlled BESS operates within 50% of the total peak load demand of the airport (-599 kW, 599 kW). The Cost-Optimal controlled BESS even reduced the peaks to -155 kW and 155 kW. As a result, the cable loads are decreased to 0-8% and 0-2% of the grid cable capacity, respectively. Lastly, the voltage fluctuations range between 99-100% and do not cause a severe risk of exceeding the allowable threshold of 95-105%.

Subsequently, the analysis of the economic performance indicator (section 4.4.3) concluded that a BESS, depending on the control strategy, was accomplished to significantly reduce LCOE compared to the Business-as-Usual case. The induced CAPEX, OPEX, and financing costs of the BESS are extinguished by the lowered grid electricity and peak load costs. The Cost-Optimal control strategy achieved a reduction of 24.7% compared to the case without a BESS, resulting in a LCOE of 0.381 $/kWh. In contrast, the Self-Consumption control strategy obtains a relatively small cost reduction of 0.031 $/kWh compared to the solar-only case, while Peak-Shaving realizes a cost of 0.425 $/kWh. The lifetime of the BESS ranged between 15-16 years for the control strategies, resulting in no significant deviations between the control strategies in annual BESS CAPEX costs.

Lastly, the environmental performance indicator presented in section 4.4.4, revealed that while a 9-pax adoption level of EA is introduced, the CO_2 emissions from the electricity production at the island level of Bonaire decreased by -1.09% due the solar park and the BESS at the airport. Installing solely a solar park results in a CO_2 reduction of 1.16%. The emission reduction does not differ among the BESS control strategies for the used system sizing and adoption level of EA. However, compared to the Business-as-Usual case where no solar park and BESS are deployed, an increase of 0.82% in CO_2 emissions was observed.

4. How sensitive are the results of the performance indicators to changes in input parameters and data for future scenarios?

The results of the three different scenarios with different adoption levels of EA and its sub-scenarios can be found in Chapter 4.5.

Considering peak loads on both demand and feed-in sides of the airport, the sensitivity analysis showed that the Self-Consumption control strategy causes the highest peak demand with an increasing adoption level of EA. In combination with an annual demand growth rate of 8% in the optimistic sub-scenario, this results in a peak demand of 3063 kW, the highest peak load among all scenarios and control strategies, causing a grid cable load of 44.0% of its capacity.
Additionally, voltage fluctuations arise that reach the acceptable threshold with the 8% demand growth rate in the optimistic sub-scenario. At maximum, the voltage dropped to 96.30% of 12.2 kV for the Self-Consumption BESS in the 30-pax adoption level, while the conservative and moderate sub-scenarios do not cause severe risks.
Furthermore, the analysis of the economic performance indicator's sensitivity revealed that the Self-Consumption control strategy was more sensitive to an increased adoption level of EA, while the LCOE for the Peak-Shaving control strategy and the Cost-Optimal control strategy was less sensitive to an increased adoption level.
Lastly, for all scenarios, each control strategy was able to reduce the CO_2 emissions of the island's electricity production. However, in the optimistic sub-scenarios that include a demand growth rate of 8% the CO_2 emissions originating from grid electricity are increasing.

Main Research Question

'What is the effect of different BESS control strategies on the technical, economic, and environmental performance so that it can facilitate both the grid operator and the airport to enable electric aviation?'

To enable electric aviation at Bonaire International Airport a battery is required, as regardless of the adoption level of EA, the transformer capacity is overloaded. A battery is able to defer the transformer capacity upgrade, lower costs, and reduce the CO_2 emissions at the island. However, the extent depends on the control strategy.

Regarding the technical performance, the Self-Consumption strategy is not capable of mitigating all the transformer overloads, while the Peak-Shaving and Cost-Optimal control strategies effectively manage the peak loads, even in 2030 with the highest demand growth rate and adoption level of EA. However, in sub-scenarios with a high demand growth rate, for all the control strategies nearly critical voltage drops are seen. Evaluating the grid cable load, a significant increase to 41-44% is noticed when the BESS is controlled by Self-Consumption with the highest adoption level of EA.
In economic terms, the Cost-Optimal control strategy was able to reduce the LCOE for all considered scenarios most significantly, while Self-Consumption leads to a limited reduction in costs. In future scenarios, the Self-Consumption control strategy shows the most sensitivity to an increased adoption level of EA, while the LCOE for the other scenarios remains relatively constant.
Lastly, from an environmental perspective, all control strategies achieved a similar reduction in CO_2 emissions for the 9-pax adoption level and its system sizing. However, in a future scenario with high demand growth rates, CO_2 emissions are increasing at the island level, where the Cost-Optimal strategy leads to the most significant rise.

5.2. Discussion

The discussion section aims to elaborate on the uncertainty and the limitations of the methodology used in this research. Moreover, the contribution of this research is included.

Electric Aviation

In prior research, an approximation of the energy demand for a hybrid electric fleet was made for the large airport O'Hare Airport, where it was concluded that due to the adoption of a hybrid fleet, grid infrastructure upgrades were necessary [45]. This research concluded that independent of the adoption level of full-electric aircraft also upgrades are needed for the transformer capacity, while other infrastructure components such as the transmission grid cables are strained depending on the adoption level but not overloaded. However, this research focused on a small airport where the flight scheme is dominated by small regional aircraft that are suitable for electrification, while the study in [45] analyzed the adoption of a hybrid fleet in a large airport flight scheme.

The research methodology used is exposed to several sources of uncertainty. First of all, the input parameters for the two equations for the energy consumption of electric aircraft are based on parameters provided by aircraft manufacturers. Given that most of the aircraft designs are in the testing or conceptual phase, these parameters can potentially change in the future or are conceptual numbers. Furthermore, assumptions are made for input parameters in case the parameter is unknown. These input parameters are used in the simplified Breguet-range equation and an approximation formula for the take-off energy. It was seen that the calculated energy consumption with the Breguet range equation is lower compared to the real consumption, specifically for short-range flights, as described in section 3.1.3. The take-off equation is added to compensate for the lower energy, however, still this energy consumption tends to be lower than the real energy consumption.
Secondly, the impact of the design range of the electric aircraft design impacts the battery mass and thereby determines the energy consumption. It could be interesting to calculate the energy consumption of an aircraft specifically designed for the considered distances and seating capacity. In this research, it was seen in the results in Chapter 4.1 that the electricity consumption for the 9-pax and 19-pax aircraft are almost similar. This was due to the design range of aircraft. As the larger aircraft ES-19 is designed for a shorter operational design range compared to Alice, this results in reduced battery mass, while Alice carries a relatively heavier battery. The total masses claimed by the manufacturers of both aircraft designs are comparable. Ultimately, due to the similar masses of the aircraft, the energy consumption for both aircraft is comparable, although the aircraft have different passenger capacities and design ranges.
Lastly, in this model, the charging starts and ends immediately from one to the other timestep on full power. However, in practice, the charging power increases and decreases gradually. Depending on the flight schedule this could result in reduced peak loads due to less simultaneous charging. At the same time, when maintaining the same turnaround time, a higher peak load is reached for the charging of an aircraft in case of gradual charging.

Model

Moreover, it was seen in the literature that with a constant pricing scheme and a large price gap between the purchase price of electricity and the feed-in tariff it is economically attractive to operate the battery system by maximizing the self-consumption ratio [70]. As this is the case for Bonaire, from the results it was observed that the Cost-Optimal control strategy achieved a high self-consumption ratio.
However, in this research, with the considered system set up at the airport, for some system sizing the Cost-Optimal strategy achieved a slightly higher self-consumption ratio compared to the Self-Consumption strategy. The formulation of the optimization of the Self-Consumption model is one of the methodological limitations in this research. Optimization is not the most appropriate method for the Self-Consumption control strategy with the considered energy system set-up in this research. On the other hand, the Cost-Optimal is well-suited to the optimization method.
In the system set up of this research, the battery is able to charge and discharge to the grid, charge the battery with PV electricity, and discharge to the load. The objective function for self-consumption was formulated by maximizing the PV electricity directly consumed by the load and the PV electricity that is consumed via the battery. The PV electricity via the battery was optimized by maximizing the flow of the discharge of the battery to the load. Secondly, to prevent discharging to the load with

grid electricity and thereby achieve a high self-consumption ratio, the battery interaction with the grid was minimized. In this way, it is ensured that the battery is predominantly used for self-consumption purposes. However, the Cost-Optimal control strategy was not constrained by reduced grid interaction and achieved a slightly higher self-consumption ratio.

This research's model cannot directly be generalized, as one of the research's limitations is the constant pricing scheme used in the case study of Bonaire. For case studies with a time-based pricing scheme, a data set with prices of electricity for each step should be incorporated into the model. As a result of the constant pricing scheme, the Cost-Optimal control strategy behaves very similarly to the Self-Consumption control strategy. Therefore, it could be interesting to include a dynamic pricing scheme in the model.

Performance Indicators
The grid impact analysis is performed using the grid analysis program Vision, where the voltage fluctuations and the grid cable load are obtained. However, Vision is only capable of analyzing a one-week profile, which consists of a typical weekday, a Saturday, and a Sunday on a 15-minute basis. Therefore, this research used the worst week in terms of solar irradiance for this analysis. Moreover, some other electricity demand profiles of grid connections in Vision use a standard scaled profile. Therefore, these results should be interpreted to provide insight into the behavior of the voltage fluctuations and cable loads and give an indication of the severity of the impact.

For the economic performance indicator, the battery lifetime was determined using a rainflow counting method. The general assumptions made to use this method are discussed in section 2.3.1. However, as the optimization model runs for a single year, it is assumed that the same battery charging behavior, and thereby the same degradation rate, is repeated for each year. The degradation of each year is accumulated until the battery capacity reaches 80% of the initial capacity. However, in reality, battery the charging behavior, is affected by the new degraded capacity, the changing load profile over time, the solar profile, and the flight scheme. A whole-lifetime model including degradation would be a possible solution to this problem.

Lastly, the calculation of the CO_2 emissions is another methodological limitation of the case study in this research. The used methodology is a simplified model of electricity production for an isolated microgrid. As a consequence, it is easier to find out which production units generated the electricity and the associated CO_2 emissions. For large continental electricity grids, this would be more complex, and the simplified model for microgrids in this methodology can not directly be applied.

Contributions
Ultimately, this research's contributions in the field of a stationary BESS for electric aviation charging purposes can be summarized as follows:

- Data collection and processing of the airport demand, island demand, and PV system output, and the construction of a total demand profile including aircraft charging based on the current flight schedule and operating aircraft types at Bonaire International Airport. Analysis of the impact of electric aircraft charging for different adoption levels on the local grid infrastructure of Bonaire focusing on voltage fluctuations, transmission grid cable load, and peak loads at the transformer.
- Develop three different control strategies for a BESS in combination with the considered PV system at Bonaire International Airport focusing on self-consumption, reduction of peak loads on the grid, and minimization of the operational cost through an optimization model.
- An analysis and comparison of the different control strategies on a threefold of indicators: the impact on the local grid infrastructure, the LCOE of the airport's system, and the CO_2 emissions from used grid electricity.
- Formulate various future scenarios for a BESS serving electric aviation at Bonaire and assess the sensitivity of each BESS control strategy for the various future scenarios.

5.3. Future Work

This section elaborates on future fields of research related to this topic. This research focused on the contribution of a BESS in an energy system and its impact on the grid infrastructure, the LCOE of the airport's system, and the change in CO_2 emissions.

First, a more accurate study can be done on the energy consumption of electric aircraft as it was seen from the sensitivity analysis that the demand profile of electric aircraft charging had a significant impact on all the performance indicators. In this study, the energy consumption is based on two equations that approximate the total energy consumption of a battery-powered aircraft. Moreover, the input parameters of these equations are based on claimed parameters of aircraft designs in the conceptual or testing phase. Therefore, it is recommended to perform a more in-depth calculation of the energy consumption of electric aircraft by considering the energy consumption per flight phase of the trajectory. Additionally, the energy consumption for an aircraft that is specifically designed for the operating range of Aruba and Curacao can be analyzed.

Two other important assumptions in this research, are the perfect foresight of the load data and solar irradiation, and the system sizing. First, to be able to analyze a more realistic situation without the perfect foresight assumption it can be interesting to perform an optimization study that includes uncertainty in the load and solar data and analyze the impact on the performance indicators. Secondly, an interesting topic for further research is the determination of the optimal sizing of the system for each control strategy. In this research, three control strategies are modeled, where the optimal sizing for each control strategy is outside the scope of this research, and the sizing of the system is based on assumptions. However, there is a trade-off for the Cost-Optimal control strategy between the sizing and the reduction in costs. Where the influence of the sizing is even more with a fluctuating energy pricing scheme. For Self-Consumption and Peak-Shaving a trade-off can be made for the optimal system sizing for peak load reduction or grid independence and the associated costs.

As was stated earlier, this case study at Bonaire leads to a limitation of this research since there is a static pricing scheme at Bonaire. With a dynamic pricing scheme, the charging behavior of the Cost-Optimal control strategy could potentially change due to energy arbitrage, while the other control strategies are not operating on price incentives. By actively charging and discharging the battery in the Cost-Optimal strategy the total electricity purchase costs and revenue from feed-in could potentially significantly change as was seen in the study of [40]. Therefore, research should be done on the impact of a fluctuating pricing scheme on the charging battery behavior and the resulting costs, grid impact, and CO_2 emissions, and the difference among the distinct control strategies.

Lastly, the implementation of the BESS at the airport should be studied further on the electrical infrastructure set up at the airport, the electricity selling price to the electric aircraft, and additional grid service of the batteries.
This research focused on the impact on the current grid infrastructure, however, the optimal infrastructure design at the airport and how the BESS, the PV system, and the chargers are connected was out of the scope of this research. Therefore, the physical location of each system component at the airport, the voltage level, the cables, and the power losses with high charging rates should be researched further. In this research, it is assumed that the system operates on low voltage with the currently used transformer. However, due to the high power of electric aircraft charging and PV production, as well as the potentially large distances between the solar park, BESS, and chargers, a high voltage level can be beneficial to limit power losses and avoid unnecessary use of large-diameter cables. Therefore, in appendix A.4, a system set up operating on 12.2 kV and without the transformer is given that can be used for further research for the electrical system design and the locations of the system components at the airport.
Secondly, as the airport is charging the aircraft with self-produced electricity, the airport should determine an electricity price for the electricity that is used for aircraft charging and sold to airlines. With this, revenue can be made to obtain a more profitable business case.
Lastly, an interesting topic of further research is the support of the BESS at the airport for grid support. As Bonaire is a microgrid and needs to handle the high peak loads, there could be a potential role for the BESS at the airport to support the grid of Bonaire peak load times.

References

[1] International Civil Aviation Organization (ICAO). *On board a sustainable future*. ICAO, 2016.

[2] Heart Aerospace. *Learn more about the ES-30*. 2022. URL: https://heartaerospace.com/es-30/.

[3] Bonaire International Airport. *Jaarverslag 2021 Bonaire International Airport*. 2022. URL: https://bonaireinternationalairport.com/wp-content/uploads/Jaarverslag-en-Jaarrekening-BIA-2021-voor-website.pdf.

[4] Maria C Argyrou, Paul Christodoulides, and Soteris A Kalogirou. "Energy storage for electricity generation and related processes: Technologies appraisal and grid scale applications". In: *Renewable and Sustainable Energy Reviews* 94 (2018), pp. 804–821.

[5] Ida Norberg Arne Smedberg and Simon Oja. *Electric Aviation 2021, Technology Overview*. 2021.

[6] International Air Transport Association et al. "Aircraft technology roadmap to 2050". In: *IATA: Geneva, Switzerland* (2019).

[7] ERA Aura Aero. *19 seater Electric Regional Aircraft*. last accessed on 31.03.2023. URL: https://aura-aero.com/en/era/#video.

[8] HDI Global Specialty Aviation. "Technical Study Electrical Aviation in 2022". In: 56 (2022).

[9] Thomas P Barrera et al. "Next-Generation Aviation Li-Ion Battery Technologies—Enabling Electrified Aircraft". In: *The Electrochemical Society Interface* 31.3 (2022), p. 69.

[10] Ausilio Bauen et al. "Sustainable Aviation Fuels: Status, challenges and prospects of drop-in liquid fuels, hydrogen and electrification in aviation". In: *Johnson Matthey Technology Review* 64.3 (2020), pp. 263–278.

[11] BBT. *BBT Nieuwsbrief editie 1*. 2023. URL: https://www.bbtbonaire.com/wp-content/uploads/2023/02/BBT_Nieuwsbrief.pdf.

[12] Federico Bigoni et al. "Design of airport infrastructures in support of the transition to a hybrid-electric fleet". In: *Advanced Aircraft Efficiency in a Global Air Transport System Conference (AEGATS 2018)*. 2018, pp. 1–10.

[13] Thomas Bowen, Ilya Chernyakhovskiy, and Paul L Denholm. *Grid-scale battery storage: frequently asked questions*. Tech. rep. National Renewable Energy Lab.(NREL), Golden, CO (United States), 2019.

[14] Benjamin J Brelje and Joaquim RRA Martins. "Electric, hybrid, and turboelectric fixed-wing aircraft: A review of concepts, models, and design approaches". In: *Progress in Aerospace Sciences* 104 (2019), pp. 1–19.

[15] Paul Callister and Robert McLachlan. *Electric aircraft calculations*. 2021. URL: https://www.rapidshift.net/electric-aircraft-calculations/.

[16] Tania C Cano et al. "Future of electrical aircraft energy power systems: An architecture review". In: *IEEE Transactions on Transportation Electrification* 7.3 (2021), pp. 1915–1929.

[17] M. Castillo-Cagigal et al. "A semi-distributed electric demand-side management system with PV generation for self-consumption enhancement". In: *Energy Conversion and Management* 52.7 (2011), pp. 2659–2666. ISSN: 0196-8904. DOI: https://doi.org/10.1016/j.enconman.2011.01.017. URL: https://www.sciencedirect.com/science/article/pii/S0196890411000628.

[18] Chuanhai Chen et al. "Load spectrum generation of machining center based on rainflow counting method". In: *Journal of Vibroengineering* 19.8 (2017), pp. 5767–5779.

[19] Haisheng Chen et al. "Progress in electrical energy storage system: A critical review". In: *Progress in natural science* 19.3 (2009), pp. 291–312.

[20] Li Chen, Yuqi Tong, and Zuomin Dong. "Li-ion battery performance degradation modeling for the optimal design and energy management of electrified propulsion systems". In: *Energies* 13.7 (2020), p. 1629.

[21] Tianmei Chen et al. "Applications of lithium-ion batteries in grid-scale energy storage systems". In: *Transactions of Tianjin University* 26.3 (2020), pp. 208–217.

[22] Chee K Chin. *Extending the endurance, missions and capabilities of most UAVs using advanced flexible/ridged solar cells and new high power density batteries technology*. Tech. rep. NAVAL POSTGRADUATE SCHOOL MONTEREY CA, 2011.

[23] Daiwon Choi et al. "Li-ion battery technology for grid application". In: *Journal of Power Sources* 511 (2021), p. 230419.

[24] European Commission. *PHOTOVOLTAIC GEOGRAPHICAL INFORMATION SYSTEM*. 2019. URL: https://re.jrc.ec.europa.eu/pvg_tools/en/.

[25] Antilliaans dagblag. *Zonne-energie voor particulier nauwelijks rendabel*. 2022. URL: https://antilliaansdagblad.com/bonaire/26187-zonne-energie-voor-particulier-nauwelijks-rendabel.

[26] Timothy P Dever et al. *Assessment of technologies for noncryogenic hybrid electric propulsion*. Tech. rep. 2015.

[27] Ministerie van Economische Zaken. *Duurzame en betaalbare energie in the Caribisch Nederland*. 2017.

[28] Water- en Energiebedrijf Bonaire N.V. *Short annual report 2021*. 2021. URL: https://www.webbonaire.com/wp-content/uploads/2022/08/Jaarverslag-WEB-2021-11-07-22.pdf.

[29] ENTSOE. *DEVELOPING BALANCING SYSTEMS TO FACILITATE THE ACHIEVEMENT OF RENEWABLE ENERGY GOALS*. 2011. URL: https://eepublicdownloads.entsoe.eu/clean-documents/pre2015/position_papers/111104_RESBalancing_final.pdf.

[30] Alan H Epstein and Steven M O'Flarity. "Considerations for reducing aviation's co 2 with aircraft electric propulsion". In: *Journal of Propulsion and Power* 35.3 (2019), pp. 572–582.

[31] Eviation. *Alice*. last accessed on 31.03.2023. URL: https://www.eviation.com/aircraft/.

[32] Mikael Faa. "Potential Network Planning for Electric Aircraft". In: (2022).

[33] Xiayue Fan et al. "Battery technologies for grid-level large-scale electrical energy storage". In: *Transactions of Tianjin University* 26 (2020), pp. 92–103.

[34] *flightradar24*. 2023. URL: https://www.flightradar24.com/data/airports/bon.

[35] Edwin van Gastel. *Stimulering voor zonnepanelen in Caribisch Nederland niet nodig*. 2020. URL: https://solarmagazine.nl/nieuws-zonne-energie/i22545/staatssecretaris-van-t-wout-stimulering-voor-zonnepanelen-in-caribisch-nederland-niet-nodig.

[36] van der Geest and Teles. *Nexus interventions for small tropical islands: case study Bonaire, Energy*. Wageningen University, 2019.

[37] Girish Girishkumar et al. "Lithium- air battery: promise and challenges". In: *The Journal of Physical Chemistry Letters* 1.14 (2010), pp. 2193–2203.

[38] NASA Glenn Research Center. *Lift to Drag Ratio*. URL: https://www1.grc.nasa.gov/beginners-guide-to-aeronautics/lift-to-drag-ratio/.

[39] Albert R Gnadt et al. "Technical and environmental assessment of all-electric 180-passenger commercial aircraft". In: *Progress in Aerospace Sciences* 105 (2019), pp. 1–30.

[40] Zekun Guo et al. "Aviation to grid: Airport charging infrastructure for electric aircraft". In: International Conference on Applied Energy. 2020.

[41] Zekun Guo et al. "Aviation-to-Grid Flexibility through Electric Aircraft Charging". In: *IEEE Transactions on Industrial Informatics* 18.11 (2021), pp. 8149–8159.

[42] *Heart Aerospace ES-30: All We Know About It*. 2023. URL: https://airlapse.net/blog/heart-aerospace-es-30.

[43] Martin Hepperle. "Electric flight-potential and limitations". In: (2012).

[44] Bernd Hirschl et al. "PV-Benefit: A Critical Review of the Effect of Grid Integrated PV-Storage-Systems". In: *Proceedings of the International Renewable Energy Storage Conference (IRES), Berlin, 18.-20. November 2013*. Eurosolar. 2014.

[45] Boya Hou, Subhonmesh Bose, and Kiruba Haran. "Powering electric aircraft at o'hare airport: A case study". In: *2020 IEEE Power & Energy Society General Meeting (PESGM)*. IEEE. 2020, pp. 1–5.

[46] Boya Hou et al. "Impact of Aviation Electrification on Airports: Flight Scheduling and Charging". In: *arXiv preprint arXiv:2108.08963* (2021).

[47] Mohamed SE Houache et al. "On the Current and Future Outlook of Battery Chemistries for Electric Vehicles—Mini Review". In: *Batteries* 8.7 (2022), p. 70.

[48] IATA. *Net zero 2050: Sustainable Aviation Fuel*. URL: https://www.iata.org/en/iata-repository/pressroom/fact-sheets/fact-sheet---alternative-fuels/.

[49] IATA. *Net-zero carbon emissions by 2050*. 2021. URL: https://www.iata.org/en/pressroom/pressroom-archive/2021-releases/2021-10-04-03/.

[50] Ministerie van Infrastructuur en Waterstaat. *Verantwoord vliegen naar 2050, Luchtvaart nota 2020-2050*. 2020. URL: https://www.rijksoverheid.nl/documenten/rapporten/2020/11/20/bijlage-1-luchtvaartnota-2020-2050.

[51] Lloyd R Jenkinson et al. *Civil jet aircraft design*. Vol. 338. Arnold London, UK, 1999.

[52] Lonnie Johnson. "The viability of high specific energy lithium air batteries". In: *Proceedings of the Symposium on Research Opportunities in Electrochemical Energy Storage-Beyond Lithium Ion: Materials Perspectives, Oak Ridge National Laboratory, TN, USA*. 2010, pp. 7–8.

[53] Cedric Y Justin et al. "Operational and economic feasibility of electric thin haul transportation". In: *17th AIAA Aviation Technology, Integration, and Operations Conference*. 2017, p. 3283.

[54] Cedric Y Justin et al. "Power optimized battery swap and recharge strategies for electric aircraft operations". In: *Transportation Research Part C: Emerging Technologies* 115 (2020), p. 102605.

[55] Katarina Knezović et al. "Distribution grid services and flexibility provision by electric vehicles: A review of options". In: *2015 50th International Universities Power Engineering Conference (UPEC)*. IEEE. 2015, pp. 1–6.

[56] KNMI. *Wind - windspeed, direction, standarddeviation at a 10 minute interval*. 2019. URL: https://dataplatform.knmi.nl/dataset/windgegevens-1-0.

[57] Alexander Kraytsberg and Yair Ein-Eli. "Review on Li–air batteries—Opportunities, limitations and perspective". In: *Journal of Power sources* 196.3 (2011), pp. 886–893.

[58] Gaël Le Bris et al. *Preparing Your Airport for Electric Aircraft and Hydrogen Technologies*. ACRP Project 03-51. 2022.

[59] GBMA Litjens, E Worrell, and WGJHM Van Sark. "Economic benefits of combining self-consumption enhancement with frequency restoration reserves provision by photovoltaic-battery systems". In: *Applied energy* 223 (2018), pp. 172–187.

[60] Saifullah Mahmud et al. "Recent advances in lithium-ion battery materials for improved electrochemical performance: A review". In: *Results in Engineering* 15 (2022), p. 100472. ISSN: 2590-1230. DOI: https://doi.org/10.1016/j.rineng.2022.100472. URL: https://www.sciencedirect.com/science/article/pii/S2590123022001426.

[61] Autoriteit Consument en Makrt. *Beschikking tot vaststelling van de maximale productieprijs van elektriciteit per 1 januari 2023 voor ContourGlobal Bonaire B.V.* 2022.

[62] On The World Map. *Bonaire map*. 2021. URL: https://ontheworldmap.com/caribbean-netherlands/bonaire/.

[63] Christine Driessen Marlies Hak. *Roadmap Electric flight in the Kingdom of the Netherlands*. Tech. rep. 2021.

[64] Ghada Merei et al. "Optimization of self-consumption and techno-economic analysis of PV-battery systems in commercial applications". In: *Applied Energy* 168 (2016), pp. 171–178. ISSN: 0306-2619. DOI: https://doi.org/10.1016/j.apenergy.2016.01.083. URL: https://www.sciencedirect.com/science/article/pii/S0306261916300708.

[65] Ajay Misra. "Energy storage for electrified aircraft: The need for better batteries, fuel cells, and supercapacitors". In: *IEEE Electrification Magazine* 6.3 (2018), pp. 54–61.

[66] Ajay Misra. "Summary of 2017 NASA workshop on assessment of advanced battery technologies for aerospace applications". In: *AIAA SciTech Forum and Exposition*. GRC-E-DAA-TN51429. 2018.

[67] Janina Moshövel et al. "Analysis of the maximal possible grid relief from PV-peak-power impacts by using storage systems for increased self-consumption". In: *Applied Energy* 137 (2015), pp. 567–575.

[68] Valentin Muenzel et al. "A multi-factor battery cycle life prediction methodology for optimal battery management". In: *Proceedings of the 2015 ACM Sixth International Conference on Future Energy Systems*. 2015, pp. 57–66.

[69] Jayant Mukhopadhaya and Brandon Graver. *Performance analysis of regional electric aircraft*. 2022.

[70] Grietus Mulder et al. "The dimensioning of PV-battery systems depending on the incentive and selling price conditions". In: *Applied Energy* 111 (2013), pp. 1126–1135. ISSN: 0306-2619. DOI: https://doi.org/10.1016/j.apenergy.2013.03.059. URL: https://www.sciencedirect.com/science/article/pii/S0306261913002559.

[71] Hiroshi Nagata and Yasuo Chikusa. "All-Solid-State Lithium–Sulfur Battery with High Energy and Power Densities at the Cell Level". In: *Energy Technology* 4.4 (2016), pp. 484–489.

[72] Engineering National Academies of Sciences, Medicine, et al. *Commercial aircraft propulsion and energy systems research: reducing global carbon emissions*. National Academies Press, 2016.

[73] CBS Nederland. *Caribbean Netherlands tourism recovered partially in 2021*. 2022. URL: https://www.cbs.nl/en-gb/news/2022/12/caribbean-netherlands-tourism-recovered-partially-in-2021.

[74] CBS Nederland. *Caribisch Nederland; banen en lonen, geslacht, leeftijd*. 2022. URL: https://www.cbs.nl/nl-nl/cijfers/detail/82518NED.

[75] NREL. *Annual technology baseline, Commercial battery storage*. 2022. URL: https://atb.nrel.gov/electricity/2022/commercial_battery_storage.

[76] NREL. *Annual technology baseline, Commercial PV*. 2023. URL: https://atb.nrel.gov/electricity/2022/commercial_pv.

[77] Kip P. Nygren. *Breguet's Formulas for Aircraft Range Endurance*. URL: %5Curl%7Bhttps://peer.asee.org/breguet-s-formulas-for-aircraft-range-endurance-an-application-of-integral-calculus.pdf%7D.

[78] Florian Pampel, Stefan Pischinger, and Moritz Teuber. "A systematic comparison of the packing density of battery cell-to-pack concepts at different degrees of implementation". In: *Results in Engineering* 13 (2022), p. 100310.

[79] Alexia P Payan, Cedric Y Justin, and Dimitri Mavris. "On-Site Renewable Energy Generation to Support Electric Thin Haul Air Mobility Operations". In: *AIAA AVIATION 2020 FORUM*. 2020, p. 2885.

[80] Dominic Perry. *Heart details dimensions of ES-30 as Swedish start-up pushes ahead with 30-seater*. 2022. URL: https://www.flightglobal.com/airframers/heart-details-dimensions-of-es-30-as-swedish-start-up-pushes-ahead-with-30-seater/150231.article.

[81] Phase to Phase. *Vision Network Analysis*. 2023. URL: https://www.phasetophase.nl/vision-network-analysis.html.

[82] Andrés Poleri. *Dubai 2021: Tecnam unveils the P-Volt, an electric aircraft based on the P2012 Traveller*. 2021. URL: https://www.aviacionline.com/2021/11/dubai-2021-tecnam-unveils-the-p-volt-an-electric-aircraft-based-on-the-p2012-traveller/?utm_content=cmp-true.

[83] Anita Prapotnik Brdnik et al. "Market and Technological Perspectives for the New Generation of Regional Passenger Aircraft". In: *Energies* 12.10 (2019). URL: https://www.mdpi.com/1996-1073/12/10/1864.

[84] Anita Prapotnik Brdnik et al. "Market and technological perspectives for the new generation of regional passenger aircraft". In: *Energies* 12.10 (2019), p. 1864.

[85] *rainflow 3.2.0*. last accessed on 15.07.2023. URL: https://pypi.org/project/rainflow/.

[86] Md Masud Rana et al. "A review on peak load shaving in microgrid—Potential benefits, challenges, and future trend". In: *Energies* 15.6 (2022), p. 2278.

[87] Iromi Ranaweera and Ole-Morten Midtgård. "Optimization of operational cost for a grid-supporting PV system with battery storage". In: *Renewable Energy* 88 (2016), pp. 262–272. ISSN: 0960-1481. DOI: https://doi.org/10.1016/j.renene.2015.11.044. URL: https://www.sciencedirect.com/science/article/pii/S0960148115304651.

[88] Rijksoverheid. *Nederland en Bonaire investeren samen in modernisering luchthaven*. 2022. URL: https://www.rijksoverheid.nl/actueel/nieuws/2022/12/14/nederland-en-bonaire-investeren-samen-in-modernisering-luchthaven.

[89] Hannah Ritchie. *Climate change and flying: what share of global CO2 emissions come from aviation?* 2022. URL: https://ourworldindata.org/co2-emissions-from-aviation.

[90] Smruti Sahoo, Xin Zhao, and Konstantinos Kyprianidis. "A review of concepts, benefits, and challenges for future electrical propulsion-based aircraft". In: *Aerospace* 7.4 (2020), p. 44.

[91] Francesco Salucci et al. "Optimal Recharging Infrastructure Sizing and Operations for a Regional Airport". In: *1st Aerospace Europe Conference (AEC 2020)*. 2020, pp. 1–8.

[92] Hans Schermeyer et al. "Understanding distribution grid congestion caused by electricity generation from renewables". In: *Smart Energy Research. At the Crossroads of Engineering, Economics, and Computer Science: 3rd and 4th IFIP TC 12 International Conferences, SmartER Europe 2016 and 2017, Essen, Germany, February 16-18, 2016, and February 9, 2017, Revised Selected Papers 4*. Springer. 2017, pp. 78–89.

[93] Katrin Schmietendorf, Joachim Peinke, and Oliver Kamps. "The impact of turbulent renewable energy production on power grid stability and quality". In: *The European Physical Journal B* 90 (2017), pp. 1–6.

[94] Yuanyuan Shi et al. "A convex cycle-based degradation model for battery energy storage planning and operation". In: *2018 Annual American control conference (ACC)*. IEEE. 2018, pp. 4590–4596.

[95] AK Shukla and T Prem Kumar. *Lithium economy: will it get the electric traction?* 2013.

[96] AE solar. *Peak shaving - off grid system*. URL: https://ae-solar.com/peak-shaving-off-grid-system/.

[97] Min-Kyu Song, Elton J Cairns, and Yuegang Zhang. "Lithium/sulfur batteries with high specific energy: old challenges and new opportunities". In: *Nanoscale* 5.6 (2013), pp. 2186–2204.

[98] Min-Kyu Song, Yuegang Zhang, and Elton J Cairns. "A long-life, high-rate lithium/sulfur cell: a multifaceted approach to enhancing cell performance". In: *Nano letters* 13.12 (2013), pp. 5891–5899.

[99] Centraal Bureau voor Statistiek (CBS). *Forecast Caribbean Netherlands: 15 percent more inhabitants by 2030*. 2022. URL: https://www.cbs.nl/en-gb/news/2022/49/forecast-caribbean-netherlands-15-more-inhabitants-by-2030.

[100] Marco Stecca et al. "Lifetime Estimation of Grid-Connected Battery Storage and Power Electronics Inverter Providing Primary Frequency Regulation". In: *IEEE Open Journal of the Industrial Electronics Society* 2 (2021), pp. 240–251. DOI: 10.1109/OJIES.2021.3064635.

[101] Daniel Ioan Stroe. "Lifetime models for Lithium-ion batteries used in virtual power plant applications". In: (2014).

[102] Stefan Stückl, Jan van Toor, and Hans Lobentanzer. "VOLTAIR-the all electric propulsion concept platform–a vision for atmospheric friendly flight". In: *28th international congress of the aeronautical sciences*. ICAS Brisbane, Australia. 2012, pp. 23–28.

[103] Gopinath Subramani et al. "Grid-tied photovoltaic and battery storage systems with Malaysian electricity tariff—A review on maximum demand shaving". In: *Energies* 10.11 (2017), p. 1884.

[104] Yin Sun et al. "6MW solar plant integration feasibility study: Bonaire island case study". In: *2016 IEEE 17th Workshop on Control and Modeling for Power Electronics (COMPEL)*. IEEE. 2016, pp. 1–8.

[105] Mohd Tariq et al. "Aircraft batteries: current trend towards more electric aircraft". In: *IET Electrical Systems in Transportation* 7.2 (2017), pp. 93–103.

[106] *The Breguet range equation*. 2008. URL: https://web.mit.edu/16.unified/www/FALL/Unified_Concepts/Breguet-Range-U2-notes-Fall08(2).pdf.

[107] Liya Tom et al. "Commercial aircraft electrification—Current state and future scope". In: *Energies* 14.24 (2021), p. 8381.

[108] Lorenzo Trainelli et al. "Optimal sizing and operation of airport infrastructures in support of electric-powered aviation". In: *Aerospace* 8.2 (2021), p. 40.

[109] Moslem Uddin et al. "A review on peak load shaving strategies". In: *Renewable and Sustainable Energy Reviews* 82 (2018), pp. 3323–3332.

[110] Dries Verstraete. "Long range transport aircraft using hydrogen fuel". In: *International Journal of Hydrogen Energy* 38.34 (2013), pp. 14824–14831. ISSN: 0360-3199. DOI: https://doi.org/10.1016/j.ijhydene.2013.09.021. URL: https://www.sciencedirect.com/science/article/pii/S036031991302212X.

[111] Venkatasubramanian Viswanathan et al. "The challenges and opportunities of battery-powered flight". In: *Nature* 601.7894 (2022), pp. 519–525.

[112] WEB. *Bekendmaking tarieven elektriciteit en drinkwater per 1 januari 2023*. 2022. URL: https://www.webbonaire.com/2022/12/21/bekendmaking-tarieven-elektriciteit-en-drinkwater-per-1-januari-2023/.

[113] WEB. *Duurzame Energie*. URL: https://www.webbonaire.com/duurzame-energie/.

[114] *Wet elektriciteit en drinkwater BES*. 2023. URL: https://wetten.overheid.nl/BWBR0037861/2023-01-01.

[115] M Wild et al. "Lithium sulfur batteries, a mechanistic review". In: *Energy & Environmental Science* 8.12 (2015), pp. 3477–3494.

[116] Southern wings. *Aerodynamic Forces In Climbs And Descents*. 2019. URL: https://www.southernwings.co.nz/aerodynamic-forces-in-climbs-and-descents/.

[117] WorldAtlas. *Caribbean sea*. 2021. URL: https://www.worldatlas.com/seas/caribbean-sea.html.

[118] Yaling Wu et al. "Optimal battery capacity of grid-connected PV-battery systems considering battery degradation". In: *Renewable Energy* 181 (2022), pp. 10–23. ISSN: 0960-1481. DOI: https://doi.org/10.1016/j.renene.2021.09.036. URL: https://www.sciencedirect.com/science/article/pii/S0960148121013343.

[119] Yue Xiang et al. "Techno-economic design of energy systems for airport electrification: A hydrogen-solar-storage integrated microgrid solution". In: *Applied energy* 283 (2021), p. 116374.

[120] Guangmin Zhou, Hao Chen, and Yi Cui. "Formulating energy density for designing practical lithium–sulfur batteries". In: *Nature Energy* 7.4 (2022), pp. 312–319.

[121] Zhibin Zhou et al. "A review of energy storage technologies for marine current energy systems". In: *Renewable and Sustainable Energy Reviews* 18 (2013), pp. 390–400.

A

Appendix

A.1. Additional Background

A.1.1. Alternatives to Conventional Fuelled Aircraft

Sustainable Aviation Fuels (SAFs) and hydrogen are emerging as alternatives to electric aviation with batteries. In the current aviation industry, the use of alternative fuels is limited [8]. Nevertheless, there is significant progress in the commercialization of alternative fuels [10]. Hydrogen offers opportunities as an alternative in the long term since there are multiple challenges in aircraft design and infrastructure for fuelling. Battery-powered aircraft can replace conventional smaller aircraft at short range, while for larger aircraft the hybrid form offers more prospects [10].

First, an alternative to conventional fuels is the so-called Sustainable Aircraft Fuel (SAF). SAFs are the general term for fuels produced from non-fossil sources making them environmentally friendly [10]. A SAF can be produced from various sources like waste oil and fats, green waste, and other residue raw materials. In this way, SAF is able to recycle the CO_2 absorbed by the biomass in the used sources. A synthetic production process is also possible by direct carbon capture from the air. A major advantage of SAF is the possibility to directly replace conventional kerosene as SAFs have chemical similarities. The current fuel infrastructure at airports and the modern aircraft are compatible with SAFs [48]. However, the major barrier is the higher costs related to the production of SAFs compared to conventional kerosene production [10].

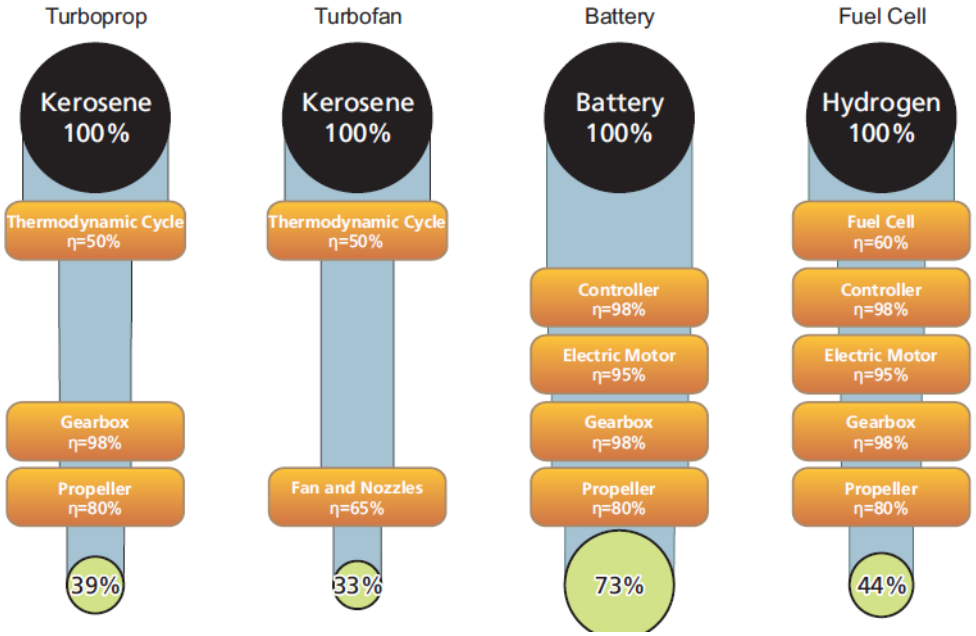

Figure A.1: Different efficiency conversion chains of onboard powering systems for aircraft [43].

Hydrogen is another alternative that can be used as a sustainable energy source in future aviation offering numerous advantages such as a reduction in noise, efficiency increase, and reduced GHG emissions as long as it is produced from renewable energy [10]. In addition, hydrogen has higher specific energy (gravimetric energy density) than kerosene. However, the downside is the lower volumetric energy density, which causes significant airframe redesigns.
The storage of liquid hydrogen can either be in the gaseous phase or in the liquid phase. Hydrogen gas typically needs to be stored in high-pressure tanks of 350 to 700 bars [43]. These tanks lead to additional weight for the aircraft and furthermore induce safety risks. Lowering the pressures results in larger volumes which could affect the drag of the aircraft [43].
For storage of liquid hydrogen, an aircraft requires highly insulated tanks in order to maintain a fuel temperature of about -250 °C. These tanks also account for additional weight, which makes the incorporation of hydrogen in aircraft designs challenging [10] [43].
The use of hydrogen does not only result in the redesign of aircraft but also the ground infrastructure needs to be adapted. A supply chain and storage facilities on the ground should be set up to enable the fuelling of aircraft with hydrogen safely [58].
Hydrogen can be used in two primary ways: in a hydrogen-fuelled turbofan and in a fuel cell. Including hydrogen as a fuel for a turbofan mainly contributes to energy utilization savings on long-distance flights, up to 11%, while on a short-range it penalized the energy utilization due to the needed storage tanks aboard [110].

Lastly, batteries are reviewed as onboard storage for electrically powered aircraft and will be considered further in this thesis. Most of the currently developed concepts are based on batteries-powered aircraft, and it is expected that this trend will continue [65]. With the vigorous development of battery technologies widely used in the transition and the reduction of emissions in the transportation sector, electric flying has attracted more interest.
The main advantages of batteries are high efficiencies, zero emissions in operation, and low maintenance, while the drawback of battery use in aircraft is the increased system weight causing a reduced flight range [107]. As can be seen in figure A.1, batteries face high total system efficiencies compared to other powering systems of aircraft. The efficiency of the kerosene-powered aircraft drivetrain is equal to either 39% or 33% for a turboprop or a turbofan, respectively. The low efficiency is mainly caused due to more dynamics in the drivetrain causing extra losses. In the drivetrain of the turboprop, the thermodynamic cycle accounted for 50% of the efficiency, the gearbox for 98%, and the propellor for 80%. In the case of the turbofan, the fan and the nozzles have a 65% efficiency as can be seen in figure A.1 [43]. Considering

electric aircraft, the drivetrain consists of a controller, electric motor, gearbox, and propeller. These components have efficiencies of 98%, 95%, 98%, and 80%, respectively. The product of these efficiencies results in a total efficiency of 73% [43].
At present, batteries based on lithium are the most promising battery technologies for electric aviation since this battery is the lightest metal and therefore will potentially lead to the highest specific energy [26]. The specific energy of a battery is measured in kWh/kg or Wh/kg. Furthermore, this type of battery technology is already heavily used in the EV industry [47]. The battery technologies among the Lithium battery include the readily available lithium-ion (Li-ion), the technologies in the research and development phase are the lithium-sulfur (Li-S), and lithium-air (Li-air) technologies [43].

A.2. Electric Aviation Parameters and Vision Model

A.2.1. Input Parameters Breguet Range Equation and Take-off Equation

Table A.1: Input parameters for Breguet range equation and take-off equation [5].

	Alice	**ES-19**	**ES-30**
R, Curacao	76 km	76 km	76 km
R, Aruba	194 km	194 km	194 km
mTO	8346 kg	8618 kg	20000 kg
L/D, steady state	16	16	16
L/D, climb	12	12	12
etatotal	0.73	0.73	0.73
vcruise	410 km/h	300 km/h	250 km/h
h, Curcao	4500 feet	4500 feet	6000 feet
h, Aruba	6000 feet	6000 feet	10000 feet
theta	5	5	5

A.2.2. Vision Grid Model

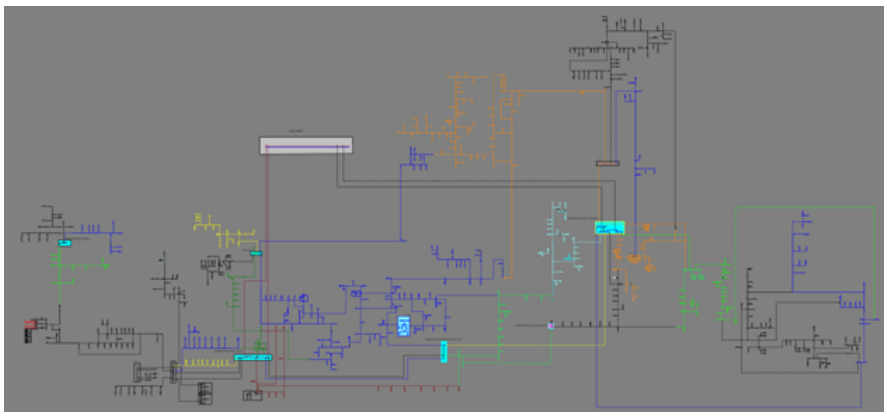

Figure A.2: Electricity grid medium voltage level (12.2 kV) model of Bonaire in Vision [81].

A.2.3. Scenarios: Historic Trends Electricity Production and Rates

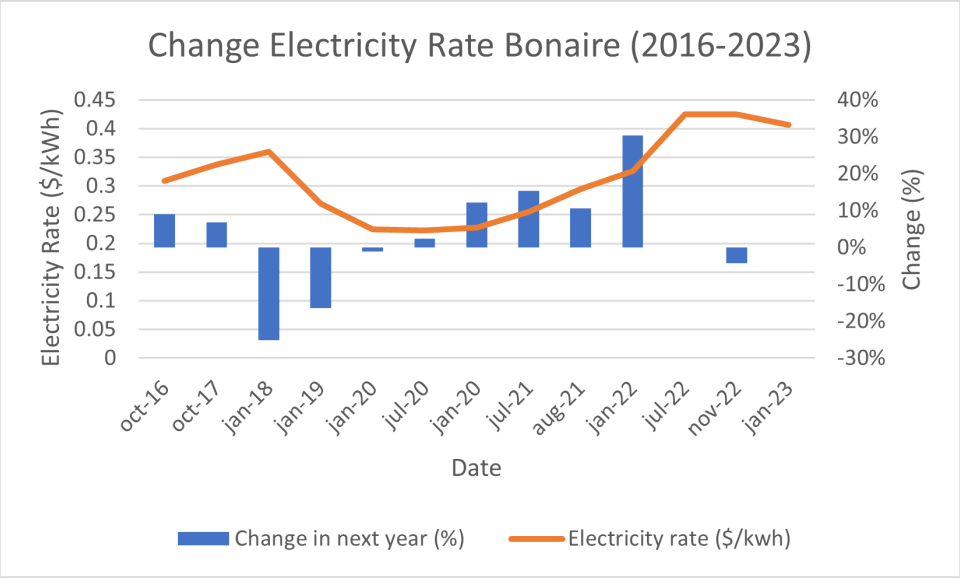

Figure A.3: Historic electricity purchase price and change. Period 2016-2023.

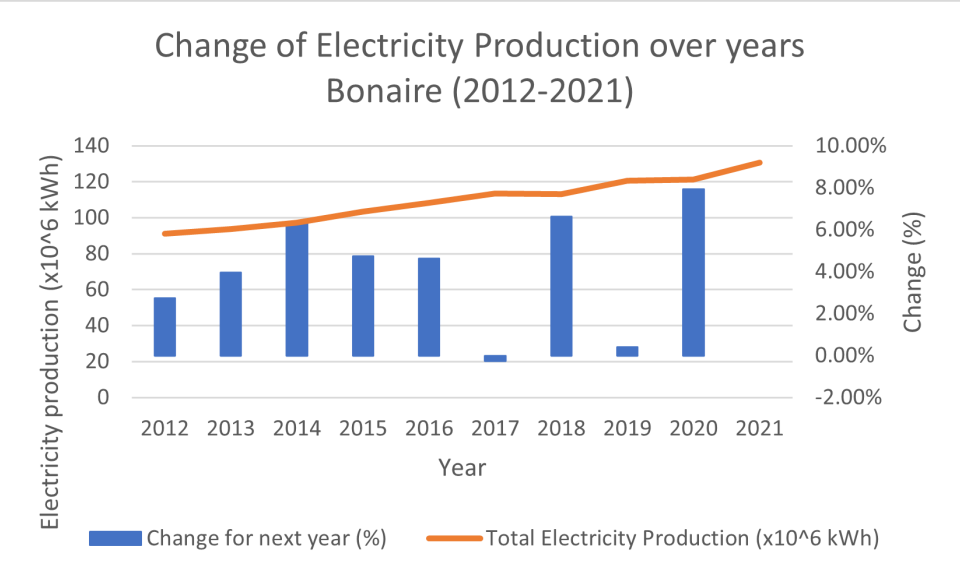

Figure A.4: Historic electricity production at Bonaire and change. Period 2012-2021.

A.3. Additional Results

A.3.1. Load Profiles Total Airport Demand

Load profiles BIA with 1.0 MWp solar

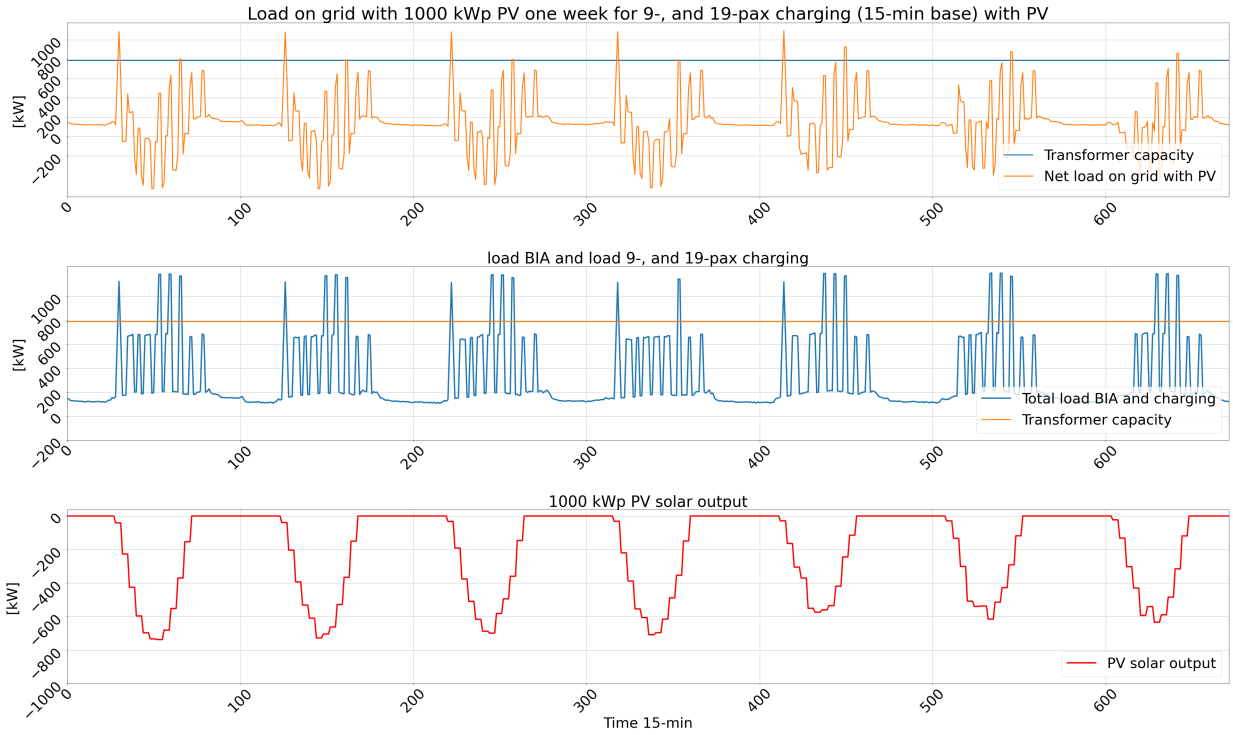

Figure A.5: Demand profile of BIA for 9-, 19-pax aircraft charging and 1 MWp PV solar park installed.

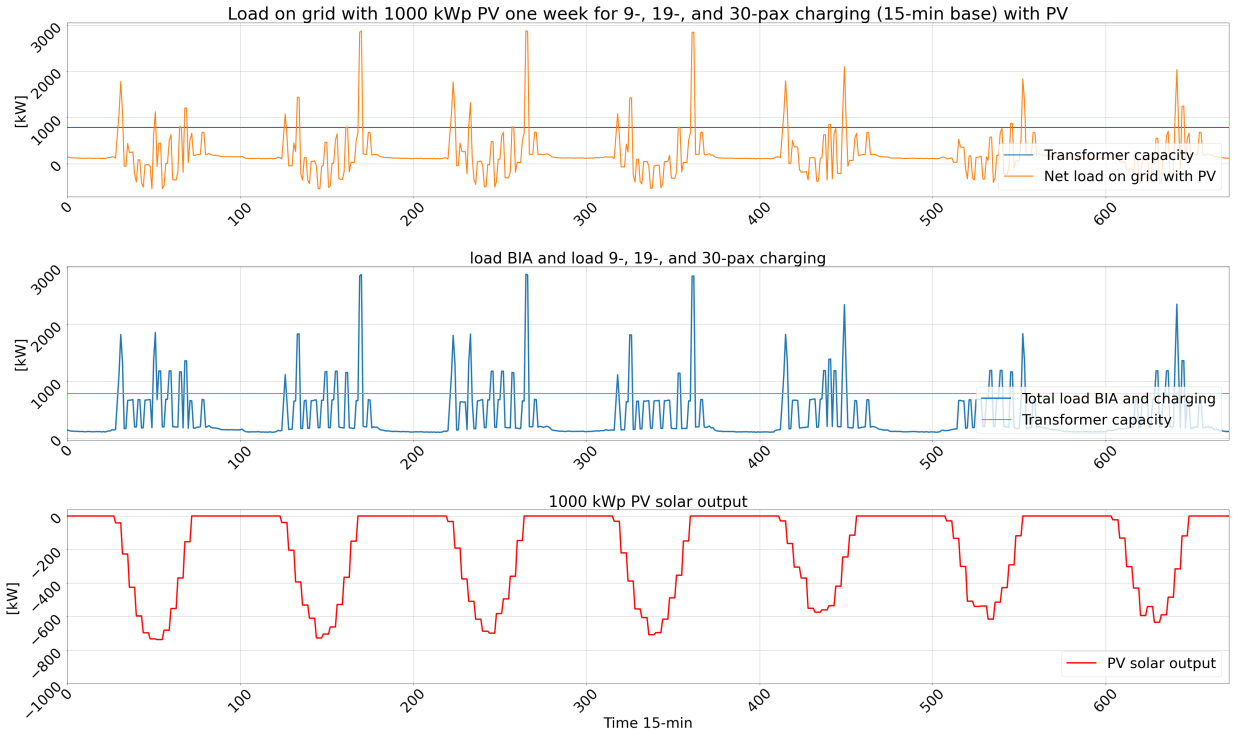

Figure A.6: Demand profile of BIA for 9-, 19-, and 30-pax aircraft charging and 1 MWp PV solar park installed.

A.3.2. BESS Control Strategies Load Flows

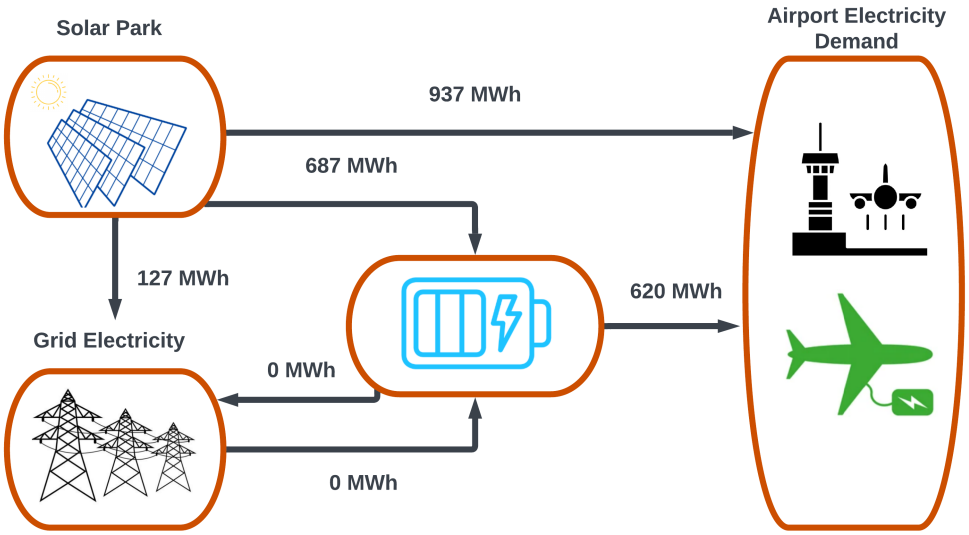

Figure A.7: Load flow of Self-Consumption for 2000kWh/1000kW BESS, 1000 kWp, 9-pax charging

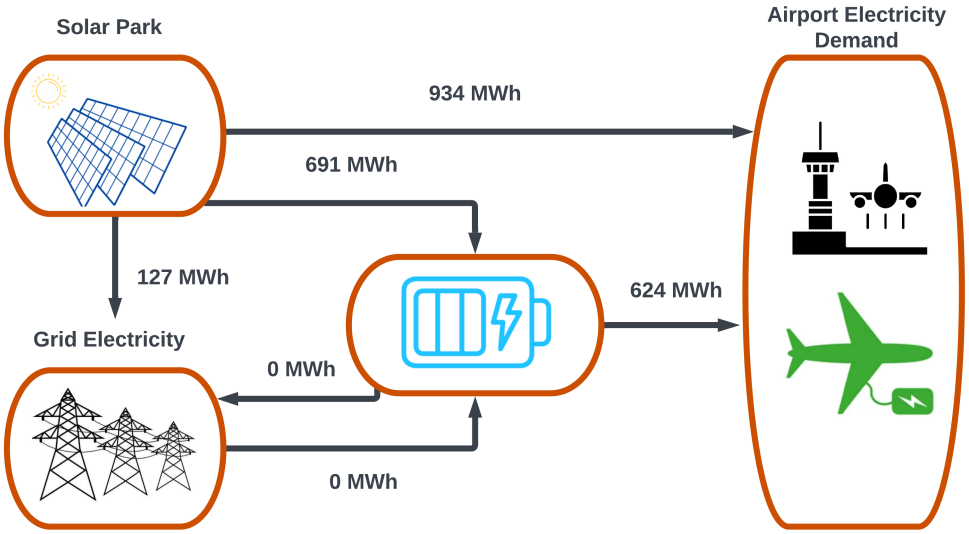

Figure A.8: Load flow of Peak Shaving for 2000kWh/1000kW BESS, 1000 kWp, 9-pax charging

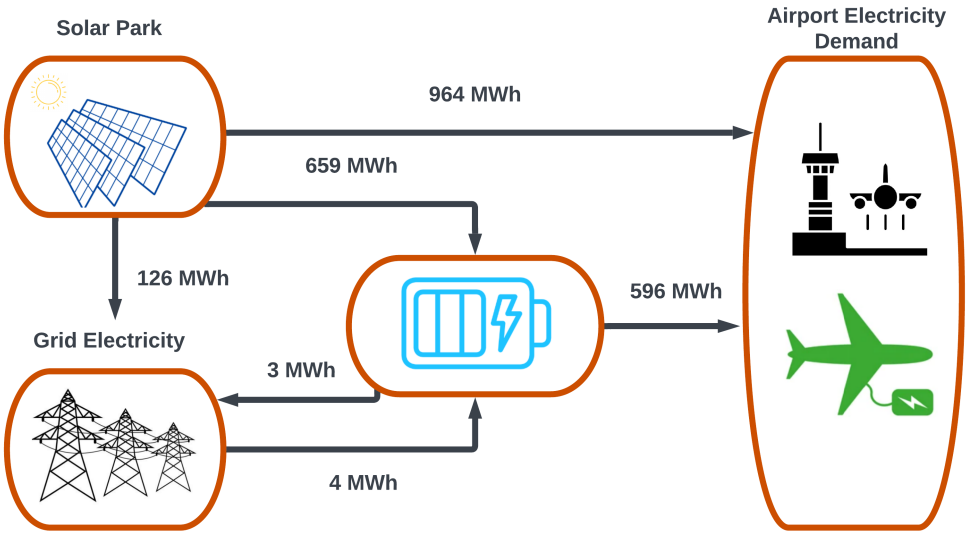

Figure A.9: Load flow of Cost-Optimal for 2000kWh/1000kW BESS, 1000 kWp, 9-pax charging

A.4. Alternative System Set Up for Future Research

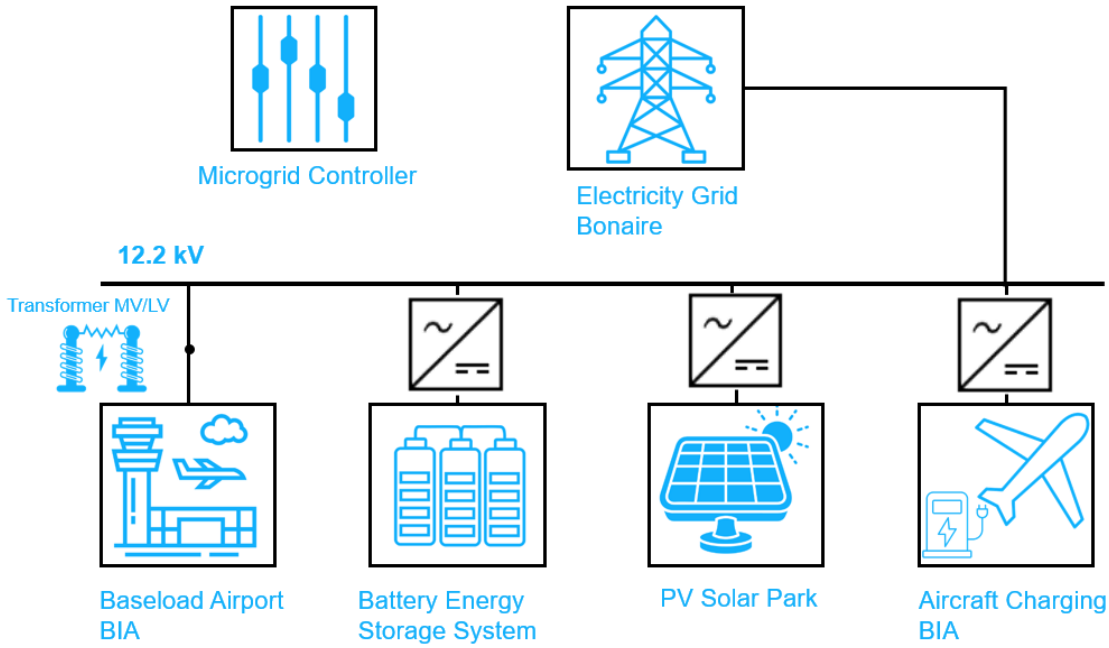

Figure A.10: Alternative system design airport: voltage level 12.2 kV to reduce the power losses over the potentially large distance at the airport.